eman ta zabal zazu

Universidad del País Vasco
Euskal Herriko Unibertsitatea

Facultad de Medicina y Enfermería

Departamento de Neurociencias

# Unraveling the role of astrocytes in the onset and spread of Parkinson´s Disease: Important contributors to neurodegeneration

PhD Thesis

**Paula Ramos González**

**2020**

Esta tesis doctoral ha sido realizada gracias a una beca del Programa Predoctoral de Formación de Personal Investigador No Doctor del Departamento de Educación, Política Lingüística y Cultura del Gobierno Vasco durante el periodo 2016-2019.

El trabajo experimental ha sido financiado por el Centro de Investigación Biomédica en Red de Enfermedades Neurodegenerativas (CIBERNED), proyectos del ministerio de Economía y Competitividad (SAF2013-45084-R y SAF2016-7592-R), proyectos de grupos consolidados del Gobierno Vasco (IT02-13 y IT03-19), proyectos de la fundación vasca de investigación e innovación sanitarias BIOEF (BIO17/ND/008) y por la fundación Euskampus.

Quizá esta sea la página de la tesis que más me ha costado empezar a escribir. Después de 5 años sois tantos los que os habéis cruzado en mi camino y a los que tengo que agradecer que no sé por dónde empezar.

En primer lugar, gracias Carlos por dejarme formar parte de este grupo. Has sabido crear no solo un equipo de grandes científicos, sino de personas con gran calidad humana, lo que me parece aún más difícil. Para mí ha sido un gusto verte trabajar y he aprendido muchísimo de tus ideas y de tus consejos, siempre oportunos. Gracias.

A mi director, Fabio. Cuando entré al labo me dijeron que tenía mucha suerte de que fueras a ser mi jefe y que iba a estar muy a gusto trabajando contigo, y no se equivocaban. Gracias por enseñarme a pensar, dejarme aportar siempre mis ideas y confiar en mí desde el primer día. Si algún día tengo a alguien a mi cargo me gustaría que se sintiera tan cómodo y tan libre como lo he hecho yo contigo. En definitiva, gracias por hacer que estos años de trabajo hayan sido tan fáciles, hemos formado un gran equipo.

I would also like to thank Proff. Richard Wade Martins, my supervisor at the University of Oxford for accepting me in such a good group for a time. It was a pleasure for me working in your lab for those three months. Thanks to all the people in the lab, Milena, Peter, Charmaine, Saba, Becky, Gabriele, Dayne… for your support, your help and for making my stay so easy. Y sobre todo, gracias Nora por estar a mi lado durante aquellos tres meses y por hacerme sentir en casa desde el primer momento. Aprendí muchísimo de ti y para mí fue un placer trabajar mano a mano contigo. Eres en gran parte responsable de que guarde un buenísimo recuerdo de mi experiencia en Oxford.

También tengo que agradeceros a todos los que formáis Achucarro. Jaime, Laura G. y Marian, gracias por vuestra ayuda y por hacer que todo funcione bien. Aitor, gracias por tu disposición a ayudar siempre y por salvarme del scanner cuando no quiere hacerme caso. Lauri, estoy convencidísima de que este centro no funcionaría sin ti. Gracias por buscar siempre la foto perfecta, por las conversaciones, las risas y los cotilleos necesarios para amenizar tantas horas en ese cuartucho. Tienes el don de convertir tres interminables horas en tres minutos. Muchas gracias también a todos los que formáis el resto de grupos de Achucarro, porque un “qué tal lo llevas”, una sonrisa en el pasillo y las conversaciones en la sala de cultivos son necesarias y siempre se agradecen. Tengo que mencionar a Zugaza y a Llavero.

Gracias por vuestros ánimos y por aparecer en nuestra salita para hacernos pasar siempre buenos ratos con vuestras matrimoniadas.

Quiero agradecer especialmente a todos los que formáis o habéis formado parte del "grupo Matute". Creo que juntos creamos un ambiente de trabajo que, sinceramente, dudo que vuelva a encontrar.

Elena, gracias por tu ayuda siempre, por preocuparte y por hacer que en las comidas siempre surja una conversación entretenida. Esti, gracias por tu apoyo, sabes transmitir la tranquilidad necesaria para quien está haciendo una tesis. Vanja, siempre tienes una buena sugerencia y sobre todo, una buena conversación. Vicky, María, Fernando, gracias por estar siempre disponibles para ayudar. Alberto, ha sido un placer compartir contigo las clases de anatomía. Susana, gracias por tu ayuda esta última temporada y por buscar siempre el experimento perfecto. Asier, gracias por hacer que cada explicación suene fácil. Fede, escucharte hablar de ciencia es un gusto, tienes siempre la respuesta a cualquier pregunta. Juan Carlos, compartir contigo las horas de electrónico hace que parezca mucho más sencillo. Anita, cuando entré al labo tu prácticamente te ibas, me ha encantado que volvamos a coincidir en mi recta final y compartir este último tiempo. Mari Paz, espero que encuentres tu lugar ideal en el mundo de la ciencia. Cuando hay ganas siempre llega, y tú las tienes. Y Saio, muchísimas gracias por todo, eres fundamental en este grupo. Seguro que el cambio que buscas llega lleno de cosas buenas.

A todos los que empezasteis un nuevo camino. Manu, Ane, Moni, Raff… fue un placer compartir poyata con vosotros. Gracias por haberme echado una mano siempre que lo he necesitado, por enseñarme cuando era una recién llegada y por recordarme que hay vida después de la tesis.

Gracias a todos los "becarios Matute". Hacer una tesis con buenos compañeros es mucho más fácil. Álvaro, gracias por mantener el sentido del humor incluso cuando tu ánimo es una montaña rusa. Venga, que ya está casi hecho. Alejandro, siempre tienes esa respuesta ingeniosa que nos hace reír. Gracias por la tranquilidad necesaria que transmites. Ana, terminarás estos años siendo una experta electrofisióloga, aunque a veces lo veas un poco gris. Mucho ánimo. Celia, muchas gracias por estar siempre dispuesta a ayudar, eres ejemplo de constancia y de trabajo bien hecho. María, se nota la pasión que sientes por la ciencia, y tienes la creatividad y las ganas de aprender necesarias para que te vaya genial en este mundo.

Adhara, llegaste en el momento perfecto y fuiste el mejor relevo que podía tener Tania. Nos trajiste la energía que necesitábamos cuando empezábamos a cojear. Gracias por estar dispuesta a ayudar siempre y por transmitir siempre buen humor. Sólo me gustan los lunes porque siempre tienes alguna aventura de fin de semana que contarnos. Gracias. A las nuevas generaciones, Laura, Leire, Uxue y Arián, habéis traído el aire fresco que siempre hace falta. Aprovechad estos años, pero sobre todo, disfrutadlos, que pasan volando. Mucha suerte y ánimo!

Y sobre todo gracias a vosotras, amigas. Aunque muchas ya no estéis sé que todavía nos quedan muchísimos momentos por compartir. Tania, Carolina y Jone, compartir mesa con vosotras ha sido lo mejor de este tiempo. No sé que habría hecho sin nuestras charlas interminables y sin vuestro apoyo diario. Tania, nunca pensé que siendo tan diferentes podríamos llegar a entendernos tan bien. El día que presidas tu pequeño país sabes que no iré a vivir contigo, pero te visitaré muchísimo. El mundo de la ciencia tiene suerte de que formes parte de él con tantísima pasión. Caroline, eres la disciplina y el trabajo bien hecho. La vida ha querido que compartamos nuestro camino desde hace muchos años, y ojalá siga siendo así. Gracias por acompañarme y animarme todo este tiempo. Jone, tenerte a mi derecha todos los días hace que el trabajo sea menos trabajo. Sé que siempre va a haber un momento para reírnos y compartir buenos momentos dentro y fuera del labo. Gracias por estar ahí siempre para ayudarme y por ser la sensatez que me falta cuando creo que lo mejor es meterme en un contenedor de basura. Alaz, hemos compartido poco en el trabajo, pero a quién le importa si puedes compartir pizza a las dos de la mañana después de una noche un poco accidentada. Eres trabajadora, divertida y la calma que hace falta cuando las cosas se tuercen un poco. Andrea, siendo el agua y el aceite, el sentido del humor y ver la vida con banda sonora de fondo han hecho que seamos mucho más que compañeras de trabajo. Gracias por las carcajadas constantes. Ainara, gracias por seguir estando después de haberte ido. Eres decidida, perseverante y sobre todo, muy valiente. Y Hazel, tú me has acompañado incluso desde antes de empezar, me diste tu confianza desde el primer momento e hiciste que todo fuera más fácil. Gracias a todas, por todo.

A mis amigas de toda la vida, mi queridísimo séquito, Aida, Ale, Ene, Glor, Lei, Lu, Marina, Nerea, Olatz, Uxu, Vic y Yas. A vosotras os agradezco simplemente que estéis en mi vida y que me deis la confianza para compartirlo todo con vosotras. Gracias por estar ahí para mí cuando lo necesito, por animarme durante estos años y siempre. Como dice parte de nuestro brindis

favorito: “brindo por ser parte de esto y por compartirlo con vosotras”. Solo espero que sigáis formando parte de todos mis mejores recuerdos. Gracias.

Carmen, eres sin duda la mejor sorpresa que me podía haber dado la tesis. Bendito el día en el que escribiste a una desconocida para compartir piso en Oxford. Los tres meses allí fueron tan increíbles porque los compartí contigo. Sé que tengo una amiga para siempre y que juntas hacemos que Sevilla y Bilbao estén mucho más cerca.

A mi castreñada favorita, gracias por regalarme siempre momentos de desconexión y de diversión. Vosotros tenéis mucha culpa de que adore tantísimo ese pueblo.

Y por supuesto, gracias a mis amigos del cole. Aunque nos veamos poco las cosas no cambian. Me conformo con saber que estáis ahí y con seguir entrando en cada año con vosotros, sé que no hay mejor manera de hacerlo.

Por último, gracias a mi familia, y a los que no sois familia pero como si lo fuerais.

Gracias a mis aitites, tíos y primos y a Memé, Jose y Elena por vuestro apoyo, los ánimos y por darle tanto valor a lo que hago.

Ama y Ángela, gracias por todo. Por intentar comprender cómo funciona este mundo sin conocerlo, sólo por intentar entenderme a mí; por escuchar mis interminables charlas en ingles sin saber de lo que hablo y por preocuparos siempre por mí. Nos toca viaje de celebración, que no se os olvide. Os quiero.

Muchas gracias a todos.

*A aita*

*“Llevo tu luz y tu olor por donde quiera que vaya.”*

*Joan Manuel Serrat, Mediterrraneo.*

**Table of contents** **I**

**List of abbreviations** **VII**

**Abstract** **XIII**

**Highlights** **XVII**

**Introduction**

1. Parkinson´s Disease **3**
    - 1.1 Prevalence, ethiology and symptoms **3**
    - 1.2 Treatments **4**
2. Alpha synuclein in Parkinson´s Disease **5**
    - 2.1 Alpha synuclein biology **5**
    - 2.2 Alpha synuclein mediated toxicity: oligomers vs fibrils **7**
        - 2.2.1 Mitochondrial dysfuntion **8**
        - 2.2.2 Lysosomal degradation defects **9**
    - 2.3 Alpha synuclein transmission: prion-like hypothesis **10**
3. Genetics **13**
    - 3.1 PD related mutations **13**
    - 3.2 LRRK2 mutation - G2019S **14**
        - 3.2.1 $LRRK2^{G2019S}$ and mitochondrial respiration **15**
        - 3.2.2 $LRRK2^{G2019S}$ and citoeskeletal dynamics **16**
4. Astrocytes´ role in CNS **16**
    - 4.1 Neuronal homeostasis and synaptic activity **18**
    - 4.2 Energy supply and metabolism **19**
    - 4.3 Homeostasis of Reactive Oxigen Species **20**
5. Astrocytes in PD **22**
    - 5.1 α- Syn mediated pathology in astrocytes **22**
    - 5.2 Impact of PD gene mutations in astrocytes **24**
    - 5.3 Reactive astrogliosis and neuroinflamation **25**
6. Models to study Parkinson´s Disease **29**

**Hypothesis and Objectives** **31**

**Experimental procedures** **35**

*Part I* **37**

1.1 Animals **37**

1.2 Rat Cell cultures **37**

1.2.1 Primary cortical neuron culture **37**

1.2.2 Astrocyte cell culture **38**

1.3 Purification of Lewy Bodies (LB) for PD brains **38**

1.4 Inhibitors and molecules **39**

1.5 Microfluidic assays **40**

1.5.1 α-Synuclein transport **40**

1.5.2 α- Synuclein Proximity Ligation Assay (AS-PLA) **41**

1.5.3 Apoptosis **43**

1.6 Immunofluorescence **43**

1.7 ELISA assays **44**

1.8 Baculovirus infection **44**

1.9 Total protein extract and Western blot **44**

1.10 α-synuclein clearance by lysosomes **45**

1.10.1 Lysosomal enrichment and FACS purification **45**

1.10.2 ELISA assay **45**

1.10.3 Fluorimetric assay for Cathepsin D activity **45**

1.11 Measurement of mitochondrial function **46**

1.12 Statistical analysis **47**

*Part II* **48**

2.1 Human Samples **48**

2.2 Human Astrocyte generation **48**

2.3 Characterization of iPSc derived Human Astrocytes **50**

2.3.1 Analysis of the GFAP positive- astrocytic population by FACS **50**

2.3.2 Calcium Imaging **51**

2.3.3 Immunofluorescence **51**

2.4 Analysis of mitochondrial ultraestructure **52**

2.4.1 Sample preparation for Electron Microscopy **52**
2.4.2 Image Acquisition and analysis **52**
2.5 Mitochondrial membrane potential measurement **53**
2.6 Measurement of mitochondrial function and glycolitic activity **53**
2.7 Western blot for detection of oxidatively modified proteins **54**
2.7.1 Sample preparation **54**
2.7.2 SDS-PAGE and western blotting **55**
2.8 Effect of astrocytes in neuronal survival **55**
2.8.1 Neuron-Astrocyte Co-cultures **55**
2.8.2 Automated Image Acquisition **56**
2.8.3 Image Processing and Statistics **57**
2.9 Statistical analysis **57**
Appendix I: Table of antibodies **58**
Appedix II: Karyotype of human astrocytes **59**

**Results - Part I** **61**
1.1 Rat cortical neurons and astrocytes internalize exogenous human α-synuclein **63**
1.2 hα-syn is uptaken by endocytosis **65**
1.3 Astrocytes display increased lysosomal activity when exposed to hα-syn compared to neurons **66**
1.4 Mitochondrial metabolism is activated in LB treated astrocytes compared to neurons **68**
1.5 hα-syn is transmitted cell-to-cell between neurons and astrocytes **70**
1.6 Astrocytes spread neurotoxicity by α-syn transmission **73**
1.7 Up taken hα-syn activates the overexpression of endogenous α-syn in both neurons and astrocytes **74**
1.8 Levels of oligomeric hα-synuclein are similar between neurons and astrocytes after transmission from astrocytes **76**
Summary I **78**

**Results - Part II** **79**

2.1 Generation and characterization of highly homogeneous iPSc derived functional astrocytes **81**

2.2 Parkinson´s Disease astrocytes display atrophic morphology in comparison to control astrocytes **83**

2.3 Astrocytes characterization by functional Calcium imaging **85**

2.4 Mitochondrial metabolism and unusual mitochondrial morphology in PD astrocytes **87**

2.4.1 PD LRRK2$^{G2019S}$ astrocytes display an impairment in mitochondrial functionality but an aerobic respiration. **87**

2.4.2 Mitochondrial morphology is disrupted in PD astrocytes compared to controls **89**

2.4.3 Parkison´s Disease astrocytes show higher levels of oxidized proteins compared to controls **90**

2.5 PD astrocytes compromise neuronal survival in neuron astrocyte cocultures **91**

Summary II **92**

**Discussion** **93**

1. Rat primary astrocytes and neurons internalize hα-syn by endocytosis and transfer the protein to each other **96**
2. Astrocytes contribute more efficiently to hα-syn degradation **98**
3. Mitochondrial function is compromised in astrocytes in our both models of the Parkinson´s Disease **99**
4. PD LRRK2$^{G2019S}$ astrocytes show an atrophic phenotype compared to healthy controls **101**
5. Astrocyte contribution to neuronal degeneration **103**
6. Future directions and concluding remarks **103**

**Conclusions** **105**

**Bibliography** **109**

| | |
|---|---|
| **6-OHDA** | 6-hydroxydopamine |
| **AFP** | α-fetoprotein |
| **AKT** | Alpha serine/threonine kinase |
| **ANOVA** | Analysis of Variance |
| **AQP4** | Aquoporin 4 |
| **ARSEP** | Association for research on multiple sclerosis |
| **AS-PLA** | Alpha- Synuclein Proximity Ligation Assay |
| **ATP** | Adenosine triphosphate |
| **ATP13A2** | ATPase type 13A2 |
| **AUC** | Area under the curve |
| **BSA** | Bovin serum albumin |
| **C1q** | Complement component 1q |
| **CNS** | Central neurvous system |
| **COMT** | Catechol-o-metyltranspherase |
| **CPH** | Cox proportional hazard |
| **CSC** | Cerebellar ataxias |
| **DA** | Dopamine |
| **DAPI** | 4',6-diamidino-2-phenylindole |
| **DBS** | Deep brain stimulation |
| **DHPG** | (S)-3,5-Dihydroxyphenylglycine hydrate |
| **DIV** | Days *in vitro* |
| **DNP** | 2,4-Dinitrophenol |
| **DNPH** | 2,4-Dinitrophenylhydrazine |
| **DMEM** | Dulbecco modified Eagles minimal essential medium |
| **Drp1** | Dynamin related protein 1 |
| **E6** | Essential 6 medium |
| **E8** | Essential 8 Flex medium |
| **EB** | Embrioid Body |
| **ECAR** | Extracellular acidification rate |
| **EDTA** | Ethylenediaminetetraacetic acid |
| **EGFP** | Enhanced green fluorescent protein |
| **EGFR** | Epidermal growth factor receptor |

| | |
|---|---|
| **EGTA** | Egtazic acid |
| **ELISA** | Enzyme-Linked ImmunoSorbent Assay |
| **F-actin** | Filamentous actin |
| **FAK** | Focal adhesion kinase |
| **FBS** | Fetal bovin serum |
| **FCCP** | Carbonylcyanide-p-trifluoromethoxy-phenylhydrazone |
| **GABA** | Gamma-aminobutyric acid |
| **GAPDH** | Glyceraldehyde 3-phosphate dehydrogenase |
| **GAT** | Gamma-aminobutyric acid transporters |
| **GFAP** | Glial fibrillary acidic protein |
| **GFP** | Green fluorescent protein |
| **GLAST (EAAT1)** | Glutamate/aspartate transporter |
| **GLT1 (EAAT2)** | Glutamate transporter 1 |
| **GS** | Glutamine synthetase |
| **GT** | Gliotransmitters |
| **GTPase** | Guanosine triphosphate hydrolase |
| **$H_2O_2$** | Hydrogen peroxide |
| **HBSS** | Hank´s balanced salt solution |
| **HCA** | High Content Analysis |
| **HCS** | High Content Screening |
| **HIFU** | High Intensitive Focused Ultrasound” |
| **Hα-syn** | Human alpha synuclein |
| **IL1β** | Interleukin 1 β |
| **IL-6** | Interleukin 6 |
| **IMDM** | Iscove's Modified Dulbecco's Medium |
| **iPSCs** | Induced pluripotent stem cells |
| **KO** | Knock-out |
| **KOH** | Potassium hydroxide |
| **LB** | Lewy body |
| **LC3** | Light chain 3 |
| **L-dopa** | Levodopa |
| **LMP** | Lysosomal membrane permeabilization |

| | |
|---|---|
| **LRRK2** | Leucine-rich repeat kinase 2 |
| **MEM** | Minimal Essential Medium |
| **MOPS** | 3-(N-morpholino)propanesulfonic acid |
| **MPTP** | 1-methyl-4-phenyl-1,2,3,6-tetrahy- dropyridine |
| **mtDNA** | Mitochondrial Deoxiribonucleic Acid |
| **MTs** | Microtubules |
| **$Na_3VO_4$** | Sodium orthovanadate |
| **$Na_4P_2O_7$** | Sodium pyrophosphate tetrabasic |
| **NAC** | Non-amyloid component |
| **NaF** | Sodium fluoride |
| **NO** | Nitric oxide |
| **NTs** | Neurotransmitters |
| **OCR** | Oxygen consumption rate |
| **p38** | Mitogen-activated protein kinase 38 |
| **PARK2** | Parkin |
| **PBS** | Phosphate-buffered saline |
| **PER** | Proton efflux rate |
| **PD** | Parkinson´s Disease |
| **PFA** | Para-formaldehyde |
| **PFF** | Preformed fibril |
| **PI** | Propidium iodide |
| **PMSF** | Phenylmethanesulfonyl fluoride |
| **PrP** | Prion protein |
| **$PrP^c$** | Cellular prion protein |
| **$PrP^{Sc}$** | Disease-associated prion proteiN |
| **PVDF** | Polyvinylidene fluoride |
| **RCA** | Rolling Circle Amplification |
| **RIPA** | Radioimmunoprecipitation assay buffer |
| **Rh123** | Rhodamin 123 |
| **ROS** | Reactive oxigen species |
| **Rα-syn** | Rat alpha synuclein |
| **SDS** | Sodium dodecyl sulfate |

| | |
|---|---|
| **SEM** | Standard error of the mean |
| **SH** | Seahorse |
| **SNARE** | Soluble NSF Attachment Protein Receptor |
| **SNCA** | α-synuclein |
| **SNpc** | Substantia nigra *pars compacta* |
| **SMA** | Smooth muscle actin |
| **TBS-T** | Tris buffered saline tween |
| **TLR4** | Toll like receptor 4 |
| **TNF-α** | Tumor necrosis factor-α |
| **TNTs** | Tunneling nanotubes |
| **Tris** | Tris(hydroxymethyl)aminomethane |
| **UCHL 1** | Ubiquitin carboxy- terminal hydrolase L1 |
| **WB** | Western Blot |
| **α-syn** | α-synuclein |
| **β-III-tub** | β-III-tubulin |
| **ΔΨm** | Mitochondrial membrane potential |

Parkinson´s Disease (PD) is the second most common and complex neurodegenerative disorder, mainly characterized by the presence of cytoplasmic inclusions called Lewy Bodies, and the loss of dopaminergic neurons in Substantia Nigra *pars compacta*. Astrocytes constitute the most abundant glial subtype in the brain covering essential functions for brain homeostasis and neuronal health. It has been recently reported that dysfunction of the astrocyte biology in the midbrain can derive to the dopaminergic neurons damage and further PD spreading. In this study, we used two different models to mimic PD: an in vitro chimera with rat cells and human Lewy body extracts (LB) and human iPS-derived astrocytes from PD patients. Through the use of modern technologies like microfluidic, machine learning, and molecular characterization of a-syn oligomers (AS-PLA) we aimed to understand the role of astrocytes in the onset and spreading of the PD and to decipher the cellular mechanism that characterize the astrocyte metabolism in the pathology.

Using an *in vitro* chimera with rat cells and human LB extracts, we have confirmed that both rat neurons and astrocytes internalize exogenous hα-syn by endocytosis, resulting in an increase of neuronal toxicity but astrocyte resistance. Indeed, astrocytes exhibit an increase in lysosomal activity and activate mitochondrial metabolism in response to the internalization of exogenous hα-syn as shown by the increase of basal respiration and ATP production. Moreover, we have demonstrated that exogenous hα-syn can be transported intercellularly and that interestingly, when transported from astrocytes to neurons activate an apoptotic mechanism in neurons. We explain the activation of neuronal death because of the lower lysosomal activity in the neurons and by the activation of endogenous a-syn translation.

Finally, we have generated and characterized human iPS-derived astrocytes from PD patients carrying LRRK2$^{G2019S}$ mutation, which constitutes the most common mutation of the familiar forms of PD. These PD astrocytes display an atrophic morphology, with less complexity and altered mitochondrial functionality which results in an altered morphology and higher basal protein oxidation. As a consequence, PD astrocytes show a reduced mitochondrial metabolism and increased glycolitic activity. Finally, as a consequence of the alteration of astrocytic metabolism, we demonstrated

that PD astrocytes when co-cultured with healthy rat neurons increased the risk of neuronal death.

We can conclude that dysfunctional astrocytes cover an essential role in the onset and progression of PD. Both the accumulation of α-syn and the LRRK2$^{G2019S}$ mutation induce mitochondrial unbalance leading to cell autonomous and non-autonomous damage and final neuronal degeneration. This study proposes a new possible therapeutic target directed to sustain the astrocytic functionality. Further experiments are needed to establish the pathways that astrocytes directly distress to induce the dopaminergic death.

- Modern technologies like microfluidic, machine learning, and molecular characterization of a-syn oligomers (AS-PLA) have been used to decipher the role and cellular mechanism of the astrocyte in PD.

- In an *in vitro* chimera with rat cells and human Lewy body extracts (LB), rat astrocytes are resistant to hα-synuclein but increase neuronal toxicity following hα-syn transport to neurons.

- In human iPSc-derived astrocytes, atrophic morphology and unbalance of mitochondrial metabolism, morphology and localization constitute important hallmarks of $LRRK2^{G2019S}$ phenotype.

- Our results suggest that alteration of astrocytic metabolism and function that is reflected in atrophic morphology, can participate to the neuronal death and PD progression.

# Introduction

# 1. Parkinson´s Disease

## 1.1 Prevalence and symptoms

Parkinson´s Disease (PD) is the second most common and complex neurodegenerative disorder with unknown etiology. The first detailed description of Parkinson's disease was made almost two centuries ago by James Parkinson (An Essay on the shaking palsy, 1817). Nevertheless, the conceptualization of the disease is still debated.

Age is the principal risk factor for PD, being present in 1% of people over the age of 65 years and rising up to 3% at the age of 80. Even if it is idiopathic in most of the cases, between the 5 and 10% of the cases represent familial forms of PD. In these cases, an earlier onset is possible but the age remains an additional risk factor (Crosiers et al., 2011). Other risk factors are represented by the exposure to environmental toxins, such as 1-methyl-4-phenyl-1,2,3,6-tetrahy- dropyridine (MPTP) or paraquat, head trauma or sex (men have more than 50% more probability to develop PD) (Antony et al., 2013).

The clinical evolution of PD is characterized by bradykinesia, resting tremor, rigidity, and postural instability, being bradykinesia the necessary condition for the diagnosis (Ling et al., 2012). In addition to these motor symptoms, many patients experience a wide range of non-motor symptoms that sometimes even precede the typical movement disorder, such as constipation, hyposmia, sleep disturbances or depression (Tab.1).

| Motor symptoms of PD | Non-motor symptoms |
|---|---|
| Resting tremor | Constipation |
| Rigidity | Autonomic dysfunction |
| Bradykinesia | Impaired olfaction |
| Postural instability | Dementia |
| Festinating gait | Depression |
| Micrographia | Sleep disorders |
| Masked facies | Impulse control disorders |
| Retropulsion | Psychosis |
| Hypophonic speech | |

**Table 1**. **Clinical syndrome of PD.** Motor and non-motor symptoms (Jakel and Stacy, 2014).

Pathologically, two major hallmarks identify PD: the progressive death of dopaminergic neurons in the substantia nigra *pars compacta* (SNpc), leading to the depletion of dopamine (DA) release in the striatum (Mercuri and Bernardi, 2005), and the appearance of protein deposits called Lewy bodies (LB). The latter are abnormal eosinophilic protein deposits whose primary structural component is the misfolded α-synuclein (α-syn) (Spillantini et al., 1997; Ross and Poirier, 2004; Desplats et al., 2009; Obeso et al., 2010) (Fig. 1). These features make PD an irreversible and, at the present, an incurable disease.

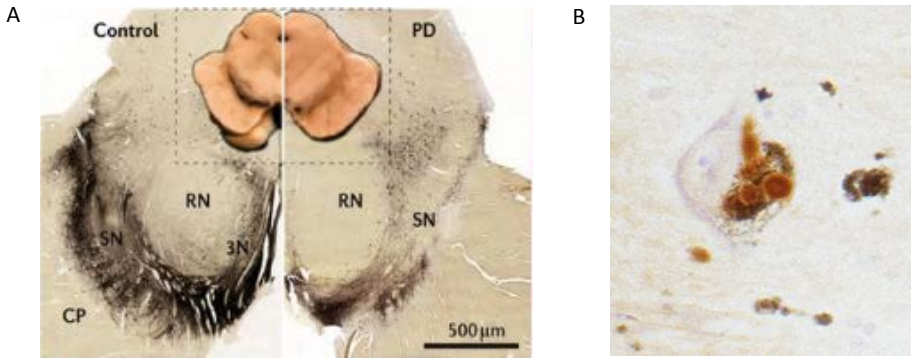


**Figure 1. Pathological hallmarks of PD.** A) Dopaminergic neuronal death in the SNpc and B) cytoplasmic inclusions, Lewy Bodies.

## 1.2 Treatments

Currently, all treatments for PD are palliative and not curative. Indeed, the therapy is dedicated to maximize patients´ quality of life and minimize disability.

Levodopa (L-dopa), the main dopamine precursor, is the most potent drug for controlling PD symptoms, particularly those related to bradikynesia. It alleviates the symptoms for approximately 5 years (Jankovic et al., 2002). After that time, the majority of the patients experience diverse adverse effects, predominantly motor fluctuations and dyskinesia (Jankovic et al., 2005). In addition to L-dopa, also dopamine agonists, catechol-o-metyltranspherase (COMT) inhibitors, or anticholinergic drugs may be used concomitantly depending on the clinical profile of the patient. Also neurological surgery has become a therapeutic strategy to ameliorate the PD

symptoms. Currently, deep brain stimulation (DBS) of the basal ganglia is considered the best alternative for disabling PD relative symptoms (Jankovic and Aguilar, 2008).

Finally, in the last couple of years, PD symptoms and tremor is reduced by using "High Intensitive Focused Ultrasound" (HIFU). This innovative technique is based on the inactivation of the subthalamic nucleus using high frequency ultrasound and is completely non-invasive and definitive (Bauer et al., 2014). In the last decade, several groups initiated cell therapy by fetal stem cells transplantation that ameliorated the symptoms after a short time evaluation but failed at longer time after the transplantation (Smith, 2016).

## 2. Alpha synuclein in Parkinson´s Disease

### 2.1 Alpha synuclein biology

α-Synuclein is a 14kDa protein composed of 140 amino acids and encoded by *SNCA* gene (Tamguney and Korczyn, 2018). It is composed of three domains, an α-helical amino terminus, a non-amyloid component (NAC), and an unstructured carboxy terminus. These domains are essential for the pathogenic progress observed in PD and other synucleinopathies. The amino terminus of α-syn forms an α-helical structure that binds to protein interactors or lipid membranes (Kim et al., 2014; Narkiewicz et al., 2014; Lawand et al., 2015).

Although the exact function of α-syn is unknown, its high concentration in presynaptic terminals (Volpicelli-Daley et al., 2011; Narkiewicz et al., 2014; Renner and Melki, 2014) and its co-localization with the reserve pool of synaptic vesicles (Lee et al. 2008), support the idea that α-syn may contribute to the cycling of synaptic vesicles. Suggested roles of α-syn are the modulation of vesicle pool size, mobilization or endocytosis (Bendor et al. 2013; Vargas et al. 2014).

Some studies suggest that α-syn is involved in the control of synaptic membrane processes (Bellucci et al., 2012) and participates in the control of neurotransmitter release via interactions with members of the SNARE family (Tsigelny et al., 2012). According to other studies, α-syn could also be transported in the nucleus (Goers et al. 2003; Huang et al. 2011) and modulate some mitochondrial transcription factors having a negative impact on mitochondria homeostasis (Desplats et al. 2012; Siddiqu et al. 2012).

However, the precise physiological functions of α-syn remain uncertain and studies are often conflicting (Luk et al., 2009).

Soluble α-syn is natively unstructured and monomeric. Emerging biophysical and biochemical studies have demonstrated that interaction between α-syn and lipids influences α-syn oligomerization and aggregation revealing the toxic function of the aggregates.

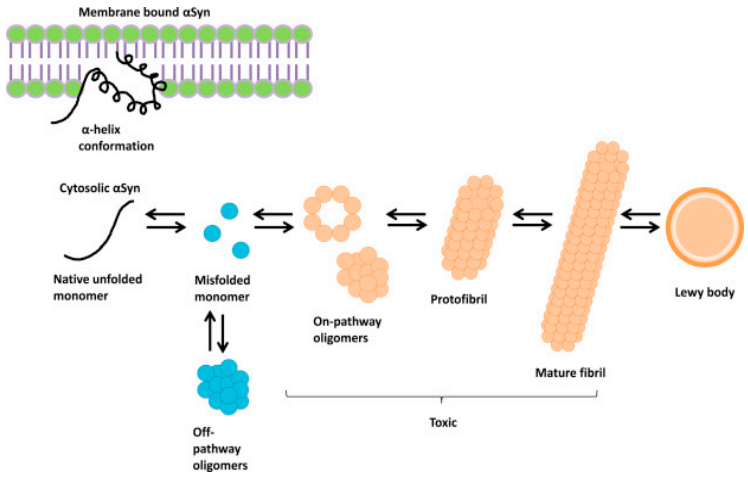


**Figure 2. Alpha synuclein aggregation stages.** Different stages of the aggregation of α-syn, from monomeric species to fibrils, through oligomers, the suspected toxic species (Mochizuki et al., 2018).

α-Syn is able to turn into oligomeric and/or fibrillar conformations in particular pathological conditions, including gene mutations of SNCA, decreased rate of clearance, oxidative stress, iron concentration, or posttranslational modifications

(Lawand et al., 2015; Sian-Hulsmann et al., 2015) (Fig. 2). In particular, posttranslational modifications of α-syn, such as phosphorylation (mostly in the serine residue S129J), ubiquitination, acetylation, sumoylation, and nitration, have been observed to alter the structure and function of α-syn, and are related to α-syn aggregation and neurotoxicity (Hodara et al., 2004; Kim et al., 2014; Hasegawa et al., 2017). Moreover, the three most common SNCA point mutations (A30P, E46K and A53P) accelerate α-syn aggregation *in vitro.* This suggests that α-syn is heavily implicated in the pathogenesis of PD, both in familial and sporadic cases (Smith et al., 2005; Angot et al., 2012).

### 2.2 α-syn mediated toxicity: Oligomers vs fibrils

To understand the pathological implication of α-syn in PD we must look at its conformation. As described by Spillantini and colleagues (1998) α-syn is one of the main proteic component of LB, but the pathological role of α-syn in PD is still debated (Bengoa-Vergniory et al., 2017). Surprisingly, Lewy bodies have been found in post-mortem brain of neurologically normal individuals over 60 with a high rate of approximately 10% (Frigerio et al., 2011; Parkkinen, 2005). Moreover, in some cases Lewy bodies found in patients correlate poorly with the severity of symptoms such as cognitive impairment and dementia. Finally, PD carrying familial mutations in the parkin gene and with the LRRK2$^{G2019S}$ mutation, show neuronal degeneration in the absence of Lewy body formation (Colosimo et al., 2003; Parkkinen, 2008).

These evidences suggest the importance of an ultrastructural study of α-syn conformations. *In vitro* and *in vivo* data suggest that oligomers may represent toxic conformations of the protein. For example, α-syn oligomers generated in *vitro* or by recombinant overexpression may induce cell death in human H4 neuroglioma cells (Outeiro et al., 2008; Bengoa-Vergniory et al., 2017). Moreover, mice overexpressing the artificial α-syn variants E57K and E35K, engineered to promote oligomer formation, displayed a more severe loss of dopaminergic neurons as compared to regular α-syn transgenic mice, overexpressing wild-type α-syn (Winner et al., 2011).

More recent studies proposed that post-fibrillization of α-syn C-terminal truncation mediated by calpains 1 and 2 plays critical roles in fibrillation, cell toxicity and LB maturation (Mahul-Mellier et al., 2018). These results highlight the importance of developing, more immunological tools to detect LB in which α-syn is already truncated (most of the commercial antibodies are directed to the C-terminal) and encourage to develop therapeutic strategies based on targeting the C-terminus of α-syn.

Apart from causing general cellular toxicity, α-syn oligomeric forms have been related with impairments in other cellular functions, such as mitochondrial respiration, or intracellular degradation, and with non-cell autonomous responses, causing a glial mediated neuroinflamation (Fig. 3).

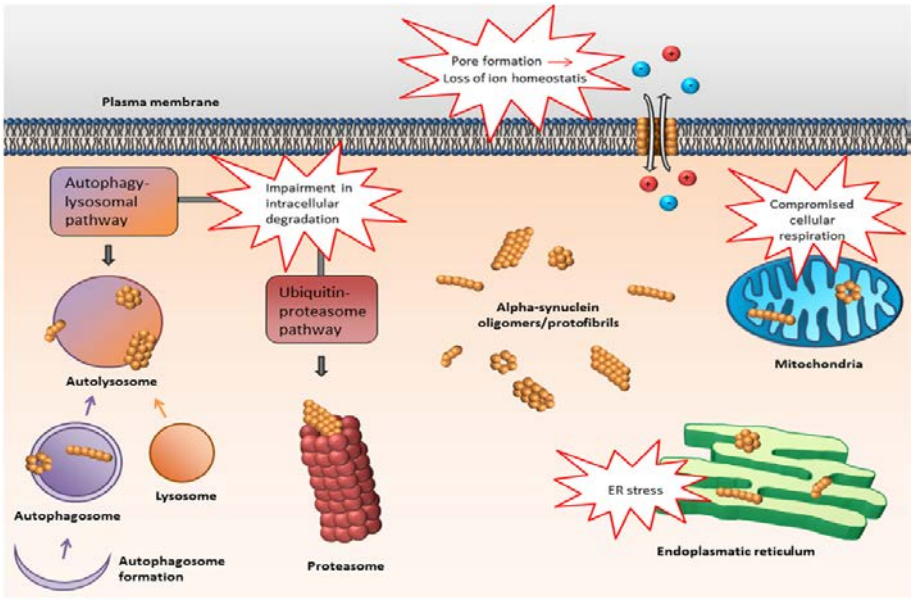


**Figure 3. Intracellular targets for α-syn-mediated toxicity**. α-syn oligomers may mediate toxicity via several intracellular targets. Mainly, impairment of various protein degradation pathways as well as damage to mitochondria (Ingelsson, 2016).

### 2.2.1 Mitochondrial dysfunction

Mitochondria play a fundamental role in energy metabolism being their primary function to provide energy for intracellular metabolic pathways. There is huge

evidence for mitochondria impairment in PD. Parker and colleagues (2008) found that mitochondrial metabolism in the substantia nigra of postmortem PD brain display a deficient complex I activity. Mitochondrial alteration via complex I deficit was also demonstrated in highly purified mitochondria from the frontal cortex of PD patients (Parker et al., 2008). Furthermore, high levels of mtDNA deletions have been observed in dopaminergic neurons from the substantia nigra of post- mortem human brains from aged individuals and idiopathic PD patients (Bender et al., 2006; Reeve et al., 2008).

Otherwise, mitochondrial morphology is disrupted by α-syn oligomers, causing fragmentation of these organelles in SH-SY5Y cells (Plotegher et al., 2014). More recently, it has been found that astrocytes can incorporate α-syn oligomers and degrade it via the lysosomal pathway. Nevertheless, if this pathway becomes saturated it may lead to mitochondrial fragmentation and toxicity (Lindström et al., 2017). Moreover, mutant and wild-type α-syn interacts with mitochondrial cytochrome c oxidase, a key enzyme of the mitochondrial respiratory system (Elkon et al., 2002), and α-syn is present in the membrane of mitochondria in normal dopaminergic neurons (Li et al., 2007). Under overexpression conditions, α-syn may translocate to the mitochondria and cause enhanced toxicity in response to subtoxic concentrations of mitochondrial toxins (Shavali et al., 2008).

All these results suggest that mitochondrial defects observed in some parkinsonian pathologies can be triggered by α-syn oligomers or by other PD linked mutations, such as LRRK2, as commented later in this Introduction.

### 2.2.2 Lysosomal degradation defects

Degradation of α-syn can be maintained via multiple degradative routes. However, because of structural constraints, the proteasome is unable to degrade protein macro-aggregates, which are instead efficiently disposed of through the autophagy-lysosomal pathway (Isidoro et al., 2009). There are several evidences in vivo and in vitro that lysosomal dysfunction can lead to increased toxicity. Thus, lysosomal

dysfunction can accelerate exosomal α-syn release inducing α-syn inclusion formation and propagating its toxicity to the neighboring cells (Alvarez-Erviti et al., 2011).

Moreover, mechanistic studies using the 1-methyl-4-phenyl1,2,3,6-tetrahydropyridine (MPTP) mouse model of PD have reported the ROS production mediated by Complex I inhibition. This induced abnormal lysosomal membrane permeabilization (LMP) with further lysosomal dysfunction, lysosomal depletion and autophagosome accumulation. (Dehay et al., 2010; Vila et al., 2011).

In addition, several indirect observations have suggested a possible link between cathepsin D, a lysosomal protein, and α-syn degradation. In cathepsin D deficient mice, extensive accumulation of endogenous α-syn was reported (Quiao et al., 2008). Conversely, the transgenic overexpression of cathepsin D decreased the accumulation of α-syn aggregates and protected the dopaminergic neuronal cells from toxicity induced by overexpression of α-syn. In astrocytes, cathepsin D mediated proteolysis is also implicated in the pathogenesis and progression of PD, even it has not been fully addressed yet. In fact, astrocytes exposed to the herbicide paraquat, a parkinsonian neurotoxin, show defective formation of autophagosome, reduced viability and inability to protect dopaminergic neurons from an oxidative stress (Janda, 2015). Predictably, astrocytes lacking cathepsin D are prone to succumb under oxidative stress and cannot protect dopaminergic neurons (Vidoni et al., 2016).

### 2.3 α-syn transmission: prion-like hypothesis

Prion diseases are fatal transmissible neurodegenerative disorders with genetic, sporadic, and acquired forms (Acquatella-Tran Van Ba et al., 2013). Prion protein (PrP), is insensitive to the chemical therapy or physical prevention that inhibits ordinary infectious agents. Cellular prion protein ($PrP^{c}$) is ubiquitously expressed on the surface of cell membranes and dominantly located in neurons. However, the specific biological functions of $PrP^{C}$ are still unknown. The central causative event in neurodegeneration is the conversion of the normal form $PrP^{C}$ into a protease-resistant, disease-associated form $PrP^{Sc}$, known as template conformation change.

Many neurodegenerative diseases like e.g. PD, share key prion-like mechanisms for protein transmission and disease spreading.

According to Braak's hypothesis (Braak et al., 2003) abnormal α-syn is spread between anatomically interconnected systems (Recasens and Dehay, 2014; Braak and Del Tredici, 2016). Braak described the presence of pathological α-syn aggregates in different brain regions, such as caudal raphe nuclei, coeruleus–subcoeruleus complex and SN. Based on this finding, he proposed the classification of PD progression in six stages that follow a caudo-rostral pattern. Although other groups confirmed the Braak hypothesis (Bloch et al., 2006; Dickson et al., 2010; Halliday et al., 2012) the clinical classification for sporadic PD is not uniform (Burke et al., 2008; Alafuzoff et al., 2009). According to the prion-like hypothesis, α-syn can be transported also from the periphery to the brain, as suggested e.g. in the "gut-to-brain" hypothesis. Holmqvist and colleagues demonstrated that human α-syn found in the SN of PD patients and distinct recombinant α-syn forms (including monomers, oligomers and fibrils) can be transported via the vagal nerve to the CNS after the injection into the intestinal wall of WT adult rats (Holmqvist et al., 2014). Likely, inoculation of α-syn PFF into the mouse gastrointestinal tract induced α-syn pathology similar to the early stages of PD, supporting the "gut-to-brain" hypothesis (Uemura et al., 2018).

The prion-like hypothesis proposes that spreading of α-syn can occur by a trans-cellular way, whose mechanisms are still under investigation.

Transgenic mice overexpressing human α-syn, transplanted with neural stem cells experienced α-syn immunoreactivity in 15% of the grafted cells (Desplats et al., 2009). In addition, dopaminergic neurons grafted into the striatum of mice over-expressing human α-syn, exhibited human α-syn immunoreactivity 6 months after transplantation (Hansen et al., 2011), thus confirming the transfer of human α-syn from host-to-graft in vivo. The authors of this study suggested that the mechanism of α-syn uptake, in terms of monomers, oligomers and fibrils, could be by endocytosis.

The first tentative evidence to demonstrate the transcellular propagation of α-syn was in the autopsy of PD patients transplanted with embryonic brain cells into the striatum to replace degenerated dopaminergic neurons (Kordower et al., 2008; Hansen et al., 2011). Over 10–16 years after the graft, examination of autoptic brain tissues showed pathologic α-syn inclusions in the cells derived from the grafting (Kaufman and Diamond, 2013; Goedert et al., 2014).

The suggested mechanisms of α-syn transmission go from classic exocytosis/endocytosis, tunneling nanotubes (TNTs), synapses or synapse-like structures, and several receptors (Goedert et al., 2010; Dunning et al., 2012; De Cecco and Legname, 2018). Moreover, α-syn can also be transported, not only between neurons, but also between glial cells, as demonstrated in in vivo model and organotypic (Reyes et al. 2014; Thakur et al. 2017; Loria et al. 2017). In particular, astrocytes cover an important role in sequestering and degrading α-syn assemblies (Cavaliere et al., 2017; Ramos-Gonzalez, unpublished data; Loria et al., 2017). Indeed, a recent study has demonstrated that although astrocytes take up a significant amount of aggregated α-syn (i.e. α-syn oligomers) for subsequent degradation, their degradative capacity can become overwhelmed, resulting in limited clearance of α-syn and its associated toxic cellular effects (Lindström et al. 2017).

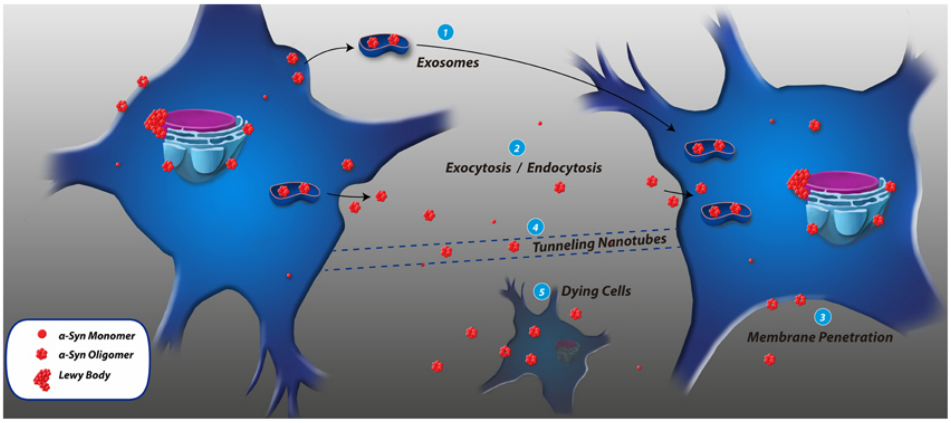


**Figure 3. Cell to cell transmission of α-syn.** Many different transmission mechanisms have been proposed for α-syn, being the most accepted (1) exosome mediated transmission, (2) receptor mediated endocytosis, (3) membrane penetration by pore formation, (4) tunneling nanotubes and (5) the reservoirs generated by dying cells (Gallegos et al., 2015)

Altogether, these data provide evidence for the "infectivity" of the α-syn, a criterion that defines a prion disease. However, the nature and mechanisms of α-syn prion-like properties is not yet well understood to refer to Parkinson´s disease as a prion disease.

## 3. Genetics

### 3.1 PD related mutations

In addition to age and environmental toxins, genetic factors may also constitute a risk factor for PD. In 5–10% of cases, PD is manifested as a Mendelian form with autosomal dominant or recessive inheritance. Currently, 28 distinct chromosomal regions are linked to PD (Klein & Westenberger, 2012). For only six of these regions, the underlying genes that cause common monogenic forms of PD have been identified, namely *snca* (α-synuclein) and *lrrk2* for autosomal dominant PD, and *pink1*, *park7* (DJ-1), *atp13a2* (ATPase type 13A2), and *park2* (Parkin) for autosomal recessive PD (Fig. 4).

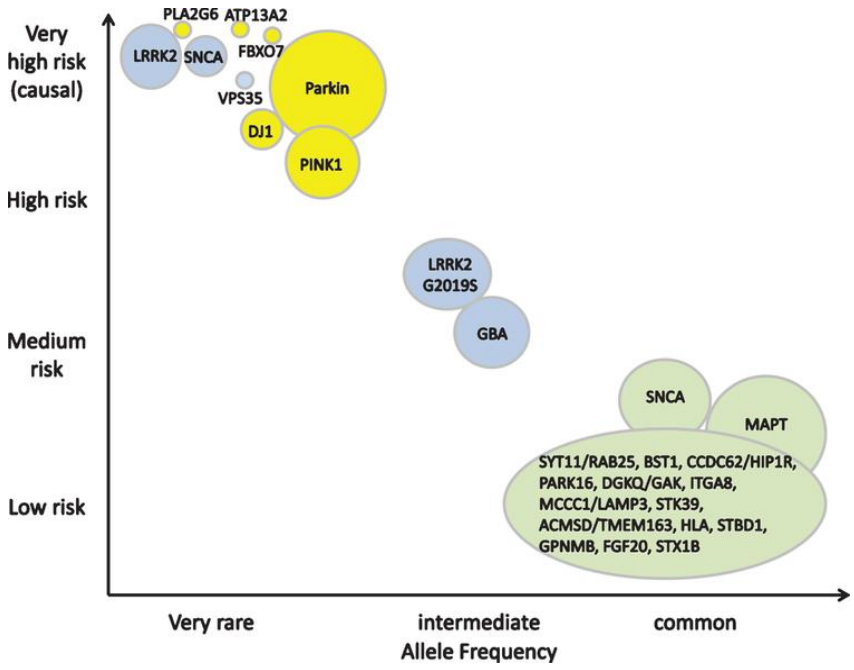


**Figure 4. Parkinson´s disease related mutated genes**. The most common mutations are usually associated with a lower risk of developing the disease, while the least common ones usually confer high risk of developing Parkinson's disease (Thomas, 2015).

Mutations on *snca* are fully penetrant, and typically cause fast-progressing early-onset to late-onset PD, with widespread and abundant Lewy body formation as a pathophysiological hallmark. In contrast, LRRK2 mutations show variable penetrance, approximately 30–70% at age 80 years, and typically cause late-onset PD, mostly without dementia, and in most cases typical Lewy body pathology (Singleton et al., 2013; Ozelius et al., 2006; Goldwurm et al., 2007). Incomplete penetrance or variable expression often cause problems in assessing whether PD is caused solely by genetic susceptibility or is modified by environmental factors. (Antony et al., 2013).

### 3.2 LRRK2$^{G2019S}$ mutation.

Leucine-rich repeat kinase 2 (LRRK2) is a large protein with dual kinase and GTPase activity that is encoded by the *lrrk2* gene (Luciano et al., 2010). Mutations in LRRK2 are the most common genetic cause of PD, and result in a patient phenotype similar to the idiopathic disease (Lobbestael et al., 2012). LRRK2 is expressed in neurons, astrocytes, and microglia (Reyniers et al., 2014) and is associated with a large variety of functions, both in terms of its physiological and cellular roles (Wallings et al., 2015) (Fig. 5).

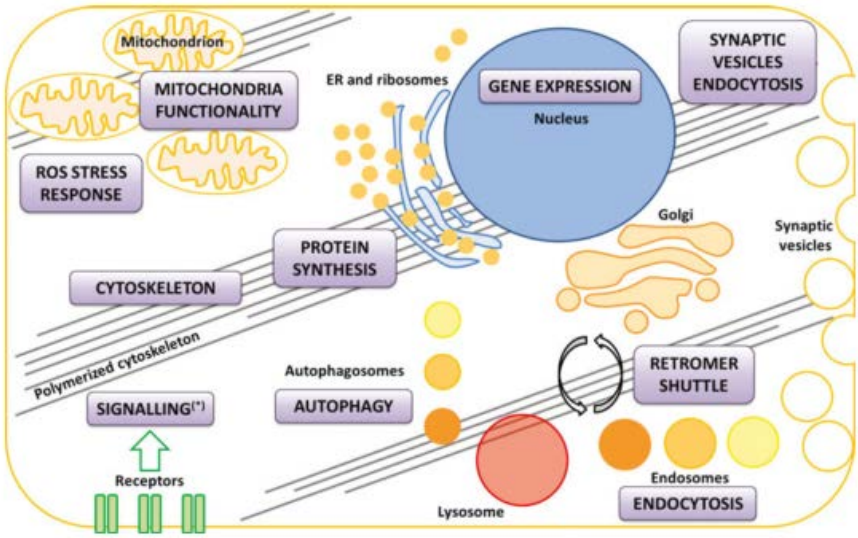


**Figure 5. Cell processes associated with LRRK2**. Representation of the cellular processes (boxes) that have been associated with LRRK2 function in physiology and/or disease. (Wallings et al., 2015)

The G2019S mutation is the most frequent pathogenic mutation in the overall LRRK2-PD population (Singleton et al., 2013). It occurs in the kinase domain of LRRK2, leading to an increase in kinase activity (West et al., 2007). This protein is involved in many different cell signaling pathways participating in mitochondrial functionality, citoskeletal dynamics, response to ROS production or autophagy. It is implicated in the autophagy-lysosome pathway in many models, not only in neurons but also in astrocytes (Xing et al, 2013; Greggio et al., 2008). I describe below the role of LRRK2 in the cellular processes that are discussed in this thesis.

### 3.2.1 LRRK2$^{G2019S}$ and mitochondrial respiration

Wild type LRRK2 interacts with a number of key regulators of mitochondrial fission/fusion, co-localizing with them either in the cytosol or on mitochondrial membranes, indicating its multiple regulatory roles (Stafa et al., 2013; Wang et al., 2012).

LRRK2 mutation causes mitochondrial dysfunction. Thus, fibroblasts from PD patients carrying the G2019S mutation showed abnormal mitochondrial morphology (Mortiboys et al., 2010). Similarly, wild-type LRRK2 overexpression in SH-SY5Y cells caused mitochondrial fragmentation, which was further enhanced by the R1441C and G2019S mutations (Wang et al., 2012). Moreover, overexpression of LRRK2$^{G2019S}$ mutation in same cells caused mitochondrial uncoupling, leading to reduced membrane potential and increased oxygen consumption (Papkovskaia et al., 2012). The G2019S mutation in LRRK2 is also implicated in defective mitophagy as it delays the digestion of dysfunctional mitochondria and the initiation of mitophagy (Hsieh et al., 2016). These alterations were found also in G2019S transgenic mice where ultrastructure examination showed the accumulation of damaged mitochondria in neuronal soma, which is consistent with altered mitophagy in aged mice (Ramonet et al., 2013).

### 3.2.2 LRRK2$^{G2019S}$ and cytoeskeletal dynamics

Many studies have established a connection between LRRK2 and both microtubules (MTs) and filamentous actin (F-actin), with multiple cytoskeletal- related proteins. A high-throughput screening to decipher LRRK2 interactome revealed proteins involved in actin filament assembly, organization, rearrangement, and maintenance, suggesting that the biological function of LRRK2 is linked to cytoskeletal dynamics. Indeed, the same study revealed LRRK2 de novo binding to F-actin and its ability to modulate its assembly in mouse primary dopaminergic neurons *in vitro* (Meixner et al., 2011). This suggests that morphological changes and abnormalities in neurite outgrowth and branching may be consequences of LRRK2-modulation of cytoskeletal dynamics.

However, the possible role of LRRK2 in cytoskeletal dynamics is intriguing, not only because it could straightly recapitulate morphological alterations observed in cellular models of LRRK2, but also because it raises the possibility that LRRK2 may be involved in development and even govern different functions in development and adult life (Wallings et al., 2015).

## 4. Roles of astrocytes in CNS

Astrocytes represent the most abundant glial cell in the CNS being responsible for a wide variety of complex and essential functions implicated in preserving the integrity of the brain.

Astrocytes form a very heterogeneous population, not only morphologically but also because of their region specificity. The main classification of astrocytes distinguishes two major groups, protoplasmic and fibrous astrocytes. Protoplasmic astrocytes are found in the grey matter and their processes contact both synapses and blood vessels. They are much ramified, with uniformly distributed processes. Fibrous

astrocytes are located in the white matter and they contact the nodes of Ranvier and the blood vessels and are less ramified than protoplasmic astrocytes (Fig. 6).

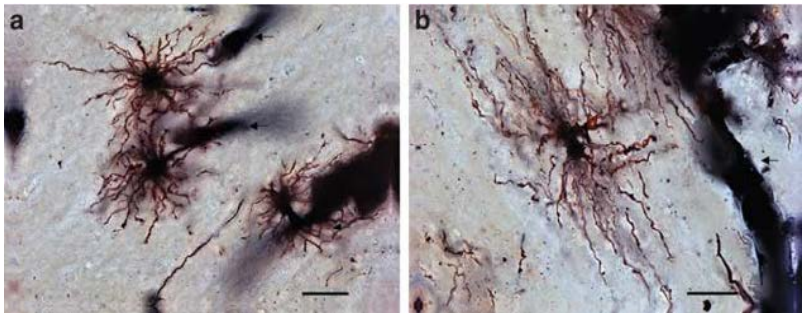


**Figure 6. Classification of astrocytes.** Based on their shape, antigen phenotype, and location, two main types are distinguished; (a) protoplasmic astrocytes, much ramified, with uniformly distributed processes and (b) fibrous astrocytes, less ramified (Torres Platas et al., 2011).

The structure of the astrocyte cytoskeleton is supported by the network of intermediate filaments. The fundamental component of these filaments is glial fibrillary acidic protein (GFAP) that is upregulated in brain damage and degeneration (Middeldorp & Hol, 2011). In addition to their structural properties, they may play other roles having to do with the transduction of biomechanical and molecular signals.

During the last 20 years, a wide variety of functions have been attributed to these cells. Astrocytes primarily support neuronal activity and function by providing important growth factors, or supporting neuronal metabolism through the conversion of glucose to ATP and glutamine to glutamate from the peripheral blood (Joe et al., 2018). They directly participate in the “tripartite synapse” by harboring each astrocyte as many as two million synapses (Oberheim et al., 2009). Moreover, they support the neuronal activity by controlling extracellular ion balance and neurotransmitter homeostasis. Table 2 lists the various functions of this glial cell type in the CNS, including biochemical support of endothelial cells, provision of nutrients to the nervous tissue, and regulation of neurogenesis and brain wiring (Vasile, 2017).

| Astrocyte functions |
| --- |
| Function |
| Blood-brain barrier (BBB) induction and maintenance |
| Metabolic support |
| Providing energy to neurons |
| Regulation of extracellular pH |
| Synthesis of precursor for glutamate and GABA production |
| Release of cytokines and chemokines |
| Forming “glial scar” after injury |
| Brain homeostasis |
| Brain energy metabolism |
| Modulate extracellular glutamate level |
| Spatial buffering |
| Neuroinflammation |

**Table 2. Biological functions of astrocytes** (Martín Jiménez, 2017).

### 4.1 Neuronal homeostasis and synaptic activity

The participation of astrocytes in neuronal homeostasis and specifically in synapse function was firstly accepted with the description of the “Tripartite synapse” by the laboratory of PG Haydon in 1999.

Synaptic plasticity is a fundamental mechanism that supports brain function (Buzsáki and Chrobak, 2005). Among the different factors that regulate synaptic plasticity, glial cells are key players in maintenance of synapse homeostasis (Eroglu and Barres, 2010). Gliotransmitters (GT) released by astrocytes modulate the synaptic activity through vescicular-dependent endocytosis, further activating intracellular $Ca^{2+}$ signals.

Astrocytes predominantly show potassium ($K^+$) conductance (Kuffler and Nicholls, 1966; Hertz et al., 2013), which is mainly mediated by Kir4.1, aquaporin-4, chloride channels, or $Na^+$-$Ca^{2+}$ exchangers (Haj-Yasein et al., 2011b; Halnes et al., 2013). This allows the rapid uptake of $K^+$ from the synaptic cleft and redistribution of $K^+$ in the extracellular space during neuronal activity (Kuffler and Nicholls, 1966; Seifert et al.,

2018). Furthermore, Aquaporin-4, that transports water, and $Na^+$-$Ca^{2+}$ exchangers are involved in the maintenance of a correct pH surrounding the synapse (Obara, 2008).

Glutamate, gamma-aminobutyric acid (GABA) and ATP are the most studied gliotransmiters. Astrocytic membranes are enriched in glutamate and GABA transporters (GAT) that are differentially expressed throughout the adult brain. These transporters serve as an efficient mechanism for clearing these neurotransmitters (NTs) from the extracellular space after neuronal activity (Borden, 1996; Bergles and Jahr, 1997; Danbolt, 2001). Glutamate transporters, concretely GLAST (EAAT1) and GLT1 (EAAT2) are responsible for removing 80% of glutamate released from the presynaptic neurons, being just 20% of glutamate taken up by post-synaptic glutamate transporters (Swanson, 2005). In astrocytes, glutamate can be metabolized to glutamine by glutamine synthetase (GS), then being released to the extracellular space to be taken up by neurons and used to resynthesize glutamate or GABA (Bergles& Jahr, 1998). GLT-1 and GLAST deficient rats developed neurodegeneration and progressive paralysis (Rothstein et al., 1996). Regarding to GABA transporters, GAT-3 is the most abundant GAT in astrocytes and is localized in astrocytic processes that are adjacent to synapses and cell bodies. Activation of GAT-3 results in a rise in $Na^+$ concentrations in hippocampal astrocytes and a consequent increase in intracellular $Ca^{2+}$ through the action of $Na^+$/$Ca^{2+}$ exchangers (Doengi et al., 2009). Thus, GABA-uptake by astrocytic GAT-3 can stimulate the release of ATP/adenosine that contributes to downregulation of the excitatory synaptic transmission, and provides a mechanism for homeostatic regulation of synaptic activity (Boddum et al., 2016).

### 4.2 Energy supply and metabolism

Astrocytes contribute to proper metabolic function in the CNS. Since their projections reach blood vessels, astrocytes take up glucose from circulation and provide energy metabolites to neurons (Guillamon-Vivancos et al., 2015). Neuronal cells show a great consumption of energy but lack energy store capacity (Barros et al., 2011) In the brain, energy is stored in form of glycogen, which is localized almost

exclusively in astrocytes, where glycolysis appears to have a larger enzymatic capacity than oxidative metabolism (Abe et al., 2006).

Astrocytic glycogen utilization can support neuronal activity in hypoglycemic conditions and through transient events where neuronal activity is increased (Brown & Ransom, 2007; Ransom & Fern, 1997; Suh et al, 2007). Moreover, while glycogen mobilization may also fulfill the astrocytes' own metabolic needs (Sickmann et al. 2009; Walls et al., 2009), glycogen breakdown typically results in lactate production and release in the extracellular space to provide neuronal energy needs (Walls et al., 2009, Dringen et al., 1993). Astrocytic glycogen mobilization is required to maintain glutamatergic synaptic transmission (i.e., neurotransmitter release) in neuron-astrocyte co-culture models (Sickmann et al., 2009; Mozrzymas et al., 2011). Glycogenolysis is facilitated by the lack of energy substrates (Gordon et al., 2008) and by elevated neural network activity (Cruz & Dienel, 2002; Swanson, 1992).

There is evidence suggesting that astrocytes have a greater metabolic plasticity than neurons. Astrocytes respond to NO with an increase in glucose metabolism through the glycolytic pathway, thereby limiting the fall in ATP levels and preventing apoptosis. In neurons, however, this response does not seem to be present, and a similar NO challenge causes a massive ATP depletion, leading to apoptosis (Almeida et al., 2001). Furthermore, metabolic astrocyte-neuron interactions (in particular through lactate release by astrocytes) also influence higher brain functions, such as long-term memory formation (Suzuki et al., 2011).

### 4.3 Homeostasis of Reactive Oxygen Species

Neuronal energy metabolism, which relies entirely on oxidative phosphorylation (Bélanger et al., 2011), constantly generates a high amount of reactive oxygen species (ROS) that the brain needs to scavenge to avoid cellular damage. This feature makes astrocytes as cellular sentinels of neuronal energy metabolism (Dringen et al., 2000). Astrocytes have significantly higher levels of various antioxidant molecules and ROS-detoxifying enzymes compared to neurons, including glutathione, ascorbic acid, heme-

oxygenase 1, glutatione peroxidase, glutathione S transferase, catalase, and thioredoxin reductase (Shih et al., 2003; Dringen, 2000; Belanger and Magistretti, 2009; Wilson, 1997). In fact, in a co-culture system, astrocytes can protect neighboring neurons from toxic doses of NO, H2O2, superoxide anion combined with NO, iron, or 6-hydroxydopamine (Wilson, 1997; Vargas and Johnson, 2009; Dringen, 2000; Belanger and Magistretti, 2009), suggesting that neurons are dependent upon the high antioxidant potential of astrocytes for their own defense against oxidative stress.

In the presence of astrocytes, neurons produce high levels of glutathione *in vitro*. Hence, removal of astroglia from the culture prevents neuronal synthesis of glutathione and facilitates ROS toxicity (Dringen et al., 1999; Makar et al., 1994). Astroglial antioxidant capacity is also mediated by ascorbic acid, the reduced form of vitamin C. Astrocytes represent the reservoir for ascorbic acid (Covarrubias-Pinto et al., 2015). Moreover, they are able to accumulate the dehydroascorbic acid derived from ROS oxidation and released by neurons and reduce it (using glutathione) to ascorbic acid (Rice, 2000; Winkler et al., 1994), avoiding ROS toxicity.

Unlike neurons, astrocytes rely on glycolysis for energy generation (Herrero-Mendez et al., 2009) and, as a consequence, have a loosely assembled mitochondrial respiratory chain that is associated with a higher generation of mitochondrial reactive oxygen species (ROS) (Lopez-Fabuel et al. 2016). However, whether this abundant natural source of mitochondrial ROS in astrocytes fulfils a specific physiological role is unknown. Very recently, Vicente-Gutierrez and colleagues (2019) found that astrocytic mitochondrial ROS regulates glucose utilization via the pentose-phosphate pathway and glutathione metabolism, which modulates the redox status and potentially the survival of neurons. This provides further molecular insight into the metabolic cooperation between astrocytes and neurons and demonstrates that mitochondrial ROS are important regulators of physiology *in vivo* (Vicente Gutierrez et al., 2019).

## 5. Astrocytes in PD

According to the role of astrocytes in neuronal metabolism and survival, it becomes clear that an alteration of astrocyte function can contribute to neuronal degeneration. The importance of astrocytes in dopaminergic neurodegeneration becomes more evident as SN has a relatively low number of astrocytes (Von Bartheld et al., 2016) lowering the threshold of metabolic support to the neurons.

### 5.1 α- Syn mediated pathology in astrocytes

In postmortem PD brains, α-syn-positive inclusions were found in astrocytes as well as in neurons (Braak et al., 2007 ; Hishikawa et al., 2001; Wakabayashi et al., 2000), raising the question if astrocytes can uptake α- syn secreted by neurons. This hypothesis has been discussed and demonstrated extensively (Braidy et al., 2013; Lee et al., 2010; Rannikko et al., 2015; Fellner et al., 2013) indicating the TLR4-independent endocytosis pathway as one of the main mechanisms (Rannikko et al., 2015; Fellner et al., 2013).

The accumulation of α-syn in astrocytes generates an imbalance in the support of neuronal metabolism and synaptic function (Fig. 7). Thus, specific *in vivo* overexpression of mutant SNCA in astrocytes causes movement disorders and developed astrogliosis before the onset of symptoms (Gu at al., 2010). The affected astrocytes exhibited decreased expression of the glutamate transporters GLAST1 and GLT1 (Gu at al., 2010) and abnormal localization of the water channel aquaporin-4 (AQP4), which is involved in blood–brain barrier function and water transport (Simard et al., 2003).

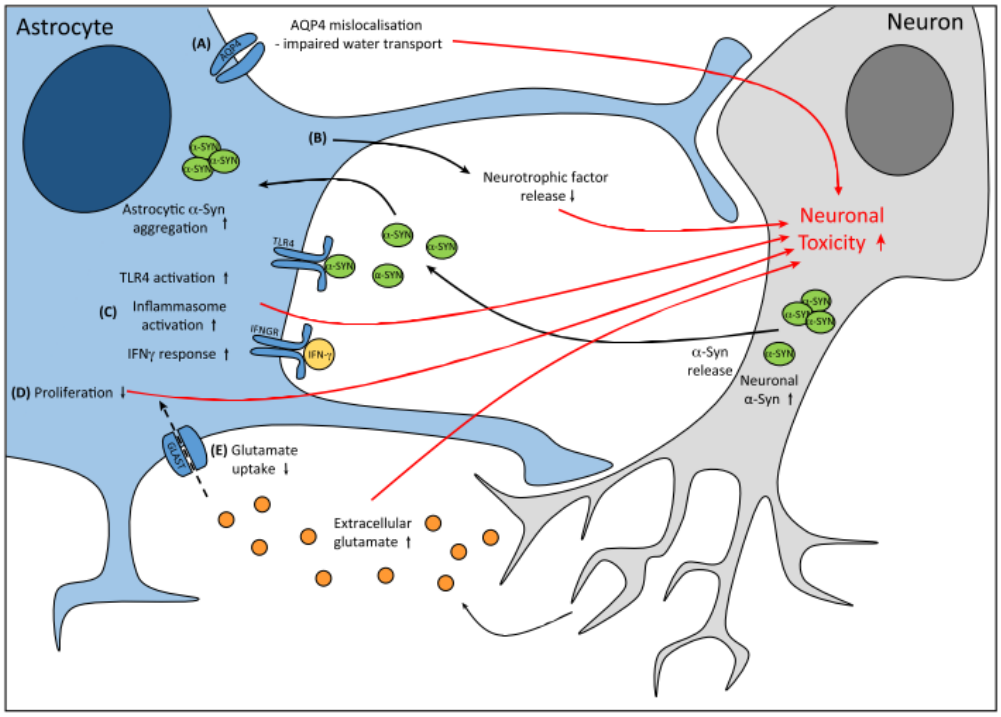


**Figure 7. Dysfunctional Astrocytes Contribute to Neuronal Toxicity**. Astrocyte dysfunction elicits neuronal toxicity via five main mechanisms. (A) AQP4 water channels are mislocated away from the astrocyte end-feet, resulting in impaired water transport. (B) neurotrophic factor release is decreased, (C) inflammatory signaling increases (D) astrocyte proliferation is impaired, and (E) Glutamate uptake is reduced, potentially resulting in increased extracellular glutamate and, therefore, neuronal excitotoxicity (Booth et al., 2017).

One of the consequences of α-syn accumulation in astrocytes is mitochondrial dysfunction. For example, in human primary astrocytes α-syn can accumulate into the mitochondria causing reduced oxygen consumption and ROS generation (Braidy et al., 2013). In a co-culture system of mouse primary neurons, astrocytes and oligodendrocytes, α-syn oligomers induced mitochondrial damage following fragmentation. Expression patterns of the fusion protein Mitofusin 1 and the fission protein Drp1, were clearly affected in oligomer exposed cells, indicating a disturbance of the mitochondria fission-fusion dynamics. All these defects lead to an increase in neuronal degeneration some days after exposure to toxic α-syn (Lindstrom et al., 2017). In fact, dysfunction of mitochondrial complex I, the primary site of redox reactions, can be the primary source of pathogenic ROS and can contribute to PD onset and spreading (Jacobson & Duchen, 2002). Consistent with these evidences,

postmortem analyses showed loss of complex I activity and oxidative damage in the brain of sporadic PD patients (Keeney, et al 2006).

As key actors in the neuroinflammation, astrocytes can contribute also to the production and release of proinflammatory cytokines like IL-6 and TNF-α (Fellner et al., 2013). As a result of the neuroinflammatory process, astrocytes become reactive as demonstrated in animal models and in SN and striatum of PD patients, increasing the expression level of IL-6 and TNF- α and increasing the risk of neuronal degeneration.

### 5.2 Impact of PD gene mutations in astrocytes

In addition to pathological α-syn, there are other PD-associated genetic risk factors of genes expressed in astrocytes, such as *park2, park7, gba, lrrk2, pink1* and *nr4a2*.

PINK1 and PARK mutations are mostly loss-fuction mutations. Proliferation of astrocytes in the brain is controlled, at least in part, by EGFR signaling, and further investigation showed that *pink1* regulates EGFR protein levels via an AKT/p38-dependent pathway. Similarly to *pink1*, Parkin has a role in astrocyte proliferation, as demonstrated by the decreased proliferation of Park2-KO astrocytes (Solano et al., 2006; Solano et al., 2008). Moreover, Park2-KO astrocytes alongside other glial cells, but no neurons, had increased levels of damaged mitochondria (Schmidt et al., 2011).

Like Parkin, PINK1, DJ-1, and LRRK2 are also implicated in the regulation of mitochondrial function and glucose metabolism (Dodson & Guo, 2007; Giasson, 2004; Saha et al., 2009). Thus, expression of PINK1 mutant decreased ATP generation, decreased oxygen consumption, and increased ROS production (Amo et al, 2011). Parkin may also regulate glycolysis since it directly regulates pyruvate kinase M2, a glycolysis rate-limiting enzyme (Liu et al, 2016). PINK1-knockout (KO) astrocytes exhibit reduced mitochondrial mass, decreased membrane potential, lower glucose uptake, and increased intracellular ROS levels (Choi et al., 2013). In addition, LRRK2 regulates vulnerability to mitochondrial dysfunction in *C. Elegans* (Saha et al., 2009). In

astrocytes, these genes regulate mitochondrial function and glucose metabolism. Moreover, LRRK2 kinase activity increases the trafficking to the membrane of autophagic vesicles of LC3 in primary mouse astrocytes (Ji et al., 2007). This may be indicative of either induction of autophagosome formation or inhibition of autophagosome/autolysosome degradation. Furthermore, expression of GFP-LRRK2 mutants (R1441C, Y1699C, and G2019S) in primary mouse astrocytes results in an increase in lysosome size.

Parkin, α-synuclein, and LRRK2 also regulate endocytosis and/or phagocytosis. Parkin deficiency promotes lipid raft-dependent endocytosis through the accumulation of caveolin-1 in mouse embryonic fibroblasts (Cha et al., 2015). In addition, LRRK2 regulates microglial phagocytic activity in a kinase dependent manner (Maekawa et al., 2016; Marker et al., 2012).

PD related genes might regulate also the microglial surveillance function. LRRK2 interacts with several actin-regulating proteins regulating actin dynamics (Chan D et al., 2011; Parisiadou et al., 2009; Meixner A et al.,2011) which are necessary for microglia continuous movement of their processes to survey microenvironments of the brain (Nimmerjahn et al., 2005; Davalos et al., 2005; Hines et al., 2009). LRRK2-KO BV2 microglia cells are morphologically different from WT microglia and are highly motile even in the absence of any stimulator (Choi et al., 2010; Ma et al., 2016). LRRK2 regulates microglial motility in a kinase-dependent manner through the inhibition of FAK, a critical player in cell movement (Ilić et al., 1995). Furthermore, $LRRK2^{G2019S}$ mutation retards microglial response to injury (Choi et al., 2010). Since defects in the ability of microglia to isolate injured brain sites increase damage (Hines et al., 2009) microglial defects caused by the G2019S mutation may contribute to the development of PD.

### 5.3 Reactive astrogliosis and neuroinflamation

One of the possible trigger factors of PD is the excessive release of oxygen free radicals during enzymatic dopamine breakdown, impairment of mitochondrial

function, loss of trophic support, abnormal kinase activity, and disruption of calcium homeostasis. In addition, inflammation, that has long been considered secondary to neuronal damage, is considered to have a role in the progression of the disease. Indeed, activation of microglia in the SNpc and striatum is profound in various types of PD animal models (Leal et al, 2013; Benner et al, 2008; Tansey et al, 2007).

The involvement of microglial phagocytosis in PD pathogenesis is further supported by the fact that microglia swallow up and digest DA cell debris (Sugama et al 2003). Moreover, microglia can also engulf α-syn, a major constituent of LBs, possibly via the TLR4 receptor (Fellner et al, 2013; Park et al, 2008). Additionally, ineffective α-syn degradation in microglia may result in α-syn release through extracellular vesicles, which in turn contributes to the diffusion of toxicity. On one hand, extracellular α-syn or neuronal debris might contribute to neurodegeneration by interfering with microglial phagocytic functions. On the other hand, there are evidences suggesting that several proteins encoded by genes implicated in the PD or positioned within PD risk loci, lower microglial phagocytic activity. This contributes to an accumulation of unwanted material, and consequently, to neurodegeneration (Tremblay et al, 2019).

Apart from microglia, astrocytes also play a critical role in neuroinflammation in PD. Astrocytes respond to pathological conditions acquiring a reactive phenotype in a process known as “Reactive astrogliosis”, in which they increase the expression of GFAP and release some proinflamatory cytokines (IL1β, TNFα). Besides, reactive astrocytic hypertrophy of cell body and cell extensions occur in various PD animal models and the disease proper, indicating the possible involvement of astrocytes in the immune processes in this disease (Yamada et al, 1992).

Recent studies also revealed that astrocytes contribute to phagocytic clearance in a similar manner to microglia during normal physiological conditions (Bellesi M. et al, 2017) and there is abundant evidence that microglia and astrocytes cooperate to remove cell debris (Liddelow et al, 2017; Clarke et al, 2018; Jha et al, 2018; Tian et al, 2012).

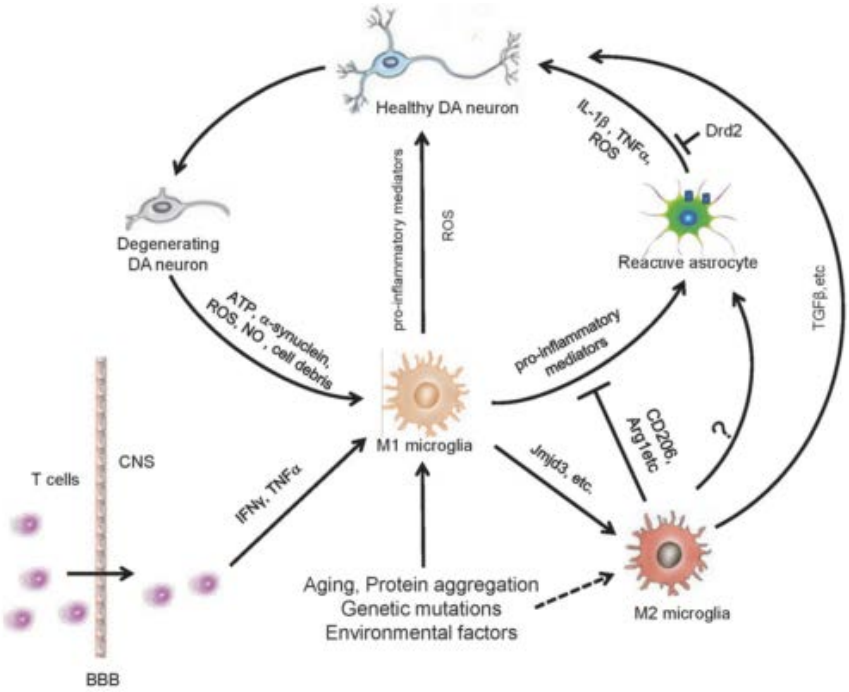


**Figure 8. Representation of inflammatory mechanisms involved in PD pathogenesis.** The molecules released from degenerative DA neurons can cause activation of microglia that respond with the release of pro-inflammatory cytokines. Concomitantly activated astrocytes acquire a reactive phenotype that enhances the inflammatory response (Wang et al., 2015)

In this context, two different classes of reactive astrocytes, named A1 and A2 have been described depending on the nature and type of insult (Clarke et al, 2018; Clark et al 2019). A2 are protective and, possibly, promote CNS recovery and repair during acute events like ischemia (Clarke et al, 2018). In contrast, A1 astrocytes are neurotoxic and lose many normal astrocytic functions, including the ability to support synapse formation and function and instead tend to phagocytize neuronal elements. Activated microglia induce A2 to A1 phenotypic conversion of astrocytes by the release of pro-inflammatory cytokines (IL-1 and TNF-a), C1q activation or, lastly, fragmented mitochondria (Liddelow et al, 2017; Joshi et al., 2019). Interestingly, the neurotoxic A1 astrocyte population is specifically observed in PD, suggesting that impaired astrocytic phagocytic clearance may contribute to increasing neuronal debris and abnormal protein accumulation, thus triggering neuroinflammation and neurodegeneration processes (Clarke et al, 2018).

The precise role of inflammation in PD is still not fully understood and future studies are necessary to understand the molecular mechanisms and the specific, possibly distinct, roles of microglial versus astrocytic phagocytic clearance in the onset and progression of PD.

## 6. Models to study Parkinson´s Disease

PD is a heterogeneous disease with a varying age of onset, symptoms, and rate of progression. This heterogeneity requires the use of a variety of cellular and animal models to study different aspects of the disease.

Primary cultured cells are simplified systems that allow us to answer specific questions quickly, clarify signaling pathways and resolve mechanistic details. Genetic or pharmacological manipulations and time-lapse imaging are easier and more reliable. In addition, specific cell types (e.g. dopaminergic neurons) can be studied in isolation, which can be important in order to determine their contribution to PD pathogenesis. At the same time, many important steps of PD pathogenesis and pathophysiology require the interaction of different cell types and thus can only be studied in animal models. Therefore, all findings from cultured cells need to be validated in animal models (Falkenburge, 2016).

In experimental animal models, that include mainly rodents, non-human primates and non-mammalian species (e.g. flies), two main approaches are used to model PD: neurotoxins and genetics. Neurotoxins (6-hydroxydopamine, (6-OHDA) or 1-methyl-4-phenyl-1,2,3,6-tetrahydropyridine MPTP) can model dopaminergic neurodegeneration derived from environmental factors (Konnova & and Swanberg, 2018). They generally induce a strong and rapid cell loss in the substantia nigra *pars compacta* (SNpc), trigger motor symptoms and behavioral changes, but lack LB formation (Blesa & Przedborski, 2014). By contrast, genetic-based models not only show variable cell loss and motor symptoms but can also exhibit α-syn pathology. Nevertheless, all animal models display some limitations. Many transgenic models [mutated LRRK2 (Blesa &

Przedborski, 2014) and UCHL1 (Setsuie at al., 2007); DJ-1, PINK1, and Parkin knockout (Dawson et al 2010)] show some functional disruption in the nigro-striatal system but are ineffective at inducing a robust display of neurodegeneration and α-synuclein pathology. Moreover, functional recovery in neurotoxic models and the lack of reliable phenotypes highlight the difficulty of replicating PD in animal models (Konnova & and Swanberg, 2018). In fact, is well evidenced the loss of translation of animal models into successful clinical trials, not only for PD but also for other neurodegenerative disorders (Mullane & Williams, 2013; Perrin 2014; Haston and Finkbeiner 2016).

Thus, the need to develop new models that can faithfully predict results in humans became imperative. Since a decade ago, when Yamanaka and colleagues discovered that adult somatic cells can be genetically reprogrammed to generate induced pluripotent stem cells (iPSCs), the use of this technology has become a common practice to model the pathology and to consider the homologous transplantation (Takahashi and Yamanaka 2006; Takahashi et al. 2007).

iPSCs offer several unique benefits as a models for PD and other complex diseases. First, it is a homologous system to study species-specific physio-pathological mechanisms. Then, as deriving from patients, they retain all of the genetic risk factors contributing to the pathology and can be differentiated in all neural cell types.

However, even if iPSCs offer the opportunity to use human, patient–specific, and disease-relevant cell types to study the molecular and cellular pathogenesis of PD, the use of iPSCs for disease modeling is not free of scientific challenges. For example, the use of multiple different protocols to generate adult neural cells makes complex the analysis of results (Krencik et al., 2011; Emdad et al 2011; Shaltouki et al., 2013; Jones et al., 2017; TCW et al., 2017).

In addition, reprogramming human somatic cells into iPSCs results in a cellular “rejuvenation”, in that age-related markers are lost (Cornacchia and Studer 2017).

Compared to differentiated adult cells, iPSCs have DNA methylation patterns, nuclear morphology, telomere lengths, DNA damage, and mitochondrial function and phenotype that resemble what is observed in young cells (Marion et al. 2009; Suhr et al. 2009, 2010; Prigione et al. 2010; Horvath 2013; Miller et al. 2013; Frobel et al. 2014). This represents a limitation in using iPSCs to model age-related neurodegeneration. Capturing the pathogenic diversity observed in patients is another significant challenge, as PD is a multifactorial disease with a high degree of heterogeneity, where patients can be classified into multiple subgroups based on their clinical features (Vidailhet 2003; Lewis et al. 2005).

The technique to reprogram post-mitotic cells in iPSCs is still in its infancy; however technical progress is fast, nevertheless, more improvements are needed to make iPSC a more reliable disease model. In this study we decided to use the iPSC model because this technology offers an unprecedented ability to mimic disease in vitro with patient-specific disease-relevant cell types. Human iPSC technology has the potential to deepen our understanding of the pathogenesis of disease, providing a more predictive platform for pre-clinical studies, and improve the success of clinical trials (Cobb et al., 2018).

# Hypothesis and Objectives

The progressive loss of dopaminergic neurons in the susbstantia nigra *pars compacta* and the presence of cytoplasmic inclusions called Lewy bodies are the principal hallmarks of Parkinson´s disease. Thus, to date, the dopaminergic neurons and their vulnerability have been the focus of the investigation of this disease. In turn, glial cells, specifically astrocytes possess a central role in regulating the well-being and well-function of neurons in both intact and injured brain. Moreover, astrocytes express the principal PD associated genes, and can contribute to familial forms of PD with the same mutations observed in dopaminergic neurons. Therefore, functional alterations of astrocytes may be directly linked to the main pathological features of the disease by impairing neuronal support or by spreading $\alpha$-syn toxicity. Here, we hypothesize that astrocytes play an important role in the degeneration and pathology of PD, favoring its onset and progression.

The global objective of this thesis is to characterize the astrocyte pathology in Parkinson's disease and to elucidate their possible contribution to neurodegeneration by using different models of the disease.

Our specific aims are:

**Objective 1.** To determine the effects of the accumulation of exogenous $\alpha$-synuclein in rat primary cultures of astrocytes and neurons, as well as the role of astrocytes in the onset and spreading of neurotoxicity.

**Objective 2.** To generate and characterize patient-specific iPSC-derived astrocytes from healthy donors and LRRK2$^{G2019S}$ patients and to elucidate the pathological crosstalk between astrocytes and neurons.

# Experimental procedures

***Part I***

## 1.1 Animals

All experimental procedures followed the European Directive 2010/63/eu, and were approved by the Ethic Committees of the University of the Basque Country UPV/EHU.

Animals were housed in standard conditions with 12 h light cycle and with *ad libitum* access to food and water. All possible efforts were made to minimize animal suffering and the number of animals used. Experiments were performed in Sprague Dawley rats at different age, according to the experimental procedures (see below).

## 1.2 Rat Cell cultures

### 1.2.1 Primary cortical neuron culture

Cortical neurons were obtained from E18 Sprague-Dawley rat embryos according to previously described procedures (Ruiz et al., 2009). Brain hemispheres were separated, meninges and basal nucleus were removed and cortical lobes were extracted.

Selected cortical tissue was digested with 0.25% trypsin and 0.004% deoxyribonuclease in Hank´s balanced salt solution (HBSS, Sigma-Aldridch) for 5 min at 37°C. Afterwards, the enzymatic reaction was stopped by adding Neurobasal medium (Invitrogen) supplemented with 10% FBS, B27 (Invitrogen), 2mM glutamine and antibiotic-antimycotic mixture, centrifuged at 1000 rpm for 5 min and the cell pellet was resuspended in 1ml of the same solution. Mechanical dissociation was performed by using 23-,25-, and 27G-gauge needles, and the resulting cell suspension was filtered through a 40 µm nylon mesh (Millipore). An aliquot of 10 µl of filtrate was collected to determine the cell number and viability by trypan blue staining (Sigma-Aldridch), and

all the rest was seeded onto 6/24 well plates, glass coverslips (12 mm) or AXIS microfluidic chambers (Millipore) in different densities depending on the experiment. Microfluidic chambers were placed onto previously poly-lysine treated 35 mm glass coverslips.

Twenty-four hours after seeding cells, culture medium was replaced by supplemented Neurobasal medium without FBS in order to avoid astroglial growth. Cell cultures were essentially free of astrocytes and microglia and were maintained at 37 °C and 5% $CO_2$. Cortical neuron cultures were used at 8-10 days *in vitro* (DIV).

### 1.2.2 Astrocyte cell culture

Primary cultures of cerebral cortical astrocytes were prepared from newborn (P0–P2) Sprague-Dawley rats as described elsewhere (McCarthy and de Vellis, 1980). Cortical lobes were extracted and enzymatically digested with 400 µl of 2.5% trypsin and 40 µl of 0.5% deoxyribonuclease in Hank´s balanced salt solution (HBSS, Sigma-Aldridch) for 15 min at 37°C. The enzymatic reaction was stopped by adding IMDM medium supplemented with 10% FBS (Gibco) and centrifuged at 1200 rpm for 6 min. The cell pellet was resuspended in 1 ml of the dame solution and mechanical dissociation was performed by using 21- and 23G-gauge needles. Resulting cell suspension was centrifuged at 1200 rpm for 6 min and plated onto 75$cm^2$ flasks coated with 30 µg/ml Poly-D-Lysine.

After 8 DIV, cells were trypsinized and astrocytes were plated (15,000 cells/cm2) onto 6/24 well plates, glass coverslips (12 mm) or AXIS microfluidic chambers (Millipore) in different densities depending on the experiment.

## 1.3 Purification of Lewy Bodies (LB) for PD brains

The samples were obtained from post-mortem brains collected in a Brain Donation Program of the Brain Bank “GIE NeuroCEB” run by a consortium of Patients

Associations: ARSEP (association for research on multiple sclerosis), CSC (cerebellar ataxias), France Alzheimer and France Parkinson. The willingness or consents were signed by the patients themselves or their next of kin in their name, in accordance with the French Bioethical Laws. The Brain Bank GIE NeuroCEB (Bioresource Research Impact Factor number BB-0033-00011) has been declared at the Ministry of Higher Education and Research and has received approval to distribute samples (agreement AC-2013-1887).

Human SNpc was dissected from fresh frozen post-mortem midbrain samples from 3 patients with sporadic PD exhibiting conspicuous nigral LB pathology on neuropathological examination (mean age at death: 77; GIE Neuro-CEB BB-0033-00011). Tissue was homogenized in 9 vol (w/v) ice-cold MSE buffer (10 mM MOPS/KOH, pH 7.4, 1 M sucrose, 1 mM EGTA, and 1 mM EDTA) with protease inhibitor cocktail (Complete Mini; Boehringer Mannheim) with 12 strokes of a motor- driven glass/Teflon homogenizer. For LB purification, a sucrose step gradient was prepared by overlaying 2.2 M with 1.4 M and finally with 1.2 M sucrose in volume ratios of 3.5:8:8 (v/v). The homogenate was layered on the gradient and centrifuged at 160,000 × *g* for 3 h using a SW32.1 rotor (Beckman). Twenty-six fractions of 1500 µl were collected from each gradient from top (fraction 1) to bottom (fraction 26), and analyzed for the presence of α-synuclein aggregates by filter retardation assay, as previously described (Recasens et al., 2014). In all cases, samples were bath-sonicated for 5 min prior to the in vitro applications.

### 1.4 Inhibitors and molecules

The following drugs and molecules were used: D15, Tocris (Endocytosis inhibitor that blocks the interaction of dynamin with amphiphysin 1 and 2) y CLR01 (molecular tweezer that prevents assembly and promotes disaggregation of protein fibrils that are associated with neurodegenerative diseases).

## 1.5 Microfluidic assays

Microfluidic experiments were performed using the AXIS chambers from Millipore. These chambers contain 4 wells interconnected by a channel on each side of the device. The two channels are connected by microgrooves (in red or green; see zooming in Fig. 9) of 450µm length. Each microgroove is approximately 5µm in height by 10µm in width allowing the passage of neurites and processes but impeding the cell migration from one side to another. For our experiments, astrocytes and neurons in different combinations (50,000 cells/channel), were seeded on poly-lysine or poly-ornithine into the two different channels as described above.

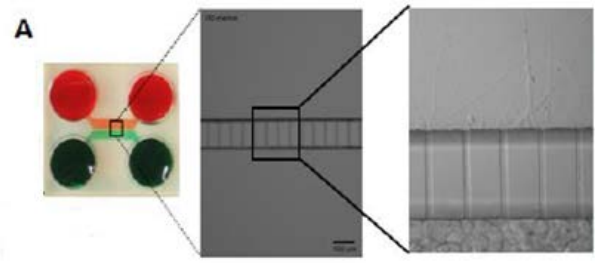


**Figure 9. AXIS Micofluidic chamber**. Two channels interconnected by microgrooves. Two wells are connected to each channel. Zoom of the microgrooves connecting both channels.

### 1.5.1 α-Synuclein transport

To study α-syn transport, neurons and astrocytes were seeded in both microfluidic channels in all possible combinations (neuron-neuron, neuron-astrocyte, astrocyte-astrocyte). LB was incubated in one channel for 5 days and hα-syn was detected in the opposite channel by immunofluorescence with the antibody against hα-syn (LB509). To avoid passive transport of α-syn, LBs were added to cells in the 'donors' chamber in a lower volume of medium (half) than in the 'receptor' side, generating a negative liquid tension, which impedes molecules to transit passively through the micro-vessels (Fig. 10).

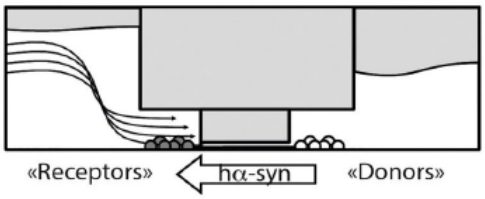


**Figure 10. Schematic representation of the diffusion of LB through the microgrooves**. "Donor" cells are incubated with half medium compared to the receptor cells to avoid the passive transport of the protein.

The inhibitor of endocytosis and axonal transport, D15 was used to prove the active transport of the α-synuclein. Neuronal cultures were seeded in microfluidic chambers and the "donor" side was incubated PBS, LB or LB with 50 µg/ml of D15 for 5 days. To prevent non-specific hα-syn uptake, "receptor" cells were seeded one week later than "donors" (Delayed) to prevent neurite spreading into "receptor" chamber.

### 1.5.2 α- Synuclein Proximity Ligation Assay (AS-PLA)

α-Synuclein Proximity Ligation Assay represents a combination between immnufluorescence and PCR that specifically recognizes α-synuclein oligomeric forms. Proximity Ligation Assay is able to detect 40 nm distances between two target proteins or, in our case, two α-synuclein monomers. Briefly (Fig. 11), the primary antibody syn211 (El-Agnaf et al., 2006) recognizes the monomers and only if at adequate proximity to form oligomers, the complex formed by a pair of oligonucleotide-labeled secondary antibodies (PLA probes) and the hybridizing connector oligonucleotides, are able to amplifying a fluorescence signal. This allows up to 1000-fold amplified signal that is visualized by a fluorescence spot by microscopy image analysis.

AS-PLA experiments were carried out using Duolink kits (Sigma) according to the manufacturer's instructions. We chose an α-synuclein antibody for the AS-PLA probes that displays blocking activity (syn211; El-Agnaf et al., 2006). Briefly, the conjugates were prepared using the Duolink Probemaker kit by incubating overnight 20 mg of

antibody (mouse anti- α-synuclein 211, 1 mg/ml, no BSA or azide, Abcam) with the Probemaker activated oligonucleotide (Minus or Plus) at room temperature.

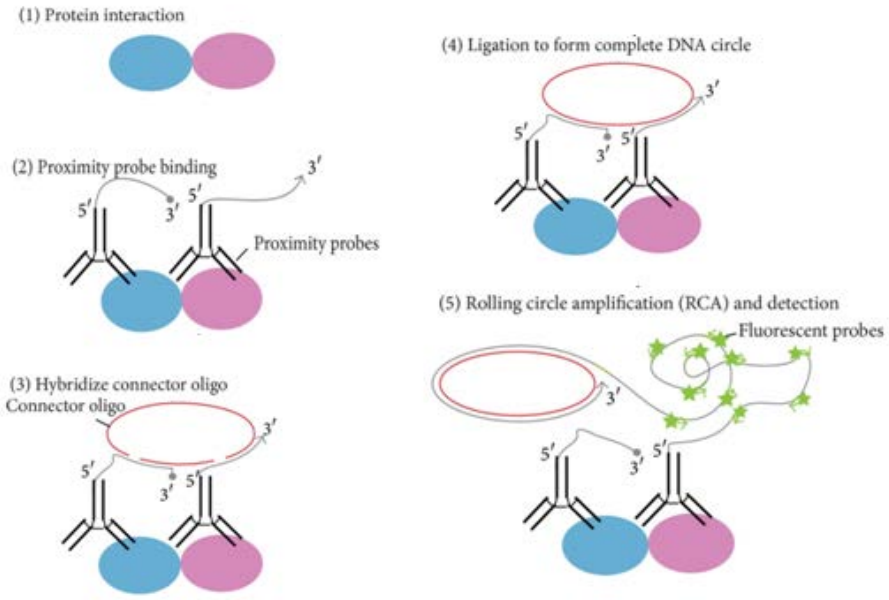


**Figure 11. Scheme of Proximity ligation assay (PLA).** 1) Protein interaction: the complex is formed between target proteins (light blue and pink). (2) Proximity probe binding: antibodies (black) with individual proximity probes (gray, 5'-3') bind to each of the target protein complexes. (3) Hybridization of connector oligo-DNAs: target protein complex serves to template the hybridization of connector oligo-DNAs (red). (4) Ligation to form complete DNA circle: adjacent connector oligos that are perfectly complementary to the target template are connected by DNA ligase. (5) Rolling Circle Amplification (RCA) and detection: after ligation, the RCA is initiated by the Phi29 DNA polymerase, by turning the target molecule primed by one of the proximity probes. The RCA product is detected through the hybridization of fluorescently labeled probes (green).

To analyze the ratio of oligomers vs monomers in astrocytes and neurons we performed an AS-PLA co-immunofluorescence. First, we immunolabel the cell cultures respectively with GFAP and/or β III tubulin. After secondary antibody detection, samples were incubated in Duolink block solution at 37ºC for 1 h. Total α-synuclein were detected incubating the syn211/activated oligonucleotide conjugates in Duolink PLA diluent (1:750) for 1 h at 37ºC and then overnight at 4ºC. After 3 cycles of washing in TBS + 0.05% Tween 20, circle DNA template for AS-PLA amplification were formed in Duolink ligation solutions and ligase for 1 h at 37ºC. Oligomers were detected in red fluorescence (594nm) after polymerase amplification of fragments in proximity distances. Only after AS-PLA, the monomers or fibrils were immune-labelled using the

specific secondary antibody anti-mouse Alex-Fluor 647. The ratio of oligomers vs monomers were calculated as a ratio between the red and the yellow signal.

### 1.5.3 Apoptosis

Neuronal apoptosis induced in different paradigms (i.e. α-synuclein transport or CLR01 protection) was visualized by nuclear morphology after DAPI staining. Cells were fixed as previously described and stained with DAPI (Molecular probes). Apoptosis was calculated as a percentage of nuclei with condensed chromatin versus total nuclei. We also used an alternate method using propidium iodide (PI) on the same experimental setting. After 5 days of incubation cells were treated with 1 mg/ml of PI for 10 min and then fixed with 4% PFA and counterstained with DAPI. PI was incorporated only in the damaged cells whereas all nuclei were stained with DAPI. Apoptosis was calculated as a percentage of PI positive vs DAPI positive.

## 1.6 Immunofluorescence

Cell cultures were fixed in 4% para-formaldehyde, permeabilized with 0.1% Triton and non-specific epitopes were blocked with 5% normal goat serum in phosphate-buffered saline (PBS). Primary antibodies (Table 1, Appendix I) were incubated overnight and then washed three times with 0.1% Triton in PBS. Secondary conjugated antibodies Alexa 488, Alexa 594, Alexa 647 or Alexa 405 (Invitrogen, 1:500), were incubated for 1 h in the dark at room temperature. After three washes with 0.1% Triton in PBS, cells were counter-stained for 1 min with DAPI. Finally, cover slips were mounted with Glycergel (Dako, Barcelona, Spain) and analyzed by fluorescence using the confocal microscope Leica TCS STED CW SP8.

### 1.7 ELISA assays

Astrocytes (50.000 cells) and neurons (100.000 cells) were seeded respectively on poly-lysine and poly-ornithine and treated with LB for 0, 1, 3 and 5 days in vitro. After treatment cells were lysed in buffer solution (10 mM Tris, 100 mM NaCl, 1 mM EDTA, 1 mM EGTA, 1 mM NaF, 20 mM $Na_4P_2O_7$, 2 mM ortho vanadate, 1% Triton X-100, 10% glycerol, 0,1% SDS, 0,5% deoxycholate 1 mM PMSF and proteases inhibitor cocktail from Sigma) and analyzed by ELISA using the commercial kit for hα-synuclein (Invitrogen). Amount of α-synuclein was calculated plotting the results on a standard curve (from 0 to 15ng/ml) and normalized for μg of total protein after Bradford analysis.

### 1.8 Baculovirus infection

Rat Astrocytes (20,000 cells) and neurons (50,000 cells) were seeded respectively on poly-lysine and poly-ornithine. Cell cultures were infected for 16 h with the commercial baculoviruses CellLight eEndosome:GFP or LysosomJe:GFP (both 30 Particles Per Cell – pcc– after titration and following the manufacturer indications; from Molecular Probes) and then treated with LB. After 3 days of treatment, cells were fixed with 4% para-formaldehyde. Cell cultures were immunostained with hα-synuclein (LB509 or syn211), GFAP or βIII-tubulin. GFP positive cells were analyzed for the colocalization with hα-synuclein using the Leica microscope TCS STED CW SP8.

### 1.9 Total protein extract and Western blot

Total protein was extracted on ice using RIPA buffer (50 mM Tris-HCl pH 7.4, 1% NP-40, 0.25% Na-deoxycholate, 150 mM NaCl, 1 mM EDTA, 1 mM PMSF, 1 μg/ml each aprotinin, leupeptin, an pepstatin, 1 mM $Na_3VO_4$, 1 mM NaF) in the presence of protease inhibitor cocktail (Complete, Mini EDTA-free tablets, Roche). Proteins were denatured for 5 min at 90 °C in the presence of sample buffer (6.25 mM Tris pH 6.8,

12.5% glycerol, 2.5% SDS, 0.025% bromophenol blue, and 5% β-mercaptoethanol). Samples were processed automatically (gel running, transfer and fluorescence detection) using the Amersham WB system based on fluorescence detection. Briefly, proteins were separated on gradient gels and transferred on PVDF membranes. After blocking solution (TBST, 5% goat anti serum) membranes were hybridized with the rat-specific primary antibody (D37A6 from Cell Signaling Technology). Primary antibody was detected using the secondary antibody goat anti rabbit Cy5 (Amersham) and quantification was performed automatically after normalization with GAPDH expression.

## 1.10 α-synuclein clearance by lysosomes

### 1.10.1. Lysosomal enrichment and FACS purification

Astrocytes and neurons (500.000 cells/cm2) were seeded on poly-lysine and poly-ornithine respectively and infected for 16 h with the commercial baculovirus CellLight Lysosome:GFP. After washing with PBS, cells were treated with 120pg/ml LB for 3 days. Lysosomal were extracted and enriched using the commercial kit Lysosome Enrichment Kit for Tissue and Cultured Cells (Thermo Scientific 89839). Isolated lysosomes previously labelled with CellLight Lysosome:GFP were purified by FACS using the sorter BD FACSJazz (USB, inFlux Compat.) with the Blue 488 laser, and collected in RIPA buffer (50 mM Tris-HCl pH 7.4, 1% NP-40, 0.25% Na-deoxycholate, 150 mM NaCl, 1 mM EDTA, 1 mM PMSF, 1 µg/ml each aprotinin, leupeptin, an pepstatin, 1 mM $Na_3VO_4$, 1 mM NaF).

### 1.10.2 ELISA assay

To quantify the α-synuclein content in lysosomes isolated from astrocytes or neurons, previously collected lysosomes were analyzed by ELISA using the commercial kit for hα-synuclein (Invitrogen, KHB0061H). Amount of α-synuclein was calculated

plotting the results on a standard curve (from 0 to 5ng/ml) and normalized for number of lysosomes (x1000).

### 1.10.3 Fluorimetric assay for Cathepsin D activity

Cathepsin D activity was evaluated using the commercial kit Cathepsin D Activity Fluorometric Assay Kit (BioVision #k143-100). Briefly, astrocytes (50000 cells/cm2) and neurons (200.000cells/cm2) were seeded on poly-lysine and poly-ornithine respectively and treated with 120pg/ml LB for 3 days. Cells were collected by centrifugation and lysed in the provided lysis buffer. Cell lysate was incubated with the commercial substrate for 1 hour at 37ºC. Cathepsin D activity was quantified in the fluorimeter (Biotek Synergy HT) with a 328-nm excitation filter and 460-nm emission filter. Results were normalized for µg of total protein after Bradford analysis.

## 1.11 Measurement of mitochondrial function

Oxygen consumption rates (OCRs; as indicator of mitochondrial respiration) of cortical neurons and primary astrocytes treated with LB were calculated with the Seahorse XF96, extracellular flux analyzer (Seahorse Bioscience, North Billerica, MA, USA) using the XF cell Mito Stress Test.

Astrocytes (20000 cells/mm2) and neurons (30000 cells/mm2) were seeded in the 96 well microplate previously coated with Poly-L-Ornitine or Poly- D-Lysine respectively, and treated or not with LB 120pg/ml for 3 days. The day of the experiment, cell medium was changed to Mito XF Medium (XF basal medium, 0.001 M piruvic acid, 0.002 M glutamine, glucose 0.01 M, pH 7.4) and the plate was incubated in a $CO_2$-free incubator at 37°C for 1 hr to equilibrate for temperature and pH. The microplate was then loaded into the XF96 and further incubated for 12 min to initialize and calibrate. The baseline was calculated by a series of 3 measurements every 3 min mix. The OCRs were obtained after the sequential treatment with oligomycin (2 µM), an inhibitor of ATP synthase, the proton ionophore carbonylcyanide-p-

trifluoromethoxy-phenylhydrazone (FCCP, 0.5 µM), and rotenone combined with antimycin A (0.5 µM), a mitochondrial complex I and III inhibitor respectively. Four replicates were performed for each condition or cell type for every experiments (n=3). Data was analyzed with the Wave 2.4.0 software.

### 1.12 Statistical analysis

Data are presented as means with SEM. Statistical analysis was carried out with the Student *t*-test or ANOVA and subsequently analyzed by Tukey's or Dunnet's tests (Graph Pad Prism 6 software). In all instances, a value of $p < 0.05$ was considered significant.

***Part II***

## 2.1 Human samples

Human fibroblasts were obtained from two healthy donors (Ctrl 1 was purchased from AXOL and Ctrl 2 from Coriel stem cell bank) and two Parkinson´s disease patients with $LRRK2^{G2019S}$ mutation (PD 1 from Coriel and PD 2 provided by BioDonostia Hospital) (Table 3). Controls did not manifest any neurological symptoms and they were matched with PDs by age and gender. All procedures with human cells were approved by the National and local ethical committees (with code M30_2018_030) according to the National law 14/2007 on Biomedical research.

| Sample | Type | Code | Biopsy | Sex | Age | Mutated gene | Mutation | Karyotype |
|---|---|---|---|---|---|---|---|---|
| **Ax0083** | Healthy | Ctrl1 | Skin | F | - | - | - | Normal |
| **38530A** | Healthy | Ctrl2 | Skin | M | 55 | - | - | Normal |
| **PD33879** | PD | PD1 | Skin | F | 66 | LRRK2 | G2019S | Normal |
| **FH1509** | PD | PD2 | Skin | M | 58 | LRRK2 | G2019S | Normal |

**Table 3. Summary of fibroblasts used for reprogramming and generation of astrocytes.**

## 2.2 Generation of Human Astrocytes

Fibroblasts were grown in DMEM F12 (Gibco) + gentamicin (50mg/ml, Sigma) and infected with the CytoTune iPS 2.0 Sendai Reprogramming Kit (Thermofisher). Sendai Reprogramming kit consists of three CytoTune™ 2.0 reprogramming viral vectors that are used for delivering and expressing key genetic factors necessary for reprogramming somatic cells into iPSCs (Klf4/Oct3-4/Sox2-KOS, hc-Myc, Klf4). Fibroblasts were co-infected with a –EmGFP fluorescent reporter plasmid to evaluate the efficiency of infection. The day after, medium was freshly replaced and infection was corroborated by checking GFP fluorescence. Seven days later, transduced fibroblasts were seeded in Geltrex pretreated 60/100 mm plates in Essential 8 Flex medium (E8, Gibco) with gentamicin. Medium was changed every other day until iPSc

colonies formation on week 3 or 4 post-infection. Colonies were manually picked up using a 27G Braun Sterican Needle and replated in laminin-521 coated 6 well plates with E8 medium with gentamicin and Rock Inhibitor (Millipore, Y-27632). The day after, medium was changed to remove Rock inhibitor (see figure 12).

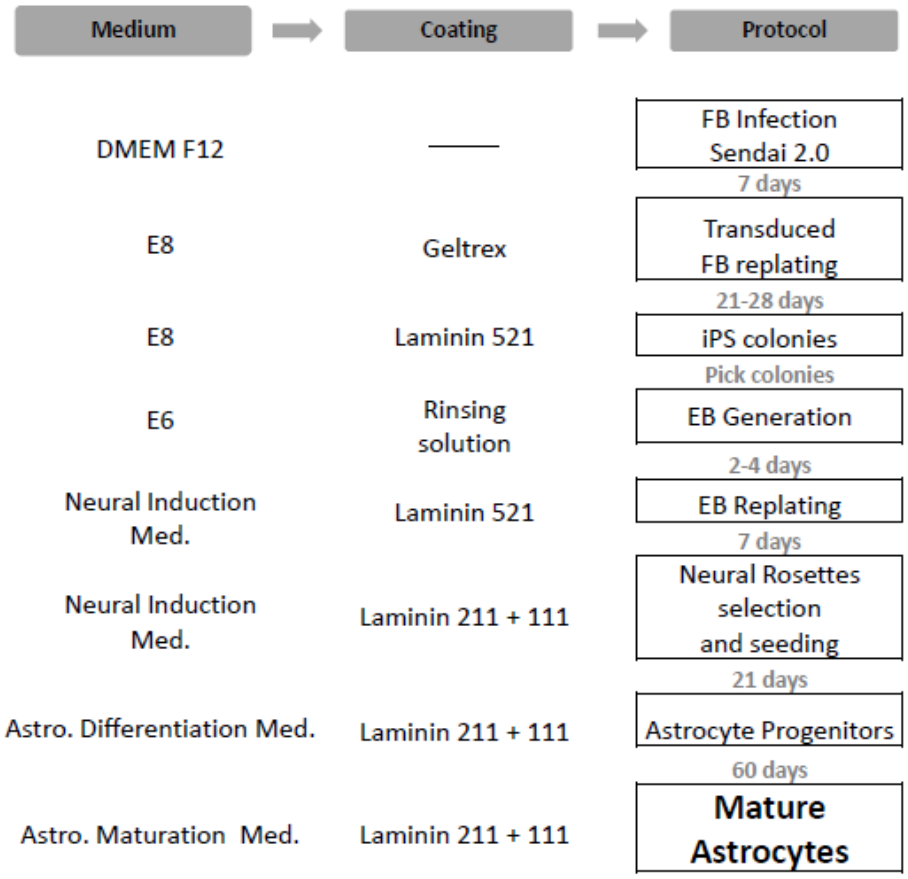


**Figure 12. Schematic summary of fibroblast reprogramming and astrocyte generation.**

Colonies were sequentially picked up, disaggregated and expanded until obtaining enough colonies. Embryoid bodies (EB) were generated culturing the cells in Essential 6 medium (E6, Gibco) for 2-4 days in the Aggrewell$^{TM}$800 plates (StemCell, 34825). Microwells of Aggrewell plates were previously treated with Rinsing Solution (StemCell, 07010) to maintain the colonies in suspension. Fresh medium was added everyday by removing half-medium of the wells. EBs were then replated and attached in a laminin 521-211 mix (50% each) coated 6 well plates in the same medium. Medium was changed daily using the STEMdiff Neural Induction Medium (Stemcell, 05835) to promote the differentiation of the cells to neural lineage until the formation of Neural Rosettes. After 7 days, Neural Rosettes were selected and detached using

the STEMdiff Neural Rossete Selection Reagent (Stemcell, 05832). Cells were incubated for 2 hours with this reagent at 37$^{o}$C with 5% $CO_2$ and then, mechanically disaggregated and seeded again at single cell level in laminin 211 + 111 (50% each) precoated plates. Differentiation of neural precursor cells to astrocytes was triggered using astrocyte differentiation medium (StemCell, 08540). To maintain the appropriate cell density (70% of confluence) cells were passed every week in the same coating mix during 21 days. Finally, astrocytes precursor cells were maturated in the Astrocyte Maturation Medium (StemCell, 08550) for 60 days. Passages of the cells were done when the cells reached approximately 80% of confluence and cells were always maintained in laminin 211 + 111 (50% each) precoated plates.

During the whole protocol, the correct state of the cells in each step was checked using the EVOS FL microscope (Life Technologies, AME4300).

## 2.3 Characterization of iPSc derived Human Astrocytes

### 2.3.1 FACS Analysis of the GFAP$^{+}$ astrocytes

Cells (500.000) from each cell line were detached with TryPLE (Sigma) and fixed as a single cell suspension with 500 µl PFA 4% for 10 minutes. Cells were washed in PBS at 400g 5 min and resuspended in blocking solution (0.5gr BSA in PBS with 0.01% Triton) with agitation overnight at 4ºC. The following day cells were washed and incubated with the primary antibody goat anti GFAP (Abcam, 53554) for 2 h at 4$^{o}$C. After further wash for 5 min in PBS-T 0.01% cell suspension was incubated with the secondary conjugated antibody Alexa fluor 488 donkey anti-goat for 1 h in the dark at 4$^{o}$C. After a wash with PBS-T 0.01%, cells were finally resuspended in PBS 1x. Cells were analyzed in the BD FACSJazz (USB, inFlux Compat.) analyzer using the Blue 488 laser. Unstained cells were gated and used as a negative control.

### 2.3.2 Calcium Imaging

Intracellular calcium ($Ca^{2+}$) levels were estimated by the 340/380 ratio method as described previously (Mato et al., 2013). Astrocytes were first loaded with fura-2 AM (5 μM; Invitrogen). Cells were subsequently washed in the recording solution containing 137 mM NaCl, 5.3 mM KCl, 0.4 mM $KH_2PO_4$, 0.35 mM $Na_2HPO_4$, 20 mM HEPES, 4 mM $NaHCO_3$, 10 mM glucose, 1 mM $MgCl_2$, 2.5 mM $CaCl_2$, and 0.5 mg/ml BSA, pH 7.4. Experiments were performed in a coverslip chamber continuously perfused with buffer at 1 ml/min by exposing the cells to ATP (100 μM) or FCCP (1 μM). The perfusion chamber was mounted on the stage of a Zeiss (Oberkochen, Germany) inverted epifluorescence microscope (Axiovert 35), equipped with a 150 W xenon lamp Polychrome IV (T.I.L.L. Photonics, Martinsried, Germany), and a Plan Neofluar 403 oil immersion objective (Zeiss). Cells were visualized with a high-resolution digital black/white CCD camera (ORCA, Hamamatsu Photonics Iberica, Barcelona, Spain) and images were acquired every 5 s. Image acquisition and data analysis were performed using the AquaCosmos software program (Hamamatsu Photonics Iberica). Intracellular $Ca^{2+}$ measurements were expressed as the ratio of F340/F380 and normalized to baseline values. Results for statistical comparison were calculated as area under the curve (AUC) of the response for each cell from the start of each compound application. Data were normalized to compound-induced effect as 100% for representation.

### 2.3.3 Immunofluorescence

Immunofluorescence for Sox2, Nanog, Oct 4, Tuj1, SMA, AFP, GFAP, S100β, MAP2, NG2 and βIII-tubulin were performed as described previously in "Experimental Procedures" Part I, 6. Working concentrations of primary antibodies are specified in Table 4 (Appendix I).

For morphological analysis, cells from the four astrocyte lines were seeded in glass bottom Cellvis 24 well plates. After fixation in PFA 4% for 8 minutes, cells were immunostained for GFAP (Goat anti GFAP, Abcam 53554). Alexa fluor Donkey anti goat was used as a secondary antibody. Images were taken with the

CellInsight CX7 High Content Screening (HCS) system (Thermo Scientific) using a 10x objective. Morphological parameters for area (defined as the number of microns squared of the object), perimeter (length of the boundary of the object) and ShapeP2A (measure of the ratio of the perimeter squared of the object to 4 times π times de area of the object) were calculated with High Content Analysis (HCA) platform. More than 100 cells per cell line were analyzed.

## 2.4 Analysis of mitochondrial ultrastructure

### 2.4.1 Sample preparation for Electron Microscopy

Cells were fixed in 4% PFA for 10 min and post-fixed in 3% glutaraldehyde for 30 min. After a wash in phosphate buffer (PB) samples were osmicated (1% $OsO_4$ in 0.1 M PB; pH 7.4) for 30 min. After 3x10 min washes in 0.1 M PB, samples were dehydrated in graded ethanol concentrations (50-100%) to propylene oxide and embedded in epoxy resin (Sigma-Aldrich) by immersion in decreasing concentration of propylene oxide (1:3 for 30 min, 1:1 for 1 h and 3:1 for 2 h). Samples were then embedded in fresh resin overnight and allowed to polymerize at 60°C for 2 days. Following visualization at the light microscope, selected portions were trimmed and glued onto epoxy resin capsules. Semi-thin sections (500 nm-thick were cut from epoxy blocks using a Power Tome ultramicrotome (RMC Boeckeler, Tucson, AZ, USA and stained with 1% toluidine blue. Ultrathin (50-60 nm-thick) sections were then cut with diamond knife (Diatome, Hatfield PA, USA), collected on nickel mesh grids and stained with 4 uranyl acetate for 30 min and 2.5% lead citrate for electron microscope visualization.

### 2.4.2 Image Acquisition and analysis

Electron microscopy images of mitochondria were taken from randomly selected fields with a Jeol JEM 1400 Plus electron microscope at the Service of Analytical and High-Resolution Microscopy in Biomedicine of University of the Basque Country

UPV/EHU. Images were taken at a magnification of 12000X. Circularity and aspect ratio (ratio of circularity vs. elongation) were measured with Image J- Software using a self made plug-in. More than 100 mitochondria were analyzed for each line.

## 2.5 Mitochondrial membrane potential (ΔΨm) measurement

Rhodamine 123 (Rh123) was used for the assessment of ΔΨm in human astrocytes. Rh123, a highly positive dye, accumulates in the mitochondria, the most negative organelle inside the cell in a manner which is dependent on membrane polarization. Mitochondrial energization itself induces quenching of Rh123 fluorescence. FCCP, a protonophore that dissipates membrane potential is used as a de-quench inductor. Adding FCCP, Rh123 leaves mitochondria and accumulates in the soma, increasing fluorescence. The fluorescence intensity in the soma will be directly proportional to the membrane potential.

Cells were seeded in Ibidi (35mm/plate) glass bottom plates in a mean density confluence of 50-70%. Cells were treated with Rh123 10µM for 15 min in the incubator at 37ºC in 5% $CO_2$. Then, Rh123 was washed with 900µl HBSS. At this point, time lapse was performed using the confocal microscope Leica TCS STED CW SP8. After the first minute, 100 µl FCCP 1 µM were added to the plate. Time lapse recording was performed for a total of 5 min (Snap every 15 sec). Fluorescence intensity after FCCP treatment was measured with the Leica LASX Software and data (n=3) was analyzed with GraphPad Prism 5.

## 2.6 Measurement of mitochondrial function and glycolytic activity

The oxygen consumption rate (OCR), as an indicator of mitochondrial respiration, the extracellular acidification rate (ECAR), as indicator of glycolytic activity, and the proton efflux rate (PER) which correlates with lactate production, were measured with the Seahorse XF96, extracellular flux analyzer.

For the analysis of mitochondrial respiration, human astrocytes (30000 cells/ mm2) were seeded in laminin 211+111 precoated wells. The day of the experiment, cell medium was changed to Mito XF Medium (XF basal medium with phenol red, 0.001 M piruvic acid, 0.002 M glutamine, glucose 0.01 M, pH 7.4). The OCRs were obtained after the sequential treatment with oligomycin (2 µM), FCCP (1 µM), and rotenone combined with antimycin A (0.5 µM). To measure the glycolytic activity, the same protocol was followed with some important modifications. The day of the experiment, cell medium was changed to Glico XF Medium, which does not contain phenol red (DMEM Base Medium without Phenol Red with 5 mM HEPES, 10 mM glucose, 1 mM sodium pyruvate, 2 mM glutamine, pH 7.4 at 37ºC). The ECAR and PER were obtained after the sequential treatment with rotenone combined with antimycin A (0.5 µM) and 2DG (50mM) respectively. Four replicates were performed for each condition or cell type for every experiments (n=3). Data was analyzed with the Wave 2.4.0 software.

## 2.7 Western blot for detection of oxidatively modified proteins

### 2.7.1 Sample preparation

Cells (30.000/well) were seeded in 24 well plates and solubilized by adding equal volume of 2X Extraction Buffer to the culture media directly to the cells. The mixture was incubated for 20 in on ice. The carbonyl groups in the protein side chains were derivatized to 2,4-dinitrophenylhydrazone (DNP-Hydrazone) by reaction with 2,4 –dinitrophenylhydrazine (DNPH). Two aliquots of each sample were prepared to be analyzed simultaneously. One aliquot was treated with “derivatization reaction” (DNPH Solution) and the other aliquot, that was used as control was treated with “derivatization control reaction”. Samples were prepared according to manufacturer’s instruction with all the reagents provided in the kit (Oxidized protein Western Blot detection kit, Abcam, ab178020). Protein concentration was quantified with a detergent-compatible assay reagent

(Pierce BCA Protein Assay Kit) according to the manufacturer's instructions (ThermoFisher Scientific).

### 2.7.2 SDS-PAGE and western blotting

Protein samples were separated by SDS-PAGE using Criterion TGX Precast Any KD Tris-Glycine polyacrylamide gels (Bio-Rad). Electrophoresis was performed in a Tris-Glycine buffer (25 mM Tris, pH 8.3, 192 mM glycine, 0.1% SDS in $dH_2O$) by using the Criterion cell system (Bio-Rad). Gels were transferred to Trans-Blot Turbo Midi Nitrocellulose Transfer Packs (Bio Rad, Hercules, CA, USA). For immunoblotting, unspecific epitopes were blocked in PBST buffer (1,4mM $KH_2PO_4$, 8mM $NA_2HPO_4$, 140 mM NaCl, 2.7 mM KCl containing 0,05% Tween 20, pH 7.3) in the presence of 4% BSA (Sigma-Aldrich) during 1h at RT. Then, membranes were incubated overnight with the specific primary antibody (Rabbit anti DNP antibody, 5000x) at $4^oC$ with gentle shaking. Afterwards, membranes were washed three times with PBST and incubated with secondary antibody (Conjugated Goat anti rabbit HRP, 5000x) in the blocking solution for 1 h at RT. Finally, membranes were again washed three times with PBST and once with PBS. Immunoreactive bands were detected by using enhanced electrochemical luminescence (Super Signal West Dura, Pierce) and visualized using the ChemiDoc XRS Imaging System (Bio-Rad).

## 2.8 Effect of astrocytes in neuronal survival

### 2.8.1 Neuron-Astrocyte Co-cultures

Primary cultures of cortical neurons were established from E20 Sprague–Dawley rat embryos (CharlesRiver Laboratories) as described elsewhere (Arrasate et al., 2004), with minor modifications. Pregnant rats were killed with $CO_2$, and their embryos were extracted and decapitated. The brain cortices were isolated from the embryos and dissociated with 1.5% papain (Worthington) for 10 min at 37 °C, followed by a 10-min

treatment with DNAseI (Sigma). Finally, the tissue was treated for 20 min with a trypsin inhibitor (Sigma) to inhibit the papain, and individual neurons were obtained by mechanical digestion in Opti-MEM (Gibco) supplemented with 0.8% glucose (Sigma), gentamicin (Gibco), and fungizone (Gibco). The neurons were plated at a density of 5 × $10^5$ neurons per well in 24-well plates (Costar) coated with laminin (BD Biosciences) and poly-D-lysine (Millipore), prewarmed to 37 °C. For immunofluorescence, 2.5 × 105 neurons per well were plated in 24-well plates with glass coverslips (Thermo Scientific) coated as described previously. After 1 h, once the neurons had attached to the coverslips, the Opti-MEM was replaced with Neurobasal medium (Gibco) supplemented with 5% FBS (HyClone), 1% GlutaMAX (Gibco), 2% B27 (Gibco), gentamicin, and fungizone. Neurons were then incubated at 37 °C in 5% $CO_2$ for 5 days until transfection with a plasmid expressing the fluorescent protein m-Cherry with Lipofectamine 2000 (Invitrogen, Carlsbad, CA)

Human Astrocytes (75,000 or 150,000 cells/well) were added to the wells 1d after neuronal transfection. The co-cultures were longitudinally tracked for 8 days for survival analysis.

### 2.8.2 Automated Image Acquisition

Transfected primary cortical neurons co-cultured with astrocytes in 24-well plates were placed on a Zeiss Observer Z1 microscope equipped with a chamber that maintains stable temperature and $CO_2$ at 37 °C and 5% $CO_2$ (Zeiss). Images were automatically acquired at determined positions with a 10× long-distance objective in one or different channels designating those positions with particular spatial coordinates. Once the full set of images had been acquired, the plate was returned to the incubator until a new set of images was acquired. For a typical survival experiment, 10 positions per well and four wells per condition were used. Positions were chosen randomly, making the selection of neurons to be analyzed unbiased. A template with the same initial spatial positions is used throughout the experiment, following exactly the same neuronal fields.

### 2.8.3 Image Processing and Statistics

For survival experiments, MATLAB-based semi-automated ad hoc programs were developed for image analysis and to estimate the survival times of individual neurons. The program shows the same neuronal field sequentially at all the different experimental times. At the initial time, the neurons were selected and numbered. In the rest of the time series, the software opens each image, and the user compares it with the previous time. Dead neurons are identified and categorized as uncensored events. Neurons that survive until the end of the experiment are considered censored events. The data were exported to Excel, and all further survival analyses were performed with STATA 12. The Nelson–Aalen cumulative hazard function was used to plot the differences in the cumulative risk of death among the experimental groups. These differences were analyzed with a log-rank test and clustered Cox regression models, as long as a proportional hazard assumption was fulfilled (Schoenfeld residual-based test evaluation or graphical assessment). Since transfection conditions are not controlled at the level of the individual neuron, a clustered Cox regression analysis of neurons coexisting in the same well was performed to improve the accuracy of the test. In addition, and because all experiments were repeated at least twice, the variability in the baseline toxicity between experiments was adjusted by stratifying the Cox model for each experiment, as long as there was more than one well per condition in any experiment. In experiments with one well per condition in all of the grouped experiments, well and experiment become equivalent, so clustering the wells was sufficient, and no stratification was applied.

## 2.9 Statistical analysis

All data were expressed as mean ± S.E.M. Statistical analysis were performed using absolute values. GraphPad Prism software was used applying one-way analysis of variance (ANOVA) for multiple comparisons and one-tailed. Paired Student’s t test for comparison of the groups has been used when necessary.

**APPENDIX I**

| Primary Antibody | Reactivity | Reference | Dilution |
|---|---|---|---|
| GFAP | Rat, Human | Abcam (ab53554) | 1:1000 |
| βIII tubulin | Rat | Abcam (ab18207) | 1:500 |
| Human α-synuclein (LB509) | Human | Invitogen (180215) | 1:300 |
| Human α-synuclein (syn211) | Human | Abcam (ab80627) | 1:300 |
| Rat α-synuclein | Rat | Cell Signaling (D37A6) | 1:200 |
| S100b | Human | Dako | 1:400 |
| SOX2 | Human | Santa Cruz (17320) | 1:300 |
| Oct4 | Human | Santa Cruz (sc-5279) | 1:100 |
| Nanog | Human | Abcam (ab21624) | 1:1000 |
| MAP2 | Human | Abcam | 1:500 |
| NG2 | Human | Abcam (ab50009) | 1:300 |
| βIII tubulin (Tuj I) | Human | Thermo Fisher (A25538) | 1:500 |
| Smooth muscle actin, SMA IgG2a | Human | Thermo Fisher (A25538) | 1:200 |
| α-fetoprotein, AFP IgG1 | Human | Thermo Fisher (A25538) | 1:500 |

**Table 1.** Primary antibodies for immunocytochemistry

**APPENDIX II**

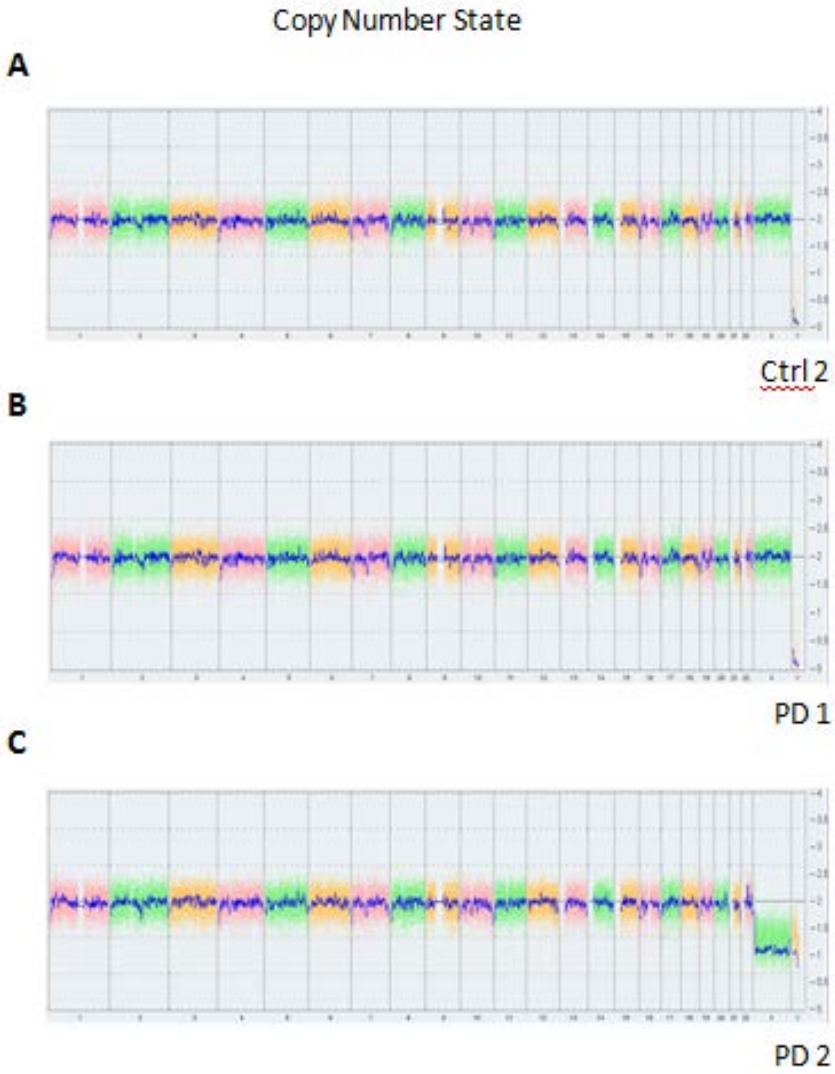


**Appendix II. Whole genome view.** The whole genome view displays all somatic and sex chromosomes in one frame with high level copy number. The smooth signal plot (right y-axis) is the smoothing of the log2 ratios which depict the signal intensities of probes on the microarray. A value of 2 represents a normal copy number state (CN = 2). A value of 3 represents chromosomal gain (CN = 3). A value of 1 represents a chromosomal loss (CN = 1). The pink, green and yellow colors indicate the raw signal for each individual chromosome probe, while the blue signal represents the normalized probe signal which is used to identify copy number and aberrations (if any). A, B and C correspond to Ctrl 2, PD 1 and PD 2 respectively, and do not show any alteration.

# Results - Part I

### 1.1 Rat cortical neurons and astrocytes internalize exogenous human α-synuclein

To determine if astrocytes and neurons internalize to exogenous human α-syn (hα-syn), we treated primary rat neuronal and astrocyte cultures with the insoluble fraction of human LB. Cells were incubated for 24, 72 or 120 h together with 120 pg/ml of LB containing hα-syn whereas untreated neuronal and astrocyte cultures (t=0) were used as a control. The ELISA assay with the intracellular extract from treated neurons and astrocytes demonstrated that astrocytes incorporated hα-syn earlier than neurons, transiently with a peak between 24 and 72 hours of incubation. In fact, we observed only a small and not significant incorporation in the neuronal cultures after 120 hours of treatment (Fig. 1.1 A). These results were confirmed also by immunofluorescence with the antibody LB509 specifically raised against the human fraction, after 120 hours of treatment (Fig. 1.1 B).

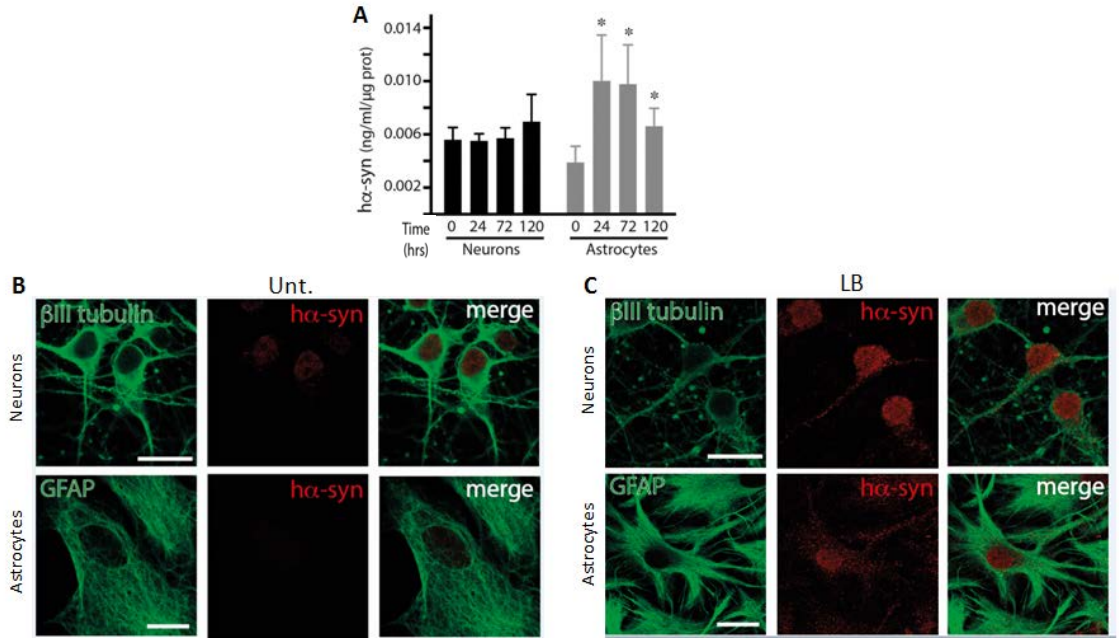


**Figure 1.1. Exogenous hα-syn uptake.** (A) ELISA assay. hα-syn was incubated with neurons (left) or astrocytes (right) for 24, 72 or 120 h. Untreated cells (0) were used as a control. After incubation, cells were washed thoroughly with HBSS and cytosolic proteins extracted for ELISA analysis. Incorporation of hα-syn was normalized for microgram of total protein analyzed. Each point was triplicated. (B) Immuno-fluorescence showing untreated (Unt.) neurons (labelled in green with anti-βIII tubulin antibodies - scale bar: 20 µm)and astrocytes (labelled in green with anti-GFAP antibodies - scale bar 20 µm) (C) Immuno-fluorescence showing hα-syn (labeled in red) incorporated in neurons and in astrocytes, after 120 h of incubation. Statistical analysis

was performed using two-way ANOVA. * indicates a significant difference ($p < 0.05$) compared to control, non-treated, astrocytes.

As demonstrated in Figs. 1.2 A and B, hα-syn uptake was toxic for the neurons, increasing the apoptotic nuclei up to 20%, but not for the astrocytes (Fig 1.2 C, D). Because LB contains other unspecific and unknown molecules apart from of α-syn, we decided to pre-treat cells with the molecular tweezer CLR01 to demonstrate that neuronal death was specifically induced by the hα-syn contained in the LB extract. CLR01 is a "molecular tweezer" that inhibits the toxic forms of the α-syn by inhibiting or deconstructing the most aggregated forms of the protein (Shina et al., 2012). In fact, we observed that CLR01 treatment previously preincubated for 10 days with LB inhibited the neuronal death.

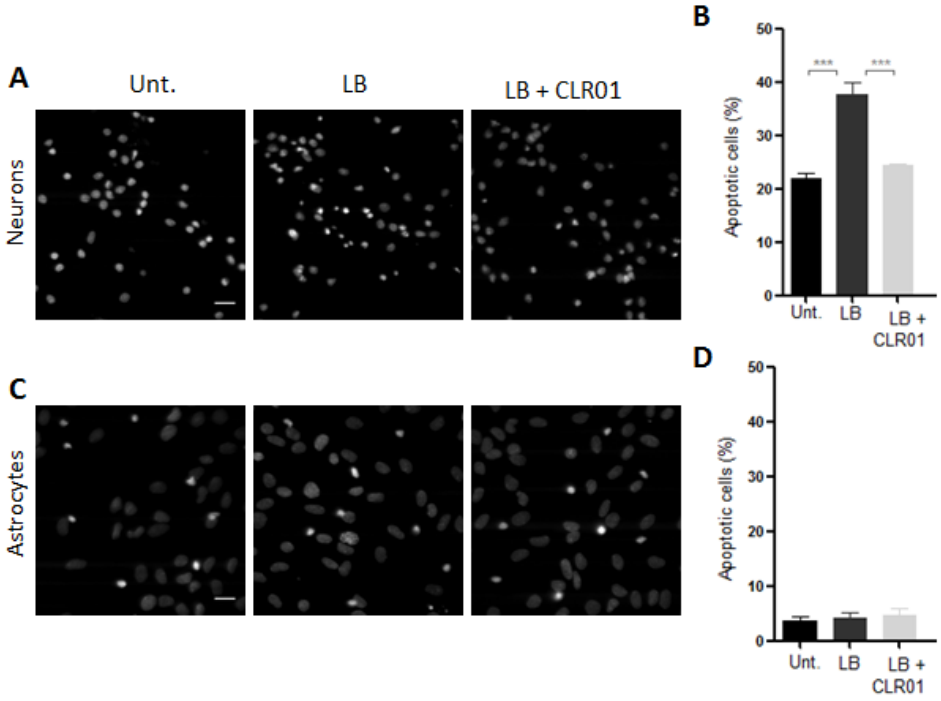


**Figure 1.2. CLR01 reduces hα-syn aggregation mediated toxicity in rat primary neurons.** Rat neurons (A) and astrocytes (C) were seeded respectively on poly-lysine and poly-ornithine and then treated with LB (120 pg/ml), CLR01 (10μM) or with the combination of LB and CLR01. LB was preincubated in gently shaking for 10 days with the CLR01 before treating the cells. After 5 days of incubation of the cells with the treatment, cells were stained with DAPI. Apoptosis was calculated as a percentage of nuclei with condensed chromatin versus total nuclei (B, D). Statistical analysis was carried out with one way ANOVA and analyzed with Bonferroni's Multiple Comparison Test ($n = 4$, * $p < 0.05$) Scale bar: 20 μm

After we demonstrated astrocytes are not sensitive to the hα-syn toxicity we decided to elucidate the mechanisms by which α-syn can be internalized and why astrocytes are resistant in contrast to the neurons.

### 1.2 hα-syn is uptaken by endocytosis

Internalization of α-syn in rat neurons occurs by different mechanisms like for example by endocytosis. In order to confirm this hypothesis (Bourdenx et al., 2015; Dehay et al., 2015a), we infected both astrocytes and neurons with a commercial baculovirus bringing the early endosome marker labeled with eGFP. After 16 h of infection (see material and methods for the detailed protocol), cells were exposed for 72 h to the LB containing the hα-syn. Hα-syn was detected by immunofluorescence inside the early endosomes in both neurons (Fig. 1.3 A) and astrocytes (Fig. 1.3 B), suggesting that cells can internalize exogenous α-syn by endocytosis. The next questions we wanted answer were: 1. Which are the possible mechanisms by which hα-syn result toxic to the cell? 2. Can resistant astrocytes transmit the toxic hα-syn to the neurons? 3. What is the conformational status of internalized hα-syn?

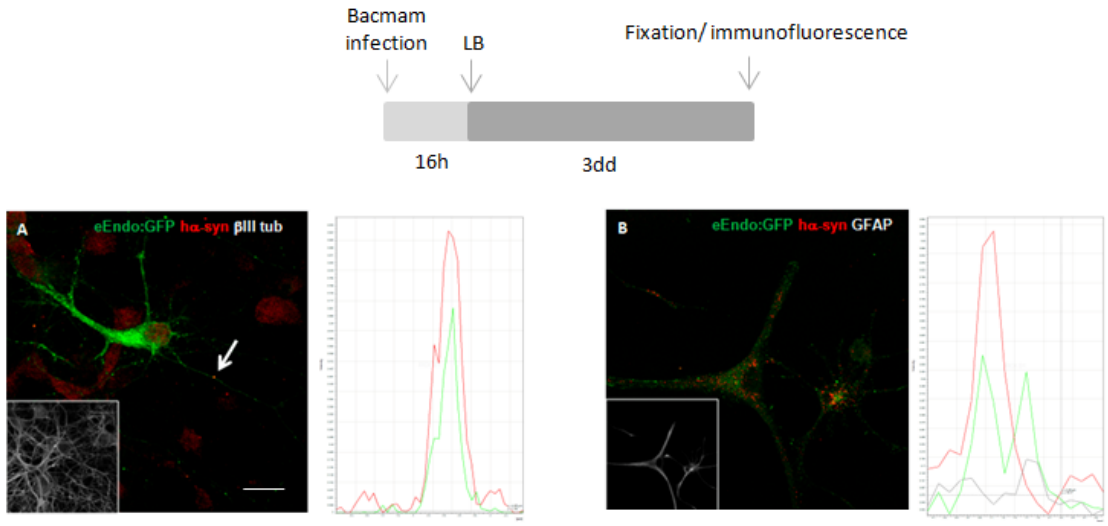


**Figure 1.3. Neurons and astrocytes uptake hα-syn by phagocytosis.** Rat cortical neurons labeled with βIII tubulin (A) and astrocytes labeled with GFAP (B) were infected by baculovirus with early endosome GFP marker (A, B). Hα-syn was detected by immunofluorescence (red) in

neurons or in astrocytes, both in white. Co-localization of endosome marker with hα-synuclein is shown in yellow and demonstrated by the respective histograms. Scale bar: 20 μm.

### 1.3 Astrocytes display increased lysosomal activity when exposed to hα-syn compared to neurons

To evaluate lysosomal activity, we infected neurons and astrocytes with baculoviruses expressing lysosome markers fused with eGFP, using the same protocol as with early endosomes. With this experiment, we wanted to understand if internalized α-syn could be processed by the lysosomes. After 72h of LB exposure, we found hα-syn colocalizing with lysosomes in both neuron and astrocytes (Fig. 1.4 A, B). To confirm that hα-syn was localized within the lysosomes and to demonstrate that lysosomes could be engaged in the α-syn metabolism, we decided to isolate the lysosomes by FACS and characterize their content (Fig. 1.4 C).

For that purpose, we labeled neuronal and astrocyte lysosomes after baculovirus infection and analyzed the sorted fractions by ELISA for the presence of hα-syn. This assay revealed that the presence of hα-syn in astrocytes was approximately 9 times higher than in neurons although it was not statistically significant (Fig. 1.4 D).

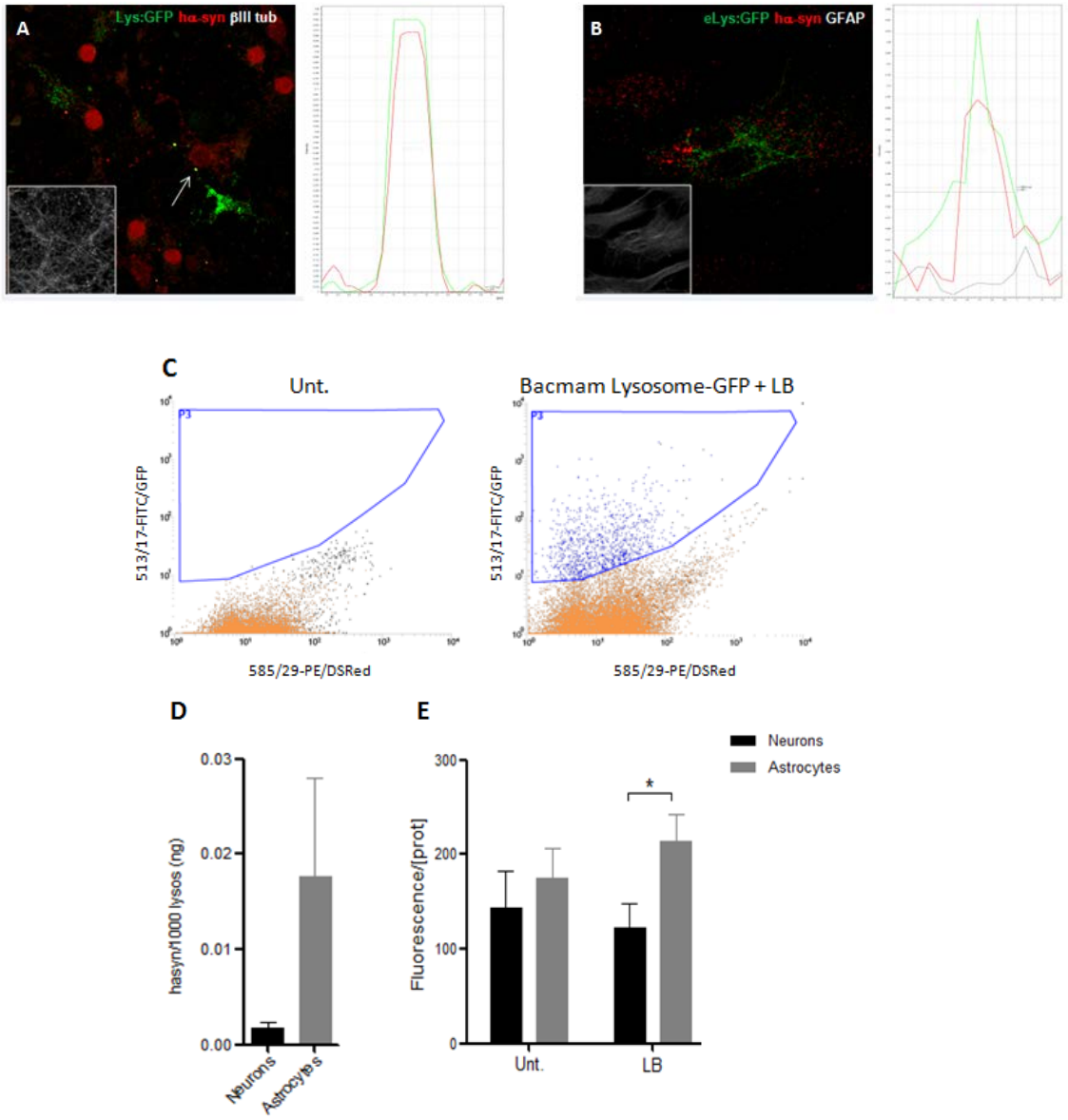


**Figure 1.4. Lysosomal clearance of α-synuclein in neurons and astrocytes.** (A) Lysosomes from treated rat neurons and astrocytes (120pg/ml LB) were labeled after baculovirus infection as in figure 1.3. Co-localization of lysosome marker with hα-syn is shown in yellow and demonstrated in the histograms. Scale bar: 20 µm. (B) eGFP labeled lysosomes were sorted by FACS. On the left part of the panel is shown the unlabeled fraction whereas in the right part the GFP fraction is gated in blue. ELISA assay detected a higher, but not significant, amount of hα-syn in lysosomes from astrocytes comparing to lysosomes from neurons. (C) Fluorimetric assay for Cathepsin D activity revealed an increase in the lysosomal activity in astrocytes compared to neurons. Statistical analysis was performed using t-test (n=3). * indicates a significant difference ($p < 0.05$).

In order to assess if the accumulation of hα-syn corresponds to a further response in the clearance machinery of the cells, we studied the lysosomal activity of treated cells. Specifically, we measured the activity of Cathepsin D, a lysosomal protein implicated in the degradation of α-syn (Sevlever et al, 2008). After 72h of LB treatment, we lysed the cells and quantified Cathepsin D activity by fluorometric assay. We found an increase in the activity of the protein in astrocytes compared to neurons when they were treated with LB. Altogether, these data suggest a more efficient metabolization of hα-syn by astrocytes compared to neurons. This indicates that hα-syn after internalization through the endocytic pathway traffics to lysosomes in both neurons and astrocytes.

### 1.4 Mitochondrial metabolism is activated in LB treated astrocytes compared to neurons

In order to study other possible metabolic alterations induced by the internalization of hα-syn, we investigated the metabolism and activity of mitochondria in neurons and astrocytes. We measured oxygen consumption rates (OCR) in cells chronically treated for 72 h with LB (Fig 1.5 A).

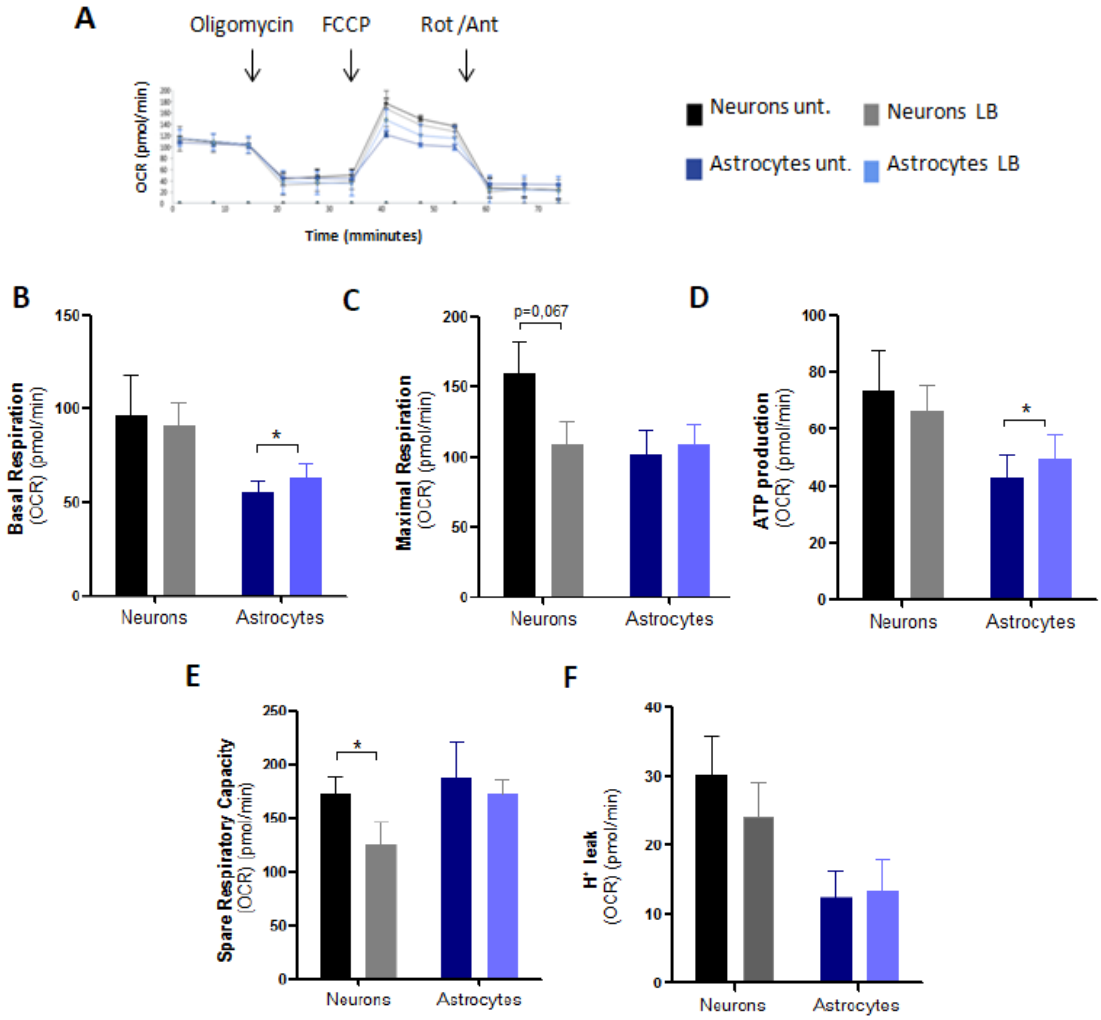


**Figure 1.5. Effects of hα-syn in mitochondrial function in rat astrocytes and neurons**. OCR is decreased in LB treated neurons compared to controls. In astrocytes, LB treatment seems to increase the OCR when treated with LB vs the controls (A). Basal respiration (B) and ATP production (D) OCR increases in LB-treated astrocytes but not in neurons. Spare respiratory capacity is decreased in LB treated neurons (E). No statistically significant changes occurred in maximal respiration (C) and $H^+$ leak (F). Statistical analysis was performed using t-test. * indicates a significant difference ($p < 0.05$).

The basal respiration and ATP production of neurons is basically higher than the astrocytes but only the latter can increase the respiration following the LB treatment, suggesting an activation of the mitochondrial metabolism in response to an energetic demand (Fig. 1.5 B, D). In contrast, neurons treated with LB decreased the spare respiratory capacity, suggesting a difficulty to produce extra ATP in case of a sudden increase of energy demand (Fig 1.5 B-F). We did not observe any significant changes in

proton leak in neurons nor in astrocytes. We also measured the OCR in cells acutely treated with LB for one day but we did not observe any significant change (data not shown). These data suggest that astrocytes, only after internalization of α-syn, respond efficiently to an energetic demand while neurons fail to activate their mitochondrial metabolism in the presence of the hα-syn insult.

### 1.5 hα-syn is transmitted cell-to-cell between neurons and astrocytes

A key feature of proteinopathies in general and synucleinopathies in particular is the occurrence of cell-to-cell passage of toxic prion-like proteins. Transport of α-syn from neurons to other cells was already described earlier (see Vargas et al., 2019 for a review) suggesting a mechanism similar to the prion toxicity. Here we wanted to confirm these results and study if astrocytes can function as vectors for α-syn transportation and/or neuronal toxicity. Using a microfluidic chamber system, we investigated whether hα-syn, once uptaken, can be transported from cell to cell. We seeded astrocytes and/or neurons in two different compartments of the microfluidic chamber at the same time. We called the cells incubated with LB as "donors" and the cells receiving the α-syn by transport to the other compartment as "receptors". The cells were in contact only through the microchannels (5 µm height and 10 µm width) and passive transport was avoided by incubating the "receptor" cells with the double of medium indeed increasing the fluidic pressure (Fig.1.6, A). We then checked by immunofluorescence if hα-syn moved from the "donors" to the "receptor" cells by using the antibody LB509 raised against the human synuclein. Interestingly, we found that, after 120 h of incubation, exogenous hα-syn was intercellularly transported from neurons to astrocytes (Fig. 1.6 B), from astrocytes to neurons (Fig. 1.6 C), from astrocytes to astrocytes (Fig. 1.6 D) and from neurons to neurons (Fig. 1.6 E). Insets in figure 1.6 feature higher magnification pictures showing that hα-syn is preferentially associated with the tight cellular contacts in the microchannels, suggesting a possible transport through such tight contacts. The fact that astrocytes take up hα-syn so efficiently and can transmit it to neighbouring cells through physical contact suggests that astrocytes can actively participate in the spreading of the LB pathology.

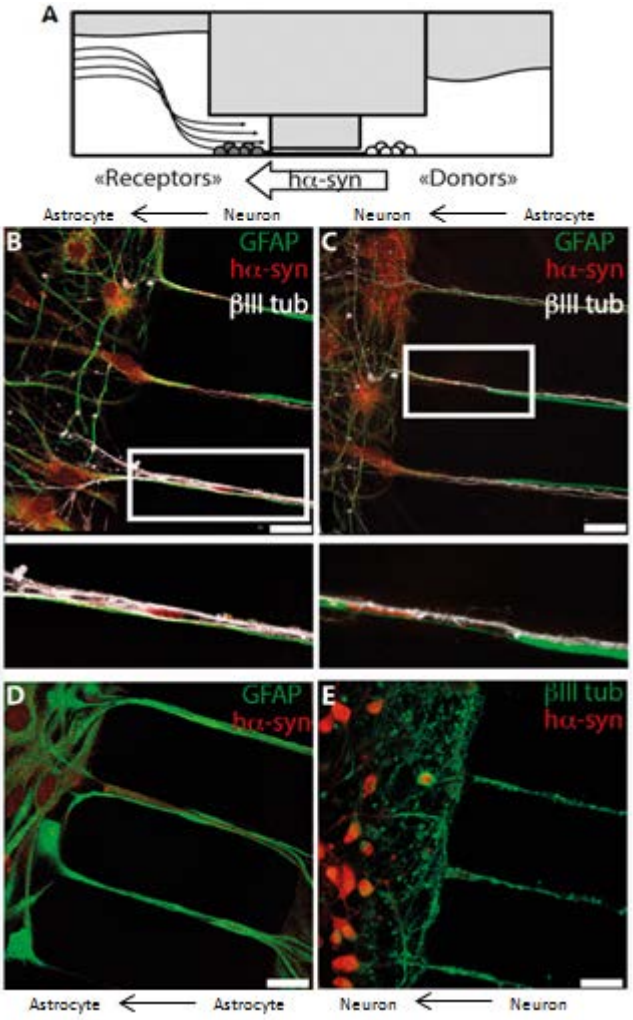


**Figure 1.6. Cell-to-cell passage of hα-syn**. (A) Microfluidic chamber scheme showing fluid level at both side and pressure direction. hα-syn was incubated with "donor" cells and transported intracellularly against fluid flow (arrows), to the "receptor" cells. The inset in A shows the microgrooves (B–E) Rat cortical neurons (βIII tubulin+ cells) and astrocytes (GFAP+ cells) were seeded in the microfluidic chamber. Human LB fractions were incubated for 120 h and hα-syn (in red) transported in the direction of the arrows. Different combinations of cells were assayed, from astrocytes to neurons (B), from neurons to astrocytes (C), astrocytes to astrocytes (D) and neurons to neurons (E). Higher magnification at the level of microgrooves (white squares) shows the tight contacts between neurites and astrocytic processes. Scale bar: 20 μm.

To exclude that "receptors" cells had spread their processes to the "donor" cells compartments during LB incubation, we first seeded the "donors" cells and let them

grow for 7 days prior to the "receptors" cells. Also in this case we observed hα-syn within the "receptors" cells after 120 h of LB incubation, confirming that hα-syn is actively transported from cell to cell (Fig 1.7, last column).

Active transport was also demonstrated by treating the "donors" cells with D15, an inhibitor of endocytosis and cellular transport (Fig. 1.7). This pharmacological treatment before and during the LB incubation prevented the endocytosis of hα-syn in "donor" cells and the further transport to the "receptors" cells, confirming the active process of α-syn transportation and the absence of passive diffusion.

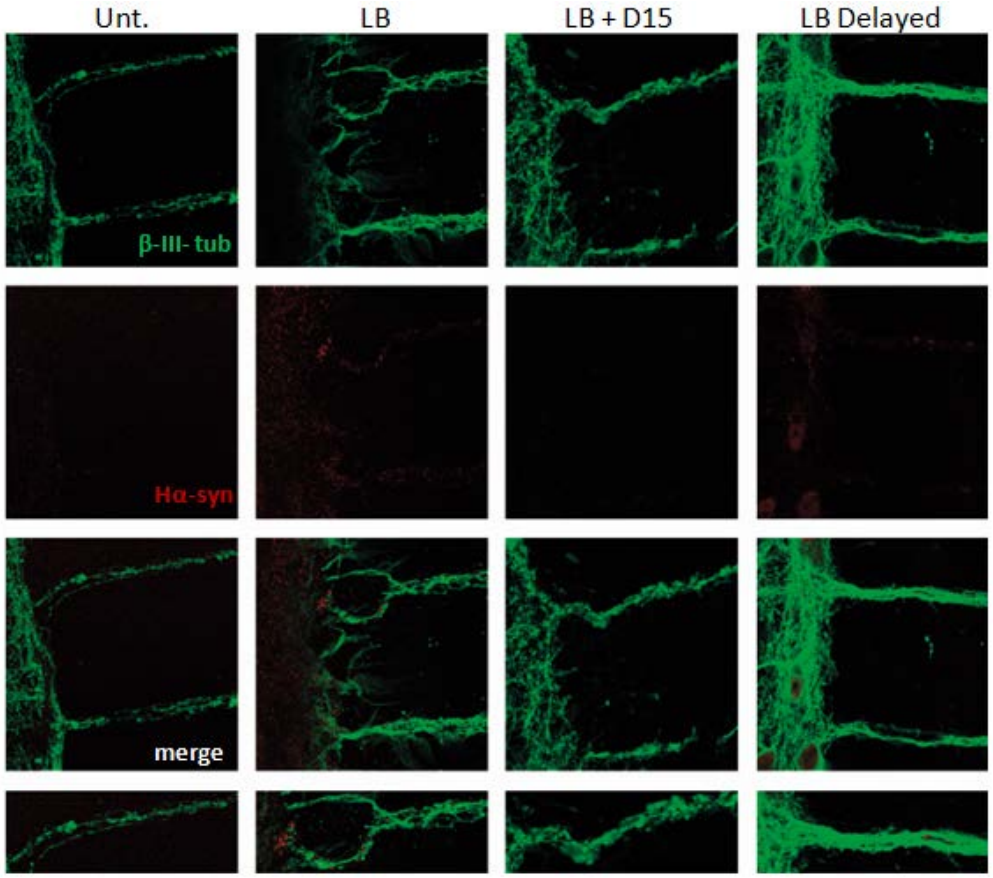


**Figure 1.7. Inhibition of hα-syn transmission**. Neuronal cultures seeded in microfluidic chambers were incubated in the presence of PBS (CTRL), LB or LB with 50 μg/ml of D15, to prevent non-specific hα-syn uptake; "receptor" cells were seeded one week later than "donors" (delayed) to prevent neurite spreading into "receptor" chamber. After 5 days, neuronal cultures were fixed and stained with βIII tubulin (green) and anti-human α–synuclein LB509 (red). Last row represents 2 × magnification of double fluorescence in microgrooves of microfluidic chambers. Scale bar: 20 μm.

## 1.6 Astrocytes spread neurotoxicity by α-syn transmission

After we demonstrated that astrocytes can internalize exogenous α-syn and transport it to neurons, we investigated if astrocytes could represent a vector for α-syn toxicity to neurons. To that end, we incubated "donors" astrocytes with LB fractions and measured neuronal apoptosis in the "receptor" compartment by DAPI or propidium iodide staining (Fig. 1.8). We observed that hα-syn had little effect on the apoptosis of "donors" astrocytes whereas apoptosis of "receptors" neurons significantly increased (approximately 40% in Fig.1.8 E). Notably, neuronal apoptosis induced by hα-syn transported from the astrocytes was higher than apoptosis triggered by direct application of LB to neurons (as shown in Fig. 1.2).

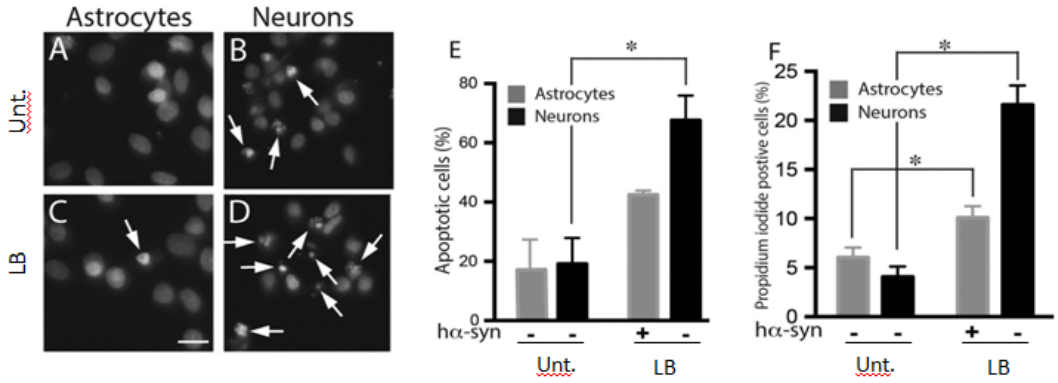


**Figure 1.8.Transmission of hα-syn from astrocytes to neurons induces neuronal apoptosis**. Rat cortical neurons and astrocytes were seeded into the microfluidic chambers as "receptors" and "donors" cells, respectively. Human LB fractions were added to the astrocyte (+) compartment. After 5 days of incubation, both astrocytes and neuronal nuclei were stained with DAPI (A–D) or with propidium iodide (F). Apoptotic cell death was calculated in both compartments as a percentage of condensed nuclei (white arrows) vs total nuclei (E) or as a percentage of PI positive cells vs DAPI (F). In the untreated "Unt." chamber, used as control for basal apoptosis, not neurons (-) neither astrocytes (-) were incubated with LB (A, B). Statistical analysis was performed by using *t*-Test Student ($n = 6$, * $p < 0.01$). (A–D) scale bar: 20 µm.

Our data clearly show that hα-syn applied, and transported, from astrocytes to neurons can kill neurons with a greater efficacy. Although we do not have an

explanation for this unexpected finding, we hypothesize that LB fractions triggers in astrocytes the release of substances that may increase LB- transported neurotoxicity further.

## 1.7 Uptaken hα-syn activates the overexpression of endogenous α-syn in both neurons and astrocytes

Next, we asked if exogenous α-syn could activate autologous mechanisms of cell death. Neurons and astrocytes were exposed for 24, 72 and 120 h to hα-syn-containing LB fractions and, after Western blot against endogenous α-syn (rα-syn) we observed interestingly, that cells taking up exogenous hα-syn responded by increasing linearly the expression of endogenous rα-syn over-time (Fig. 1.9 A and B). Both cell types up-regulated the expression of rα-syn already after 72 h of treatment (Fig. 1.9 B) with a stronger increase in neurons with levels of expression up to 19-fold after 120 h of treatment. On the other hand, up-regulation of rα-syn in astrocytes, was only 6-fold (Fig. 1.9 B). We decided to treat cells in multiwell and not in microfluidic experiments because the number of cells used in the microfluidic chambers were not sufficient to extract enough amount of total protein. In line with data obtained with Western blot analysis, immunofluorescence with specific antibody against rα-syn confirmed the upregulation of endogenous α-syn induced by LB fractions in astrocytes (Fig. 1.9 C) and neurons (Fig. 1.9 D). Taken together, these results, in accordance with those previously shown, also suggest a higher susceptibility of neurons to hα-syn-containing LB fractions. Moreover, we observed that endogenous rα-syn had an intracellular distribution different from that up taken hα-syn, localizing especially at membrane level, whereas hα-syn is more cytosolic (Fig. 1.9 C and D).

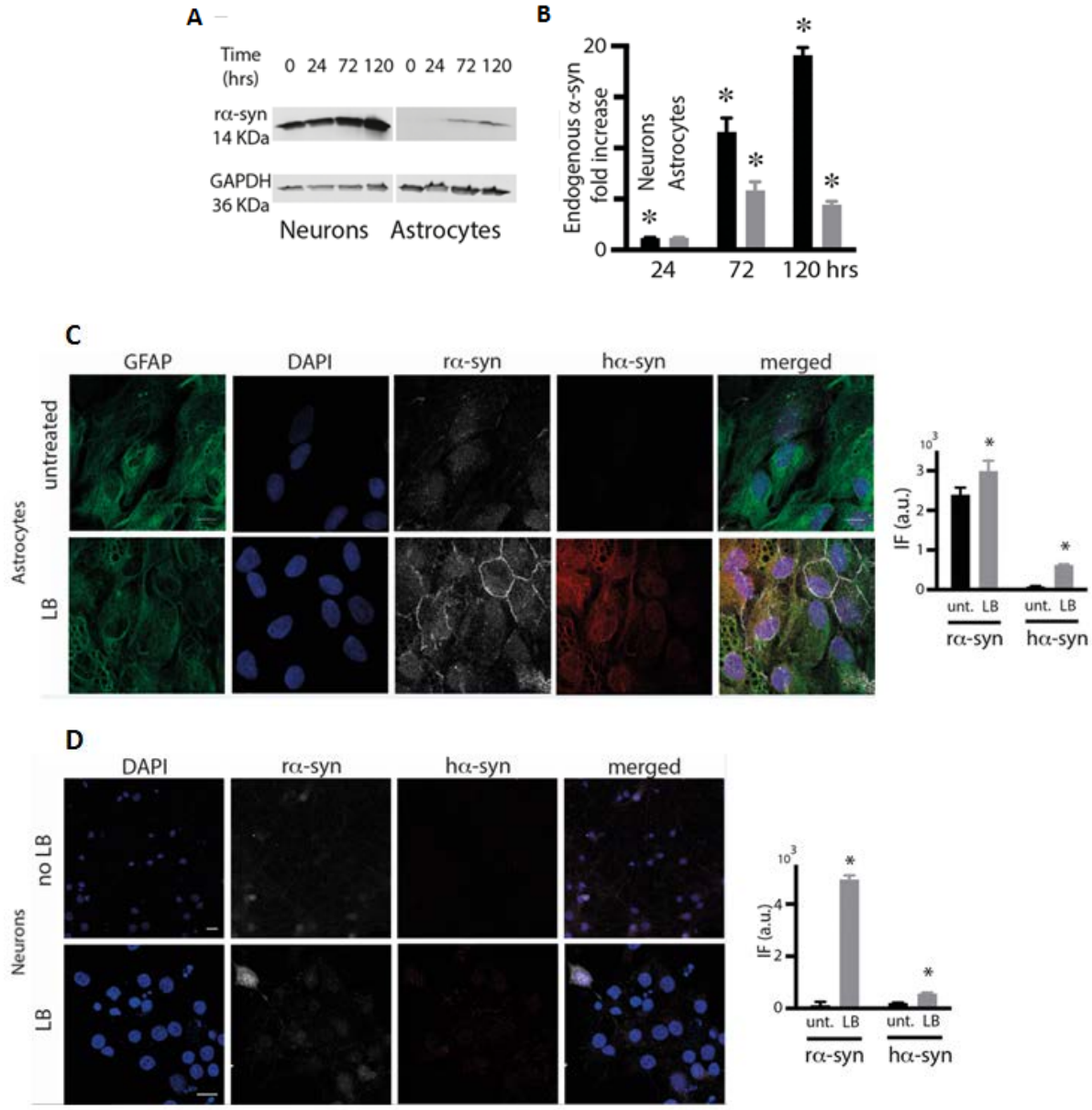


**Figure 1.9. Hα-syn induces overexpression of endogenous α-syn in both neurons and astrocytes.** (A) Western blot of endogenous rα-syn in neurons and astrocytes previously incubated with hα-syn for 24, 78 and 120 h After incubation, cells were washed with HBSS and total protein extracted for Western blot analysis. Detection of endogenous rα-syn was performed by using the rodent-specific antibody D37A6 and (B) quantified by fluorescence after normalization with GAPDH (each point was duplicated in the WB assay). Statistical analysis was performed using two-way ANOVA. * indicates a significant difference ($p < 0.05$) compared to control, non-treated, neurons and astrocytes respectively. Immunofluorescence staining of rα-syn expression after hα-syn exposure in astrocytes (C) and neurons (D) and its quantification by intensity level. Astrocyte and neuron cultures were incubated for 5 days with hα-syn, then fixed and stained with anti-GFAP (green), , anti-rα-syn (white), anti-hα-syn (red)

and nuclei, counterstained with DAPI (blue). Scale bar: 20 μm. Quantification was calculated for densitometry in 6 different fields using the public software Image J. Data are expressed as arbitrary units after threshold subtraction. * indicates a significant difference ($p < 0.05$) compared to control, non-treated cells.

## 1.8 Levels of oligomeric hα-synuclein are similar between neurons and astrocytes after transmission from astrocytes

Because none of the antibodies used to detect α-syn can discriminate between oligomeric (toxic) and monomeric form we used the α-synuclein proximity ligation assay (AS-PLA), a novel technique that allows the detection of protein-protein interactions with a very high sensitivity. In our case, AS-PLA selectively recognizes oligomers of human origin, while presenting minimal recognition of monomeric and fibrillar hα-syn. We wondered whether the α-syn we observed in astrocytes and neurons could be in form of oligomers, thus triggering the neuronal death or astrocyte resistance. We detected the typical spotted signal in both neurons and astroctytes treated with LB for 72 h, indicating the presence of oligomeric species of hα-syn. After quantification, the total number of PLA puncta was similar between the two cell types (Fig. 1.10 A).

We also performed the AS-PLA in microfluidic experiments to understand if astrocytes can transfer oligomeric ha-syn and induce neuronal toxicity. We incubated "donors" astrocytes with LB fractions and three days after the treatment, cell cultures where fixed. In order to detect oligomeric and total hα-syn we performed the AS-PLA assay and co-inmunofluorescence with the syn211 antibody respectively. AS-PLA spots and total α-syuclein were counted per field in the astrocytes ("donor") and in the neuron ("receptor") compartments. We didn't find significative differences of ha-syn oligomers (AS-PLA) nor in the total apha synuclein (antibody's signal) between the two compartments (Fig 1.10 B and C), suggesting that the increase of oligomeric species of the hα-syn is not directly responsible of the neurotoxicity.

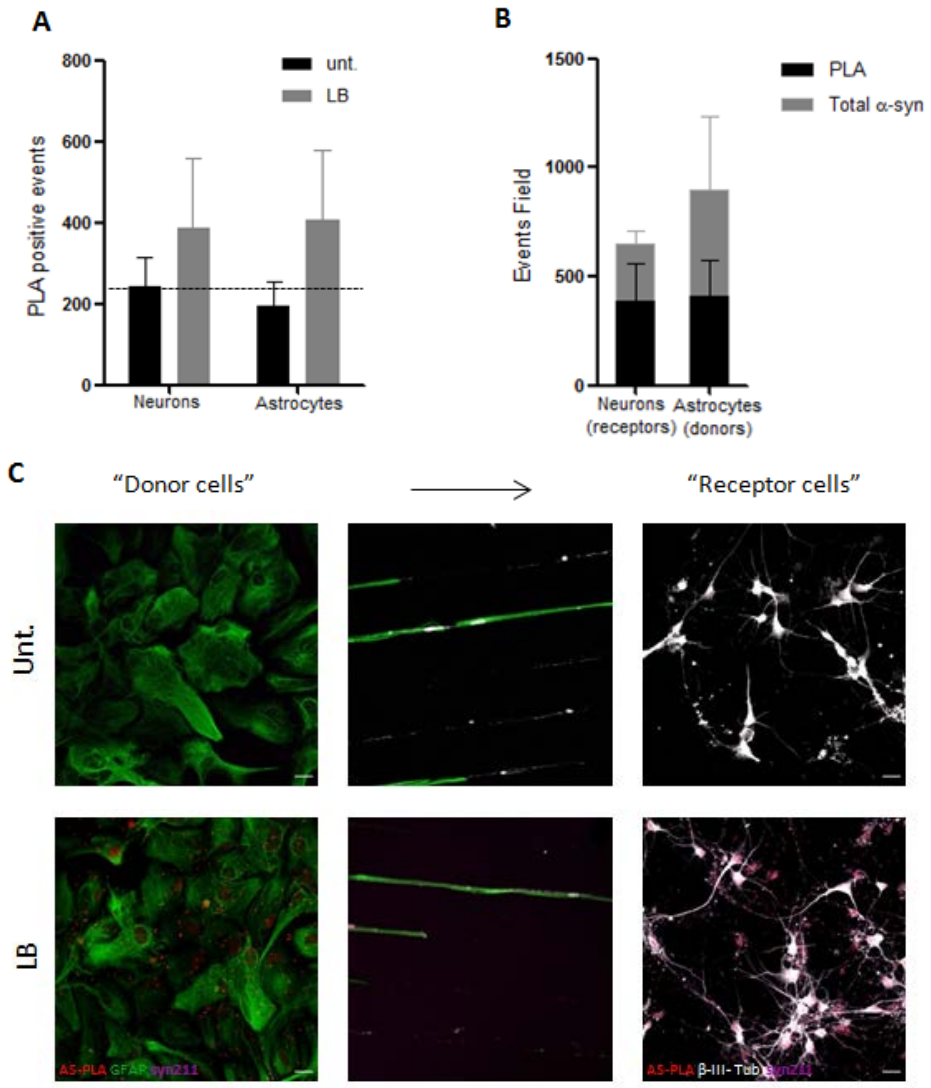


**Figure 1.10. Detection of oligomeric species of hα-syn by PLA**. (A) Rat cortical neurons and astrocytes were treated with LB fractions for 72, and then stained by PLA. PLA puncta were found both in neurons and astrocytes. (B, C) In microfluidic experiments, LB was added to the astrocyte side and five days later, oligomeric and total α-synuclein were measured both in the astrocyte (donor) and in neuron (receptor) compartments. No differences were found neither in the total hα-syn nor in the PLA puncta. Quantification of normalized puncta per field (4 fields) in triplicate experiments (n=3) using a One-way ANOVA (Bonferroni, * $p < 0.05$). Scale bar: 20µm.

## Summary I

In this first part we confirmed that both neurons and astrocytes endocytose exogenous hα-syn (LB extracts). This process results in an increase of toxicity in neurons whereas astrocytes are more resistant. Indeed, astrocytes exhibit an increase in lysosomal activity and activate mitochondrial metabolism in response to exogenous hα-syn, as demonstrated by the increase of basal respiration and ATP production. Moreover, we have demonstrated that exogenous hα-syn can be transmitted between the cells directly in every possible combination. Interestingly, astrocytes induce neuronal apoptosis through the hα-syn transportation, in part activating an endogenous program of α-syn translation. Altogether, we conclude that astrocytes represent an important element in the onset and spread of neuronal toxicity induced by α-synuclein.

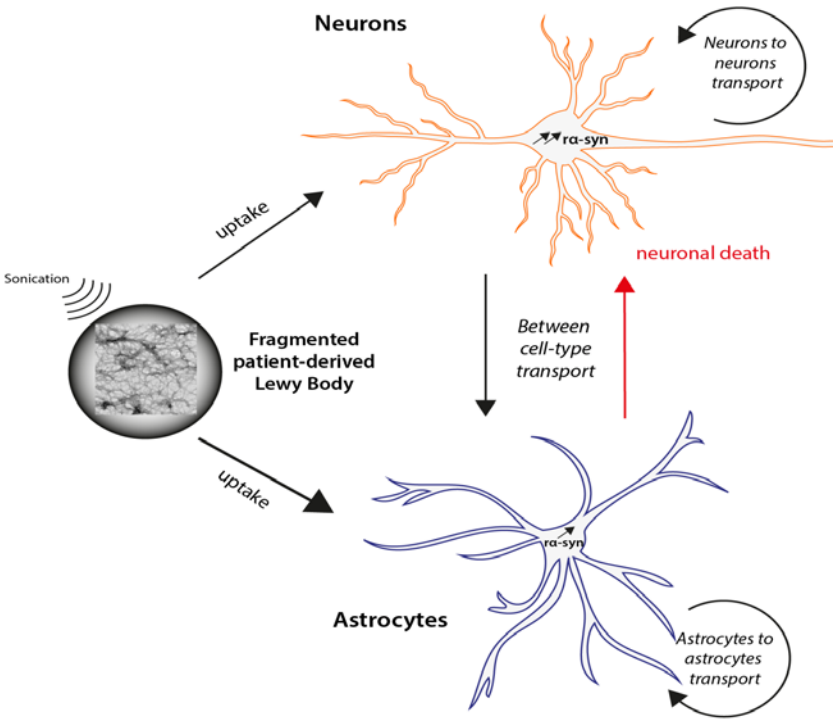


**Figure 1.11. Schematic representation of results obtained in rat primary cultures.**

# Results - Part II

## 2.1 Generation and characterization of highly homogeneous iPSc derived functional astrocytes

Human astrocytes were generated from reprogrammed fibroblast into iPS cells using modifications of previously published protocols (Mormone et al., 2014; TCW et al., 2017). Astrocytes were obtained from four independent donors: two PD patients carrying LRRK2$^{G2019S}$ mutation (PD1 and PD2), and two matched healthy controls (Ctrl 1 and Ctrl 2) (see Experimental Procedures, Table 3 for details).

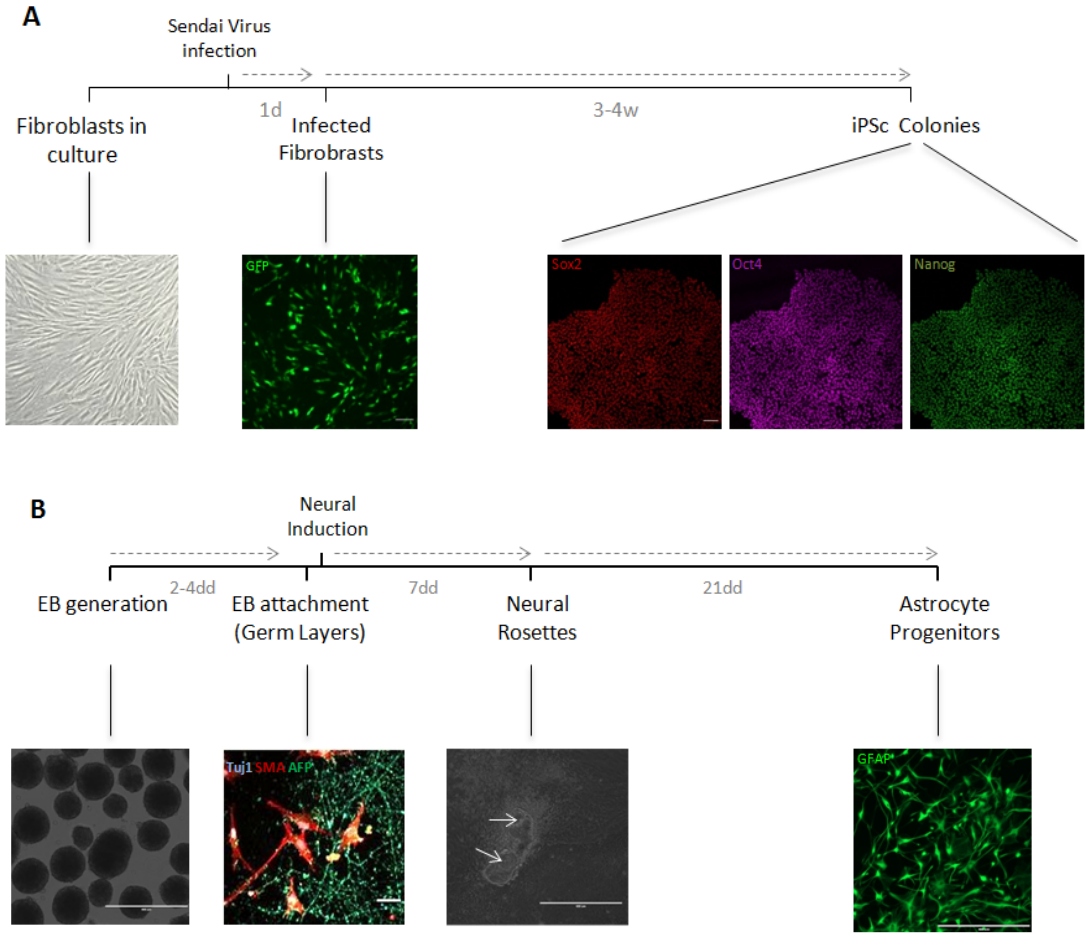


**Figure 2.1. Human astrocyte generation process.** (A) Fibroblasts were reprogrammed to iPSc by Sendai virus infection containing the 4 Yamanaka factors (MOKS). Three weeks later, reprogrammed fibroblasts generated iPSc colonies, which were positive for Sox2, Oct 4 and Nanog pluripotency markers. (B) Embryoid bodies (EBs) generated from iPSc were positive for three germ layers markers (Tuj1, SMA and AFP). One week after the neural induction, neural rosettes were formed and selected for astrocyte differentiation. Twenty one days later, almost all of the cells became astrocyte progenitors and were positive for GFAP and S100β.

The iPSc generated from fibroblasts were characterized by immunofluorescence using the pluripotency markers SOX2, Oct4 and Nanog (Fig. 2.1 A). Thus, positive iPSc colonies were picked and cultured in suspension as Embryoid Bodies (EB). We could maintain a homogenous volume and increase the number of the EB by culturing EB in the Aggrewell microwells. At this stage, cells were able to differentiate to any of the three germ layers; hence, we performed a differentiation assay by immunofluorescence for AFP (Alpha-fetoprotein, endoderm marker), SMA (smooth muscle actin, mesoderm) and Tuj1 (Neuron-specific class III beta-tubulin, ectoderm). Indeed, EBs were able to differentiate to each of the different lineages, confirming the pluripotentiality of the cells. Then, to induce the differentiation of the cells into the neural linage, we favored the formation of Neural Rosettes (Fig. 2.1 B, see also Materials and Methods for more details). Properly formed neural rosettes were selected, disaggregated at single cell level and seeded in a laminin mix (LN211+LN111) coated plates. This specific laminin mix imitates the extracellular matrix of the astrocytes, favoring the formation of astrocytes progenitors already positive for the GFAP marker (Fig. 2.1 B) (Yap et al., 2019). After 60 days of maturation, cells remained positive for GFAP and S100β, but negative for the markers of other neural derived lineage, MAP2 and βIII-tub (neurons) and NG2 (oligodendrocytes) showing the astrocyte phenotype in approximately the 95% of the population as evidenced by immunofluorescence and by cytofluorimetry assay for GFAP (Fig. 2.2 A-B).

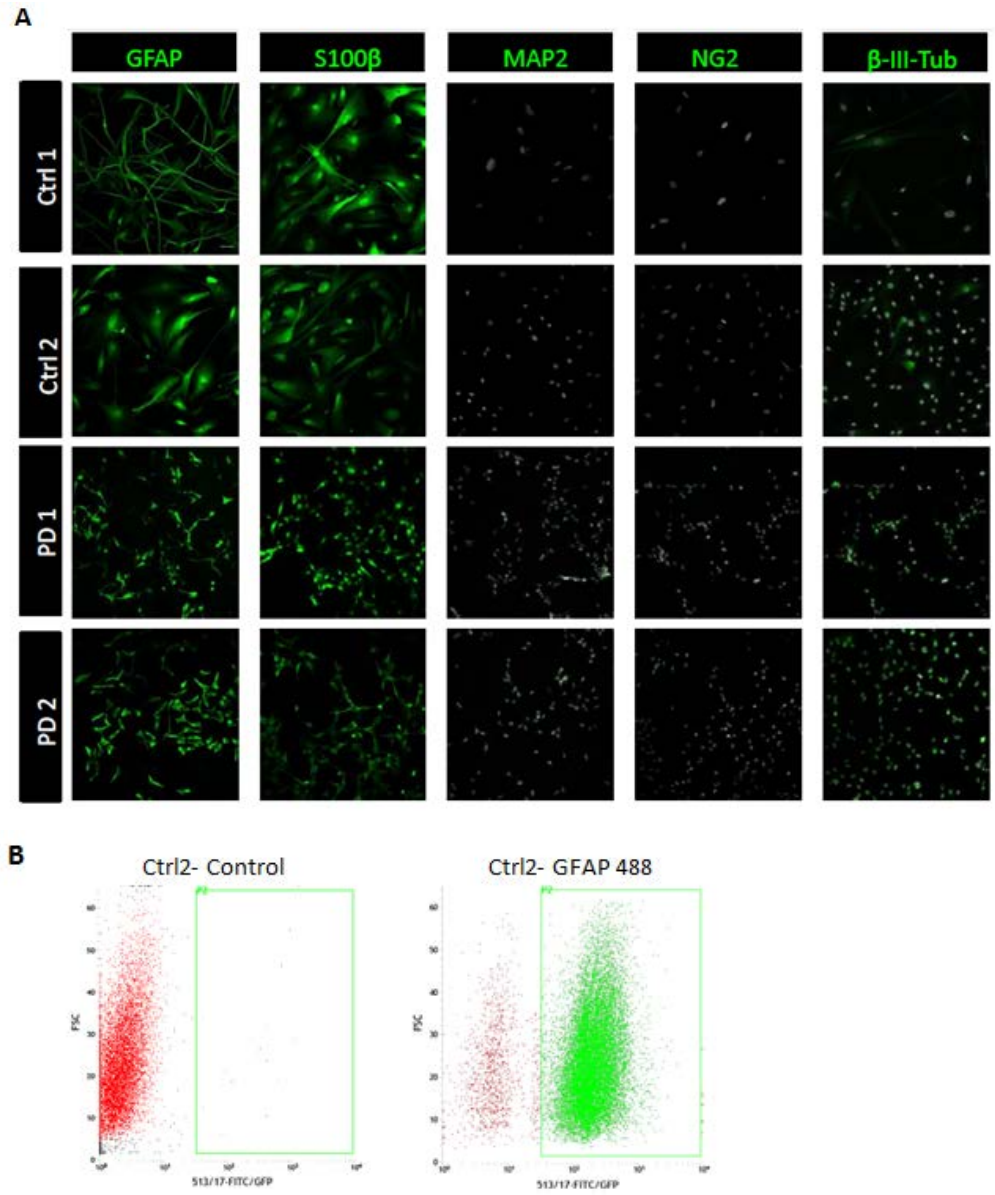


**Figure 2.2. Characterization of mature human astrocytes.** (A) After 60 DIV, mature astrocytes were positive for the astrocyte markers GFAP and S100β but negative for MAP2 (neurons) or NG2 (oligodendrocytes). Nevertheless, we observed a low expression of β-III-tub. Scale bar 20µm. (B) Cytofluorimetric analysis confirms that approximately 95% of the cells were positive for GFAP (Ctrl 2 is shown as an example).

## 2.2 Parkinson´s Disease astrocytes display atrophic morphology

During the process of final differentiation, we observed by simple phase contrast analysis that the size of the astrocytes generated from the PD patients was

dramatically smaller and with a simpler complexity compared to the control lines (see also figure 2.2A).

The morphological analysis of astrocytes was performed after immunofluorescence by measuring the area marked by GFAP. We found important differences between control and PD astrocytes in terms of size (area). As evidenced by microscopic analysis, the area of the control astrocytes was up to 8 times bigger than the PD astrocytes (Fig. 2.3).

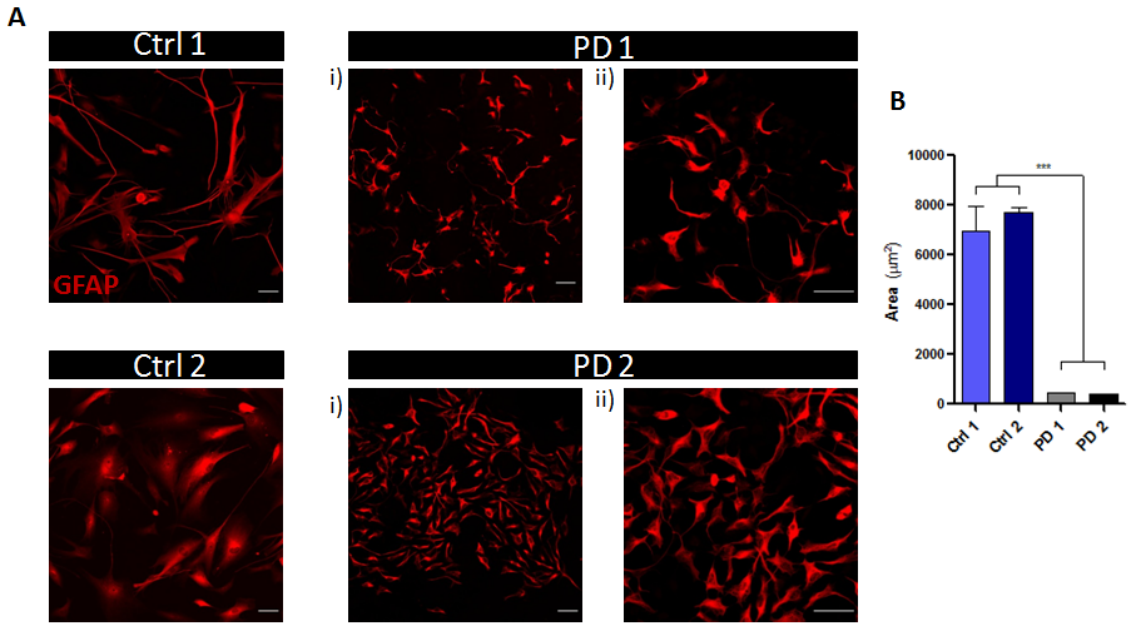


**Figure 2.3 Quantification of human astrocytes area.** (A) Immunostaining with GFAP antibody in Ctrl and PD astrocytes. ii) Represent a higher magnification of i) Scale bar: 20µm. (B) Measurement of the area reveals that Ctrl astrocytes are up to 8 times bigger than PD astrocytes. (p=0,05*; One way-ANOVA)

We further analyzed the morphology and complexity of the cells by High Content Screening technology, a machine learning method that guarantees the reproducibility of the measurement. After GFAP labeling, we confirmed the measurement of the area, together with the analysis of the perimeter and the ShapeP2A, an index for the complexity of the cells that takes in account both perimeter and area of the cells (expressed as $4*\text{perimeter}^2/\pi*\text{area}$). We found that PD astrocytes were less complex as compared to the controls (Fig 2.4).

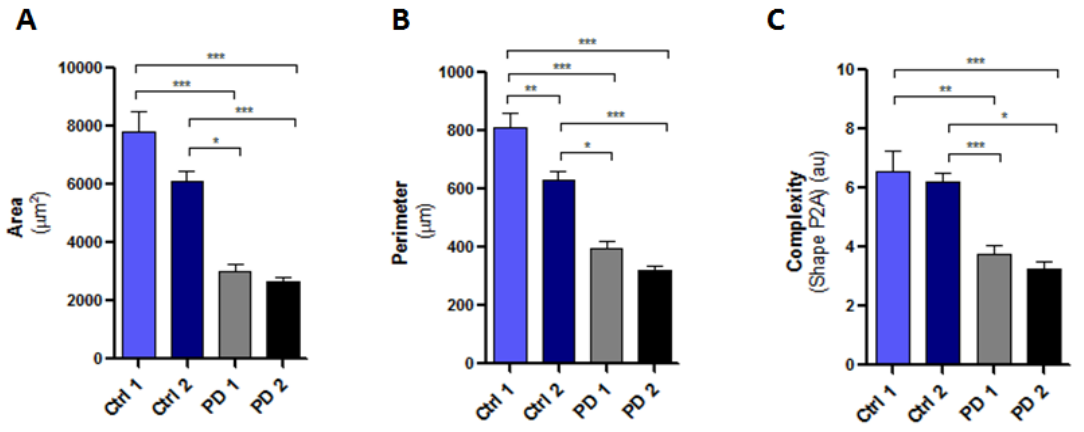


**Figure 2.4. Morphological analysis of human astrocytes.** Measurement of the area (A), perimeter (B), and the complexity index (C) of Ctrl and PD astrocytes reveals that Ctrl astrocytes are bigger and more complex PD astrocytes (p=0,05*; One way-ANOVA).

Together, these data suggest that PD astrocytes have an atrophic and less complex morphology compared to control astrocytes suggesting a deficient support for the basal neuronal functions.

## 2.3 Astrocytes characterization by functional Calcium imaging.

In order to analyze the functionality of generated astrocytes and to characterize the response to generic stimuli, we measured basal intracellular calcium and analyzed the effects of several modulators like ATP and FCCP on intracellular calcium levels $[Ca^{2+}]_i$. We did not observe $[Ca^{2+}]_i$ influx in basal conditions in any of the lines (Fig. 2.5 A). However, astrocytes responded to ATP (100 µM) and FCCP (1 µM), by increasing the levels of $[Ca^{2+}]_i$. The response to ATP was similar for Ctrl 2 and PD lines whereas Ctrl 1 showed a stronger response to extracellular ATP (Fig 2.5 B). We incubated the astrocytes with FCCP to monitor the mitochondrial membrane potential (ΔΨm) as a measure of mitochondrial health and cell viability. Exposure to FCCP did not evidence significant differences in $[Ca^{2+}]_i$ levels between Ctrls and PD (Fig 2.5 C). This result was also confirmed after time lapse recording of cell fluorescence and quenching of Rhodamine 123 with FCCP (Fig 2.5 E). Altogether, these findings confirmed that the generated astrocytes express functional receptors for ATP and have similar

mitochondrial membrane potential with no significant differences between cells originating from healthy controls and PD patients.

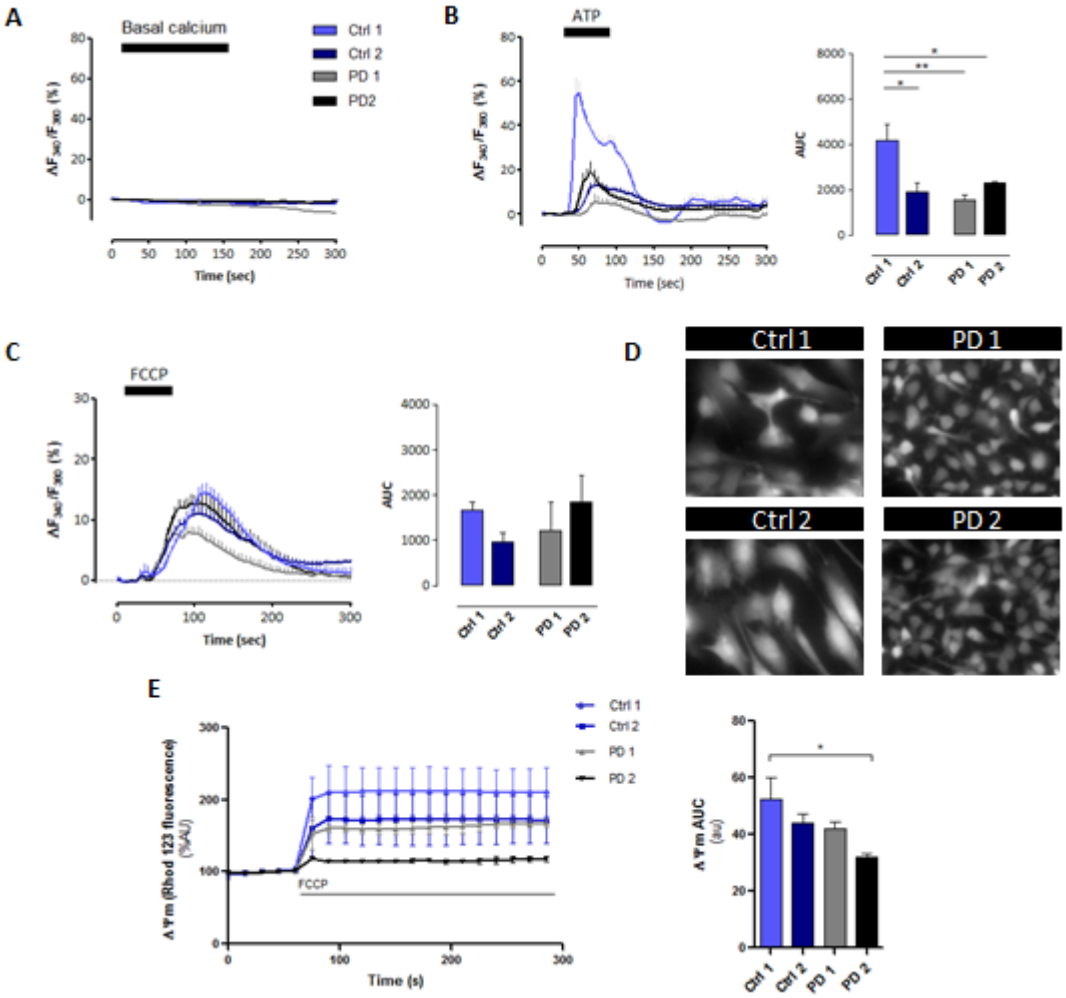


**Figure 2.5. Measurement of $Ca^{2+}$ responses to diverse modulators in human astrocytes**. (A) Measurement of the basal intracellular $Ca^{+2}$ does not show any difference in fura-2 fluorescence between lines. (B) PD astrocytes and Ctrl 2 show lower intracellular $Ca^{+2}$ levels after addition of ATP (100 µM) compared to Ctrl 1, even if all the lines respond to this agonist. (C) $[Ca^{+2}]_i$ levels increase similarly after the addition of FCCP (1 µM) in Ctrl and PD lines. (D) Representative images of the four lines after the addition of Fura-2. (E) Measurement of mitochondrial membrane potential. PD 2 shows the lower mitochondrial membrane potential than the remaining lines. Statistical analysis was performed using one way ANOVA. * indicates a significant difference ($p < 0.05$).

## 2.4 Mitochondrial metabolism and morphology in PD astrocytes.

### *2.4.1 PD LRRK2$^{G2019S}$ astrocytes display an impairment in mitochondrial functionality but an aerobic respiration.*

We next analyzed if there were alterations in mitochondrial metabolism between Ctrl and PD astrocytes. Indeed, LRRK2 protein interacts with mitochondrial membranes and many other regulators of mitochondrial respiration. The mutation in this gene affects mitochondrial functionality in fibroblasts or neurons in different PD models**.** Thus, to assess mitochondrial metabolism in PD astrocytes we used different experimental parameters. First, we measured mitochondrial oxygen consumption rate (OCR) of the two groups performing a live-cell metabolic assay. We found that PD astrocytes showed lower OCRs, in terms of maximal and basal respiration (even if not significant) and ATP production compared to healthy astrocytes (Fig 2.6 A-D).

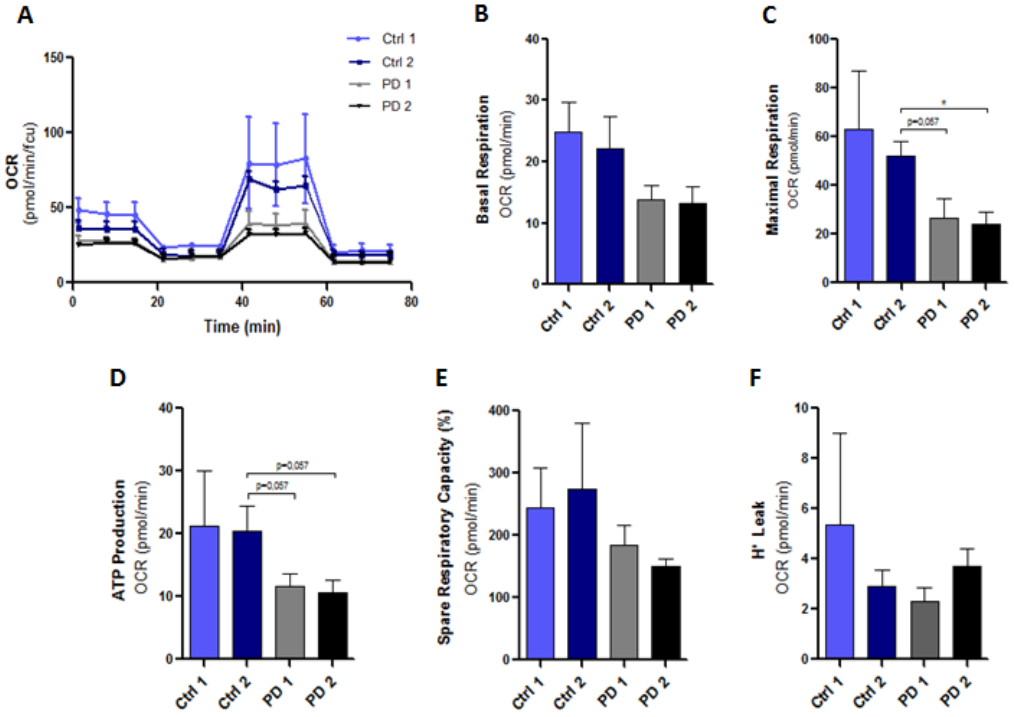


**Figure 2.6. Mitochondrial functionality of control and PD LRRK2$^{G2019S}$ astrocytes.** (A) Oxygen consumption rates (OCRs) of Ctrl and PD astrocytes. (B) Basal respiration (even if not significant), (C) maximal respiration and (D) ATP production are reduced in PD LRRK2$^{G2019S}$ astrocytes compared to controls. (E) Spare respiratory capacity and (F) H+ Leak do not show statistically significant changes (n=4). Statistical analysis was performed using one way ANOVA. * indicates a significant difference ($p < 0.05$).

According to previous results, demonstrating that cells that fail to produce ATP can switch from oxidative phosphorylation to an aerobic glycolytic respiration (Rafikov et al., 2015), we observed in PD astrocytes an increase of general extracellular acidification rate (ECAR). Specifically, we observed a significant 1.5 fold increase of the basal (Figure 2.7B) and compensatory (Figure 2.7E) glycolysis and, concordantly, a similar increase of the proton efflux rate (PER) as a meaning of lactate production (Fig 2.7E).

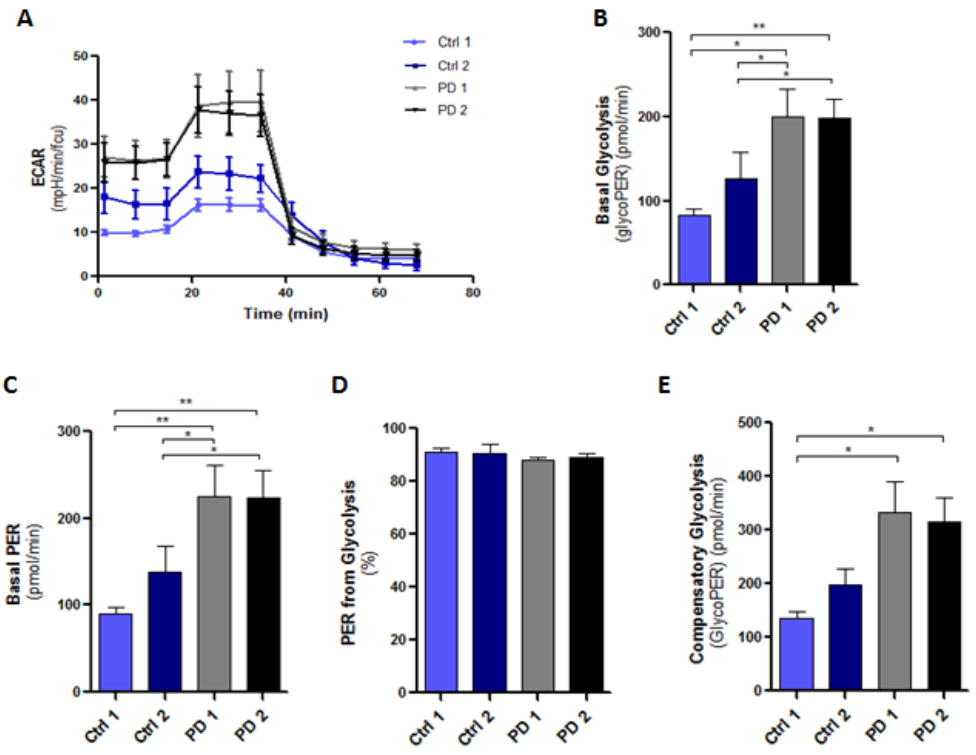


**Figure 2.7. Measurement of the glycolytic activity in control and PD LRRK2$^{G2019S}$ astrocytes.** (A) Extracellular acidification rate (ECAR) of Ctrl and PD astrocytes. (B) Basal glycolysis, (C) Basal proton efflux rate (PER) and (E) Compensatory glycolysis are increased in PD astrocytes compared to the controls. (D) PER from glycolysis is similar in the four lines (n=3). Statistical analysis was performed using one way ANOVA. * indicates a significant difference ($p < 0.05$).

*2.4.2 Mitochondrial morphology is disrupted in PD astrocytes compared to controls.*

Mitochondrial dysfunction is usually corroborated by an altered morphology of the organelle (Picard et al., 2013). Thus, we decided to compare the intracellular distribution and the ultrastructural morphology in healthy and PD astrocytes. Mitochondrial distribution was observed after cell labeling with Rhodamin 123. In healthy astrocytes, mitochondria were elongated and interconnected, forming a homogenous network distributed in the entire cytoplasm, not only in the soma but also in the projections (Fig. 2.8 A, first two images). In contrast, PD astrocytes showed less mitochondria, apparently more fragmented and mainly accumulated at the perinuclear level but not along the processes (Fig 2.8 A, last two images). This distribution was also observed and corroborated after the staining with Mitotracker (data not shown). These observations could partially explain the differences in the efficiency of mitochondrial respiration observed by the OCRs measure.

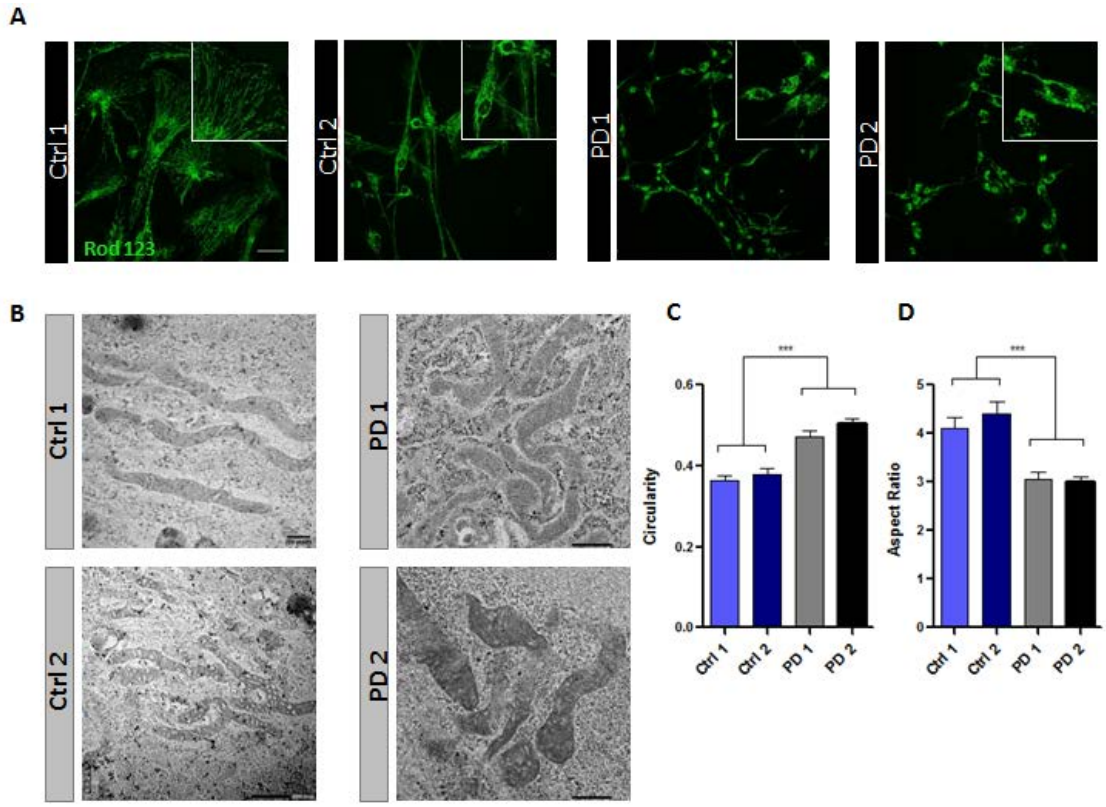


**Figure 2.8. Analysis of mitochondrial morphology.** (A) Mitochondrial staining with Rhodamin 123 showed a very different mitochondrial morphology between Ctrl and PD astrocytes. Squares represent a higher magnification of the field. Scale bar 20µm. (B) Representative

images of mitochondrial ultrastructure in Ctrl and PD astrocytes. (C) Circularity (considers the value of 1 as the perfect circle) and (D) aspect ratio (ratio of circularity vs. elongation) reveal a more rounded shape in PD LRRK2$^{G2019S}$ mitochondria compared to the control which are in contrast more elongated. More than 100 mitochondria were analyzed for each line. Statistical analysis was performed using one way ANOVA. * indicates a significant difference ($p < 0.05$).

The mitochondrial ultrastructure observed by electron microscope evidenced major differences between healthy and PD astrocytes. The measurement of the circularity, which is usually taken as an index of ROS production (Ahmad et al., 2013), evidenced that mitochondria of PD 1 and PD 2 were more rounded than in the controls (Fig 2.8 C). Accordingly, the Aspect Ratio, (the major axis vs the minor axis of the mitochondria) confirmed the difference of morphology between the control and PD lines. Ctrl 1 and Ctrl 2 showed a higher aspect ratio, suggesting the presence of more elongated mitochondria in healthy lines (Fig 2.8 D). It is worth to mention that apparently also the mitochondrial crests seemed to have an altered morphology in PD lines (work in progress).

*2.4.3 PD astrocytes show higher levels of oxidized proteins compared to controls.*

Since mitochondrial oxidative stress causes imbalance in mitochondrial fission/fusion (Wu et al., 2011) and fragmented mitochondria are associated to higher levels of ROS (Jan Ježek et al., 2018), we investigated if metabolic and morphological profiles observed in PD astrocytes corresponded to an altered level of ROS production. We measured the carbonyl groups of total proteins extracted from Ctrl and PD lines as a meaning of protein oxidative status (detected as DNP after derivatization). We found by Oxyblot assay, higher amount of oxidated proteins in both PD astrocytes lines compared to the controls (Fig 2.9 preliminary data), suggesting a basal oxidative status of PD vs Ctrl astrocytes.

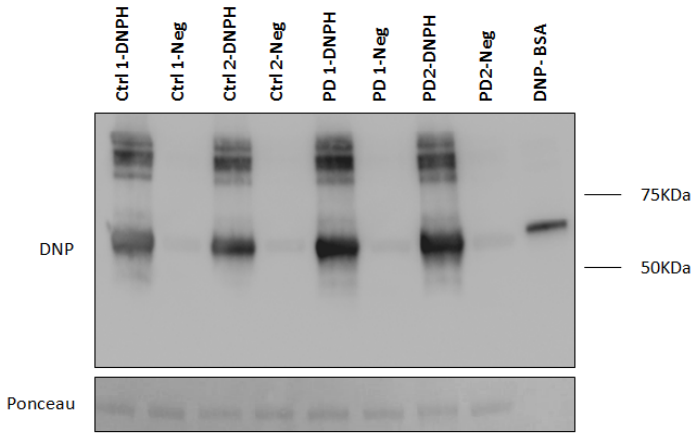


**Figure 2.9. Detection of oxidized proteins in astrocyte protein lysates.** Western Blot for DNP detection show a higher amount of oxidized proteins in PD1 and PD2 compared to both control lines. "Neg" is the non-derivatized negative control of each line. n=1, preliminary result.

Altogether, we suggest that LRRK2$^{G2019S}$ mutation corresponds to a general mitochondrial dysfunction in astrocytes, in terms of mitochondrial respiration, cellular localization and ultrastructural morphology.

## 2.5 PD astrocytes increase the risk of neuronal survival in a neuron-astrocyte co-culture.

To evaluate if astrocyte can trigger the neurodegenerative process observed in PD, we co-cultured human astrocytes with rat primary neurons. Neurons were transfected with the fluorescence protein m-cherry to follow in a longitudinal study (during 8 days in culture) the morphological changes that human astrocytes could induce. Minimal survival time was estimated for each individual neuron in the co-culture and the Cox proportional hazard (CPH) analysis (see Experimental Procedures, part II) indicated that the presence of PD astrocytes significantly increased the risk of death unlike to what observed in the co-cultures with healthy human astrocytes (Fig 2.10).

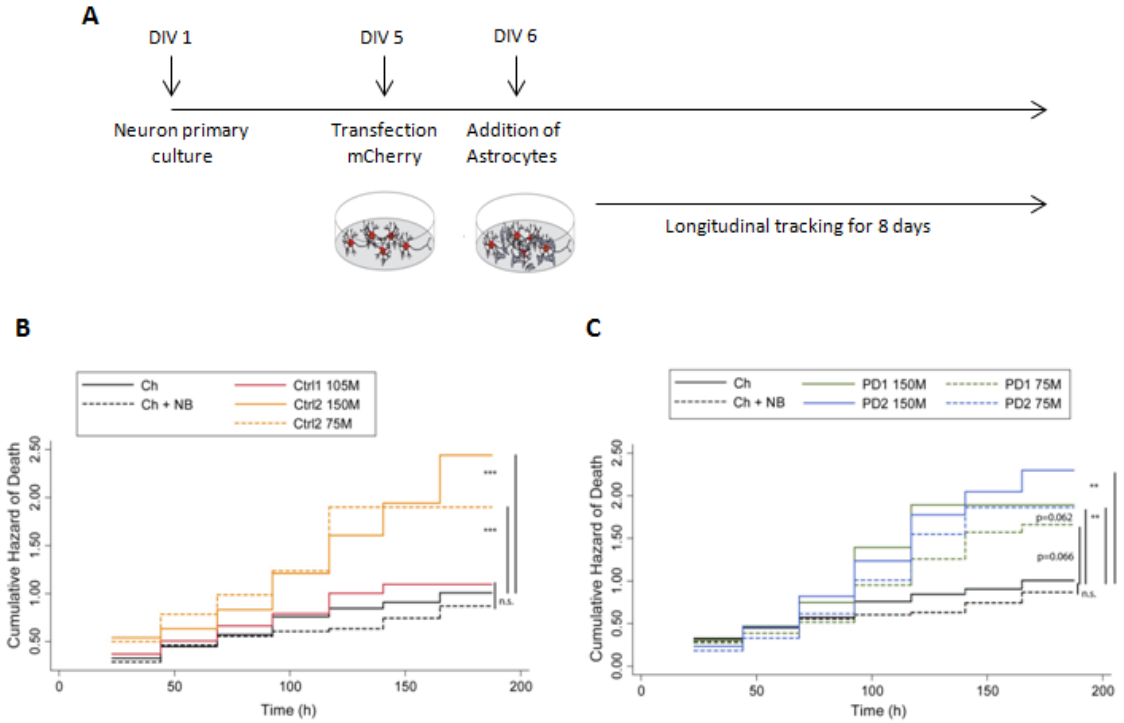


**Figure 2.10. Evaluation of the contribution of human control and PD astrocytes to the risk of neuronal death.** (A) Schematic representation of the set up of the experiment. Five days after seeding the neuronal primary cultures, cells were transfected with the plasmid pCAGG-m-cherry. The day after, human astrocytes were added to the culture and single neurons were tracked longitudinally for 8 days by epifluorescence. (B and C) Representation of the cumulative hazard risk for the neurons generated by the presence of the human astrocytes (log-rank test; n = 2, around 150 neurons per condition, **P < 0.01, ***P < 0.001).

## Summary II

In this second part we have generated and partially characterized functional human iPSc-derived astrocytes from healthy and PD ($LRRK2^{G2019S}$) donors. We have observed for the first time an unexpected atrophic morphology of the mutated astrocytes compared to the controls, with a much smaller area and less complexity than the controls. These astrocytes display compromised mitochondrial morphology, loss of ATP production, less basal respiration and increased glycolytic activity compared to the healthy controls, together with higher production of oxidized proteins. More importantly, the atypical characteristic of PD astrocytes corresponds to an increase of the risk of neuronal death when co-cultured together.

# Discussion

Astrocytes constitute the most abundant glial subtype in the brain and are responsible for a great range of functions that are essential for brain homeostasis and neuronal health. However, until now, there are few studies about their role in neurodegenerative diseases, and concretely in Parkinson´s Disease. Nevertheless, those studies have demonstrated the important implication of astrocytes in the pathophysiology of the disease, revealing that the disruption of astrocyte biology can be involved in dopaminergic neuron degeneration. In this work, we have demonstrated the implication of astrocytes in the onset and progression of PD in two different models: rat primary cultures treated with human LB extracts, which mimics the sporadic cases of PD, and human iPSc derived astrocytes with LRRK2$^{G2019S}$ mutation, as an example of the genetic forms of the disease.

In the first part of the work, we confirmed that both rat neurons and astrocytes in contact with LB extract internalized exogenous hα-syn by endocytosis. Incorporation of hα-syn resulted in neuronal toxicity whereas astrocytes were more resistant. Indeed, astrocytes exhibited increased lysosomal activity and activated mitochondrial metabolism in response to exogenous hα-syn. Moreover, astrocytes, can transport non-degraded hα-syn to neurons and induce neuronal death activating the endogenous program of α-syn translation (Fig 1.10). We propose that lower lysosomal activity, lower mitochondrial metabolism and the activation of the endogenous α-syn can be among the mechanisms responsible for neuronal death in PD (see Figure 1.11).

In the second part, we have generated and characterized human iPSc derived astrocytes carrying the LRRK2$^{G2019S}$ mutation. We have reported for the first time an atrophic morphology of the astrocytes derived from PD patients donors. It is worth to note that similar aberration has been observed also in in iPSc derived astrocytes generated from AD patients (Jones et al., 2017). Moreover, astrocytes from PD displayed altered mitochondrial morphology and compromised functionality, together with higher production of oxidized proteins. The decreased mitochondrial metabolism is reflected with increased glycolytic activity compared to the healthy controls. Indeed, dysfunctional PD astrocytes can induce neuronal death when co-cultured with healthy neurons, suggesting a detrimental role of the astrocytes in the onset of PD. Following

these general consideration, we will analyze more in detail the results obtained in this study.

## 1. Rat primary astrocytes and neurons internalize hα-syn by endocytosis and transfer the protein to each other

Although α-syn deposits are primarily found in neurons, there are several evidences demonstrating that they can be found also in astrocytes at advanced disease stages (Braak et al., 2007; Croisier and Graeber, 2006; Terada et al., 2003; Tu et al., 1998; Wakabayashi et al., 2000). These observations were made PD brains in different cortical and subcortical areas but also in transgenic α-syn mice after intracerebral injections of fibrillar and soluble forms of α-syn (Sacino et al., 2014). In line with this hypothesis, several groups demonstrated that astrocytes can readily take up recombinant forms of extracellular α-syn *in vitro* (Fellner et al., 2013; Lee et al., 2010b; Rannikko et al., 2015; Lindstrom et al., 2017).

In our study, we confirm that astrocytes can internalize exogenous hα-syn present in LB extracts. Thus, rat cultured astrocytes internalize higher quantity of hα-syn and more rapidly than neurons as shown by hα-syn ELISA (Fig 1.1 A). The mechanism of internalization we suggest is by endocytosis (Fig 1.3) though we haven't identified the receptors that mediate endocytosis yet. There are many candidates for this function; for example heparan sulfate, $PrP^C$ or lymphocyte- activation gene 3 (LAG3) can mediate the uptake of fibrillary but not of the soluble form of $\alpha$-syn in neurons (Aulić et al. 2017; Ihse et al. 2017; Mao et al. 2016). Another receptor associated with endocytosis of $\alpha$-syn is the TLR4 but its involvement has been observed in microglia but not in astrocytes (Rannikko et al. 2015; Fellner et al. 2013). Among the intermembrane proteins associated to the endocytosis, dynamin seems to be a serious candidate to $\alpha$-syn internalization in astrocytes. Indeed, the dynamin inhibitor D15 we used in this work, was effective in inhibiting the uptake and transport of h$\alpha$-syn in the microfluidic experiments, confirming the *in vitro* results obtained by other groups (Rodriguez, Marano, & Tandon, 2018). These findings support the general idea that α-

syn internalization is a complex mechanism that depends on several factors, cell-, species- and conformational-specific.

Following endocytosis, α-syn is responsible for different consequences in neurons and astrocytes. We have demonstrated that accumulation of α-syn in neurons resulted in higher toxicity and cell death than the astrocytes (Fig 1.2). To confirm the harmful role of α-syn in neurons, we use the molecular tweezer CLR01, a drug used in different animal models for PD but not yet in human, to rescue the treated neurons from the LB toxicity. CLR01 inhibits α-syn aggregation *in vitro* by binding to lysine residues primarily at the N-terminus of the protein (Sinha et al., 2011). Moreover, it reduces aggregated, pathologic, and seeding-competent α-syn in a MSA PLP-α-syn mouse model (Herrera-Vaquero et al., 2019). CLR01 effect has been compared to the sugar derivative scyllo-inositol, and the green-tea compound EGCG, having similar effect in AD and MSA and currently under clinical trial consideration (Shina et al., 2012), suggesting a potential use of CLR01 also in PD (Bengoa-Vergnory…Ramos-Gonzalez et al., under revision) .

Beside the direct effect of internalized α-syn into neurons, we proposed that astrocytes have a direct role in the neuronal death by transporting toxic α-syn intercellularly. The transport of α-syn between neurons and glial cells is a well established mechanism of neuronal death spreading (Bourdenx et al., 2015; Brahic et al., 2016; Dehay et al., 2015a; Hansen et al., 2011; Walsh and Selkoe, 2016). Nevertheless, the mechanism of α-syn transfer, especially the transport from glia to neurons, remains still intensively debated (Walsh and Selkoe, 2016). Different mechanisms for α-syn transportation have been suggested, among which the exocytosis/endocytosis, tunneling nanotubes (TNTs), synapses or synapse-like structures, and the involvement of several receptors (Goedert et al., 2010; Dunning et al., 2012; De Cecco and Legname, 2018). In our work we confirm through microfluidic experiments the neuron-astrocytes transfer whereas we demonstrate for the first time also the transport from astrocytes to neurons *in vitro* (Fig 1.6). Our current data, although not excluding other mechanisms, point out the active uptake of α-syn by endocytosis preferentially associated with the tight cellular contacts in the microfluidic microchannels.

Altogether, these data suggest that astrocytes can efficiently take up exogenous α-syn, transmit it intercellularly and contribute actively to the spreading of LB pathology.

## 2. Astrocytes contribute more efficiently to hα-syn degradation

Impairment of autophagy-lysosomal pathways (ALPs) is a major pathogenic event in neurodegenerative diseases, including PD. Together with lysosomal degradation, it is considered the main mechanism to eliminate α-syn from neurons, both under normal and pathological conditions (Lee et al., 2004; Mak et al., 2010). Pathologic α-syn itself in PD (i.e. mutated, post-translationally modified, or oligomeric/ aggregated) impairs lysosomal functions, resulting in defective clearance and subsequent accumulation of abnormal α-syn species and other lysosomal substrates (Emmanouilidou et al., 2010; Martinez- Vicente et al., 2008).

In this study, we propose a defensive mechanism of rat astrocytes based on the higher degradation and clearance of α-syn. In fact, we observed a higher co-localization of α-syn with lysosomes (Fig 1.4, A, B) as well as a higher lysosomal metabolism evidenced by Cathepsin D activity (Fig 1.4, C-E) in response to LB treatment. Cathepsin D has been widely used as an indicator of lysosomal activity, covering an active role in the degradation of α-syn (Quiao et al., 2008). Bae and colleagues demonstrated that the experimental dysfunction of Cathepsin D and the consequent reduction of 50% of the proteolytic activity in the lysosomes, promoted the accumulation of α-syn aggregates within the lysosomes and the toxic transfer of the protein to the neighbored cells (Bae et al., 2015). Our data reinforce the hypothesis that a major lysosomal degradation correspond to a higher resistance to toxic α-syn and confirm the recent finding by Loria and colleagues demonstrating an effective degradation of α-syn fibrils by astrocytes rather than by the neurons (Loria et al., 2017).

Altogether, we propose that α-syn accumulation in PD may represent both a cause and a consequence of impaired proteolytic activity, and that astrocytes in physiological conditions play an important role in the degradation of the protein, indicating that an astrocytes dysfunction can be responsible for neuronal death in PD.

## 3. Mitochondrial function is compromised in astrocytes in both rat and human models of the Parkinson´s Disease.

The involvement of mitochondrial dysfunction in PD has been reinforced in recent years by the finding that many of the mutated genes associated with familial forms of PD, including α-syn and LRRK2, either directly or indirectly affect mitochondrial function. Multiple studies have demonstrated the effects of α-syn overexpression/oligomerisation on mitochondrial function both *in vitro* and *in vivo*. These effects include the inhibition of mitochondrial complexes (Subramaniam et al., 2014) and the increase of mitochondrial fragmentation in the presence of intracellular α-syn oligomers (Plotegher et al., 2014). By direct measure of the oxygen consumption rate, we have found that after prolonged treatment with LB, rat neurons failed to activate their mitochondrial metabolism showing a decrease in maximal respiration and in spare respiratory capacity. In contrast, astrocytes increase their ATP production and Basal respiration (Fig 1.5), resulting in a more efficient response to energy demand. However, in contrast to our findings, other groups reported that the accumulation of recombinant α-syn in human fetal astrocytes, neurons and fibroblasts provoked a decrease in mitochondrial function 24h after treatment (Braidy et al., 2013). Even if we experienced the same response in neurons, our different results in astrocytes can be explained by the methods we used in our study like for example the different cell cultures used and the different α-syn concentration used to induce cell toxicity (approximately 8pM of LB extracts in our case *vs.* 5μM of recombinant α-syn in other studies).

These results, in combination with a greater degradation capacity suggest a higher resistance of astrocytes to exogenous hα-syn mediated toxicity. As mentioned

before, we suggest that astrocytes can play an initial protective role on neurons by buffering the extracellular α-syn. If astrocytes are dysfunctional or α-syn threshold reaches toxic concentrations that cannot be processed efficiently, they become vector of toxicity by transporting α-syn to the neurons.

We propose that mitochondrial function in genetic PD is altered also under basal conditions. In fact, iPSc-derived human astrocytes from LRRK2$^{G2019S}$ showed decreased OCR of the Basal and Maximal respiration and lower ATP production compared to the healthy cells (Fig 2.6 A-F), which indicates a loss of mitochondrial functionality. On the other hand, we observed in LRRK2$^{G2019S}$ astrocytes an increase in the basal glycolysis, basal PER and compensatory glycolysis (Fig 2.7) compared to healthy controls, suggesting a compensatory "glycolytic switch" for energy production. We are currently evaluating the effect of exogenous α-syn on the OCR and the ECAR of these cells in order to understand their response to one of the major features occurring in PD.

Even if our results with mutated human astrocytes don´t report any concluding difference in the mitochondrial membrane potential (Fig 2.5 E), suggesting the cells are viable, we have described important alterations of the mitochondrial morphology. As shown after mitochondrial staining with Rhodamin 123 and Mitotracker and after the ultrastructural analysis by EM (Fig 2.8 B-D), mitochondrial morphology looks different between the control lines and the LRRK2$^{G2019S}$. Healthy astrocytes evidenced elongated and interconnected mitochondria (Fig 2.8 A), forming a homogenous network covering the entire cytoplasm, distributed not only in the soma but also in the projections, while mitochondria in the LRRK2$^{G2019S}$ lines were more rounded, with tendency to accumulate perinuclearly, and did not form a very complex network. These observations suggest impairment of fusion/fission dynamics, a process that helps transmitting energy across long distances within the cell together with the loss of function in supporting the synaptic activity. Indeed, any perturbation of these dynamic processes would be prone to disease phenotypes (Singh, Zhi, & Zhang, 2019). In line with our data, there are several studies showing that LRRK2 mutation can be responsible for mitochondrial fragmentation in fibroblasts as well as in neural cells or

neuroblastoma cell lines (Grunewald et al., 2014; Niu et al., 2012; Smith et al., 2016; Su and Qi, 2013; Wang et al., 2012).

Multiple studies have demonstrated that LRRK2 mutation is also associated with an increased susceptibility to oxidative stress and increased cell death (Cooper et al., 2012; Imai et al., 2008; Mendivil-Perez et al., 2016; Ng et al., 2009; Pereira et al., 2014; Reinhardt et al., 2013). Oxidative stress is the result of disequilibrium between excessive production of reactive oxygen species (ROS) and limited antioxidant defenses and cellular consequences are oxidative damage of proteins, DNA, and lipids (Raha and Robinson, 2000). Mitochondrial dysfunction on respiratory chain complex has been linked to increased ROS production in LRRK2 mutant cells (Niu et al., 2012). In line with these results, as a consequence of mitochondrial damage, we found higher levels of carbonyl groups in LRRK2$^{G2019S}$ astrocytes than the controls, deriving to higher levels of oxidized proteins in these cells (Fig 2.9) supporting the hypothesis that LRRK2$^{G2019S}$ unchains metabolic cascade that can be harmful for neurons in genetic PD. Even if we need more studies on regard, these data strengthen the recent growing hypothesis that PD may be a mitochondrial disorder disease.

## 4. PD LRRK2$^{G2019S}$ astrocytes show an atrophic phenotype compared to healthy controls.

Abnormalities in neurite outgrowth and branching were among the earliest altered phenotypes observed in LRRK2 mutations (Kleppe et al., 2011; Tsika et al., 2014; MacLeod et al., 2006). It was initially proposed that the origin of such morphological changes could be a consequence of apoptotic processes (Tsika et al., 2014); however, further studies provided evidence for an association of LRRK2 with tubulin/actin, thus suggesting that such morphological changes may be consequences of LRRK2-modulation on cytoskeletal dynamics (Wallings, Manzoni, & Bandopadhyay, 2015). Several evidences suggested the relationship of LRRK2 protein with the cytoskeleton. The GTPase domain of LRRK2 protein can pull-down α/β tubulin from cell lysates of mouse fibroblasts and human embryonic kidney (Gandhi et al., 2009); LRRK2

was also co-precipitated with β tubulin from wild-type mouse brain and recombinant LRRK2 can phosphorylate β tubulin *in vitro* (Guillardon, 2009). Moreover, a high-throughput screening to decipher LRRK2 interactome revealed proteins of the actin family and from the actin-regulatory network as interactors of LRRK2 in the mechanism of actin polymerization *in vitro* (Meixner et al., 2011).

Here, we describe a striking atrophic phenotype of PD LRRK2$^{G2019S}$ astrocytes. The morphological analysis of these cells revealed important differences between healthy controls and LRRK2$^{G2019S}$ astrocytes. The area of PD cells is much smaller than the controls (Fig 2.3) that is reflected also in the reduction of the complexity in terms of shape or projections (Fig 2.4).

A similar phenotype has been found in astrocytes derived from AD iPSc. Astrocytes derived from both sporadic and familial AD patients exhibited a pronounced pathological phenotype, with a significantly less complex morphological appearance and overall atrophic profiles. Concretely, these astrocytes showed reduced heterogeneity, were significantly smaller than their healthy counterparts and exhibited an almost complete absence of processes (Jones et al., 2017).

To date, there are no reports describing this astrocytic phenotype in PD human brain. In fact, in 2014, Charron and colleagues found the opposite, a hypertrophic profile of astrocytes in SN of PD brains. The main cellular processes were thicker and the number of primary processes leaving the somas increased (Charron et al., 2014). In addition, they found a very large increase in striatal volume occupied by astrocytes, probably primarily due to the lengthening and the thickening of astrocyte processes (Charron et al., 2014). However, we consider that a deeper analysis of astrocyte morphology should be done in other regions of the brain that are related with dopaminergic degeneration (e.g. subthalamic nucleus or globus pallidum) and not only in degenerating regions where astrocytes are already activated.

We suggest that the atrophy observed in these PD LRRK2$^{G2019S}$ astrocytes could be a consequence of the malfunction of the mutated LRRK2 protein, being unable to modulate properly cytoeskeletal dynamics.

## 5. Astrocyte contribution to neuronal degeneration

The results of our study evidenced an atrophic and dysfunctional astrocytic population in PD, with less complexity, less processes and less mitochondrial density in the terminal processes. In terms of neuronal biology, this suggests that astrocytes in PD brain lack of the support for a correct synaptic activity and moreover, can be vectors of toxicity by transporting α-syn, as evidenced in LB experiments. The specific vulnerability of dopaminergic neurons, that represents one of the hallmarks of Parkinson´s Disease still represents one of the bottleneck of PD biology (Brichta & Greengard, 2014). Indeed, the astrocyte density in the SN is very low and each astrocyte in the caudate-putamen can "touch" up to 50,000 synapses. This evidences that the dysfunction of a single astrocyte in the SN can affect significantly the synaptic transmission and the neuronal survival of a great number of neurons. Although we still can't demonstrate the exact mechanism of neuronal death, upregulation of endogenous $\alpha$-syn (Fig 1.9), release of toxic microRNAs, an altered mechanism of $\alpha$-syn degradation or the activation of neuroinflammation may be other of the proposed mechanisms of neuronal death.

What is evident from our results is that in PD, astrocytes can be harmful to neurons. In co-culture experiments with PD LRRK2$^{G2019S}$ astrocytes and healthy neurons, astrocytes increased the risk of neuronal death compared with co-cultures with healthy astrocytes (Fig 2.10). Our results are in line with a very recent study by Lee and colleagues who observed the astrocyte-induced neuronal death in co-culture experiments (Lee et al., 2019). Treatment of LRRK2$^{G2019S}$ astrocytes with α-syn increased the expression of ER stress proteins in astrocytes and further downregulation of neurite length and neuronal viability, supporting the idea that ER stress in LRRK2$^{G2019S}$ astrocytes can aggravate neuronal damage (Lee et al., 2019).

## 6. Future directions and concluding remarks

This work represents a pioneer study on the real role of astrocytes in the onset and progression of PD. All data presented here suggest that the altered biology of astrocytes is responsible for the further neuronal death. Nevertheless, we still consider necessary to deepen the investigation on astrocytic metabolism.

First, we want to complete the characterization of human astrocytes under different aspects. The fist parameter we want to study is the differential gene expression between control and PD LRRK2$^{G2019S}$ astrocytes by qPCR or RNAseq. The differential expression analysis will reveal, among others, genes related with the inflammatory profile of the astrocytes from healthy donors and PD patients. Furthermore, in line to what observed in rat primary cultures when treated with α-syn, we want to characterize the mitochondrial metabolism of astrocytes when stimulated with exogenous α-syn and compare the response with the cell lines from rat. In addition, we believe extremely important to investigate if the atrophic morphology found in iPSc-derived astrocytes is reflected also in human brain and/or in different target regions (subthalamic nucleus, globus pallidus, cerebral cortex, and SN). Finally, considering that the severity of familiar forms of PD depends on the type of mutation, we will extend our study to other mutations, such as SNCA$^{E46K}$ or LRRK2$^{R1441G}$ that are considered two of the most aggressive mutations in the familiar PD.

Altogether, we conclude that dysfunctional astrocytes contribute to the onset and progression of PD. Both the accumulation of α-syn and the LRRK2$^{G2019S}$ mutation induce mitochondrial unbalance leading to cell autonomous and non-autonomous damage and final neuronal degeneration. This study proposes a new possible therapeutic target directed to sustain astrocytic functionality.

# Conclusions

1. Both rat neurons and astrocytes internalize exogenous hα-syn, at least by endocytosis, resulting in an increase of neuronal toxicity but astrocyte resistance.

2. Rat astrocytes exhibit an increase in lysosomal activity and activate mitochondrial metabolism in response to exogenous hα-syn.

3. Exogenous hα-syn can be transmitted between neurons and astrocytes directly in every possible combination.

4. Rat astrocytes induce neuronal apoptosis through hα-syn transportation, in part activating an endogenous program of α-syn translation.

5. Human iPSc derived healthy and PD LRRK2$^{G2019S}$ astrocytes have been successfully generated as they are functional in terms of calcium sensitivity and expression of typical astrocytic markers.

6. PD LRRK2$^{G2019S}$ astrocytes display an atrophic morphology, showing a diminished size and reduced complexity compared to control astrocytes.

7. PD LRRK2$^{G2019S}$ astrocytes exhibit a general mitochondrial dysfunction in terms of mitochondrial respiration, cellular localization and ultrastructural morphology, consequently producing higher levels of oxidized proteins and causing a "switch" to an aerobic glycolytic production of ATP.

8. PD LRRK2$^{G2019S}$ astrocytes increase the risk of neuronal death when co-cultured together.

Altogether, we conclude that dysfunctional astrocytes contribute to the onset and progression of PD. Both accumulation of α-syn and LRRK2$^{G2019S}$ mutation induce mitochondrial unbalance leading to cell autonomous and non-autonomous damage and final neuronal degeneration. This study proposes a new possible therapeutic target directed to sustain astrocytic functionality. Further experiments are needed to

establish the pathways that astrocytes directly distress to induce the dopaminergic death.

# Bibliography

Abe, T., Takahashi, S., & Suzuki, N. (2006a). Metabolic properties of astrocytes differentiated from rat neurospheres. Brain Res, 1101, 5–11.

Acquatella-Tran Van Ba, I., Imberdis, T., & Perrier, V. (2013). From prion diseases to prion-like propagation mechanisms of neurodegenerative diseases. International journal of cell biology, 2013.

Ahmad, T., Aggarwal, K., Pattnaik, B., Mukherjee, S., Sethi, T., Tiwari, B. K., & Roy, S. S. (2013). Computational classification of mitochondrial shapes reflects stress and redox state. Cell death & disease, 4(1), e461.

Ainscow, E. K., Mirshamsi, S., Tang, T., Ashford, M. L., & Rutter, G. A. (2002). Dynamic imaging of free cytosolic ATP concentration during fuel sensing by rat hypothalamic neurones: evidence for ATP-independent control of ATP-sensitive K+ channels. The Journal of physiology, 544(2), 429-445.

Alafuzoff, I., Ince, P. G., Arzberger, T., Al-Sarraj, S., Bell, J., Bodi, I., ... & Gentleman, S. (2009). Staging/typing of Lewy body related α-synuclein pathology: a study of the BrainNet Europe Consortium. Acta neuropathologica, 117(6), 635-652.

Alvarez-Erviti, L., Seow, Y., Schapira, A. H., Gardiner, C., Sargent, I. L., Wood, M. J., & Cooper, J. M. (2011). Lysosomal dysfunction increases exosome-mediated alpha-synuclein release and transmission. Neurobiology of disease, 42(3), 360-367.

Amo T, Sato S, Saiki S, Wolf AM, Toyomizu M, Gautier CA, Shen J, Ohta S, Hattori N (2011) Mitochondrial membrane potential decrease caused by loss of PINK1 is not due to proton leak, but to respiratory chain defects. Neurobiol Dis 41:111-118.

Angot, E., Steiner, J. A., Tome, C. M. L., Ekström, P., Mattsson, B., Björklund, A., & Brundin, P. (2012). Alpha-synuclein cell-to-cell transfer and seeding in grafted dopaminergic neurons in vivo. PloS one, 7(6), e39465.

Antony, P. M., Diederich, N. J., Krüger, R., & Balling, R. (2013). The hallmarks of Parkinson's disease. The FEBS journal, 280(23), 5981-5993.

Araque, A., Sanzgiri, R. P., Parpura, V., & Haydon, P. G. (1999). Astrocyte-induced modulation of synaptic transmission. Canadian journal of physiology and pharmacology, 77(9), 699-706.

Arrasate, M., Mitra, S., Schweitzer, E. S., Segal, M. R., & Finkbeiner, S. (2004). Inclusion body formation reduces levels of mutant huntingtin and the risk of neuronal death. Nature, 431(7010), 805.

Aulić, S., Masperone, L., Narkiewicz, J., Isopi, E., Bistaffa, E., Ambrosetti, E., ... & Moda, F. (2017). α-Synuclein amyloids hijack prion protein to gain cell entry, facilitate cell-to-cell spreading and block prion replication. Scientific reports, 7(1), 10050.

Bae, E. J., Yang, N. Y., Lee, C., Lee, H. J., Kim, S., Sardi, S. P., & Lee, S. J. (2015). Loss of glucocerebrosidase 1 activity causes lysosomal dysfunction and α-synuclein aggregation. Experimental & molecular medicine, 47(3), e153.

Bauer, R., Martin, E., Haegele-Link, S., Kaegi, G., von Specht, M., & Werner, B. (2014). Noninvasive functional neurosurgery using transcranial MR imaging-guided focused ultrasound. Parkinsonism & related disorders, 20, S197-S199.

Bélanger, M., & Magistretti, P. J. (2009). The role of astroglia in neuroprotection. Dialogues in clinical neuroscience, 11(3), 281.

Bélanger, M., Allaman, I., & Magistretti, P. J. (2011). Brain energy metabolism: focus on astrocyte-neuron metabolic cooperation. Cell metabolism, 14(6), 724-738.

Bellesi, M., de Vivo, L., Chini, M., Gilli, F., Tononi, G., & Cirelli, C. (2017). Sleep loss promotes astrocytic phagocytosis and microglial activation in mouse cerebral cortex. Journal of Neuroscience, 37(21), 5263-5273.

Bellucci, A., Zaltieri, M., Navarria, L., Grigoletto, J., Missale, C., & Spano, P. (2012). From α-synuclein to synaptic dysfunctions: new insights into the pathophysiology of Parkinson's disease. Brain research, 1476, 183-202.

Bender, A., Krishnan, K. J., Morris, C. M., Taylor, G. A., Reeve, A. K., Perry, R. H., ... & Taylor, R. W. (2006). High levels of mitochondrial DNA deletions in substantia nigra neurons in aging and Parkinson disease. Nature genetics, 38(5), 515.

Bendor, J. T., Logan, T. P., & Edwards, R. H. (2013). The function of α-synuclein. Neuron, 79(6), 1044-1066.

Bengoa-Vergniory, N., Roberts, R. F., Wade-Martins, R., & Alegre-Abarrategui, J. (2017). Alpha-synuclein oligomers: a new hope. Acta neuropathologica, 134(6), 819-838.

Benner, E. J., Banerjee, R., Reynolds, A. D., Sherman, S., Pisarev, V. M., Tsiperson, V., ... & Gendelman, H. E. (2008). Nitrated α–synuclein immunity accelerates degeneration of nigral dopaminergic neurons. PloS one, 3(1), e1376.

Bergles, D. E., & Jahr, C. E. (1998). Glial contribution to glutamate uptake at Schaffer collateral–commissural synapses in the hippocampus. Journal of Neuroscience, 18(19), 7709-7716.

Blesa, J., & Przedborski, S. (2014). Parkinson's disease: animal models and dopaminergic cell vulnerability. Frontiers in neuroanatomy, 8, 155.

Bloch, A., Probst, A., Bissig, H., Adams, H., & Tolnay, M. (2006). α-Synuclein pathology of the spinal and peripheral autonomic nervous system in neurologically unimpaired elderly subjects. Neuropathology and applied neurobiology, 32(3), 284-295.

Boddum, K., Jensen, T. P., Magloire, V., Kristiansen, U., Rusakov, D. A., Pavlov, I., & Walker, M. C. (2016). Astrocytic GABA transporter activity modulates excitatory neurotransmission. Nature communications, 7, 13572.

Booth, H. D., Hirst, W. D., & Wade-Martins, R. (2017). The role of astrocyte dysfunction in Parkinson's disease pathogenesis. Trends in neurosciences, 40(6), 358-370.

Borden, L. A. (1996). GABA transporter heterogeneity: pharmacology and cellular localization. Neurochemistry international, 29(4), 335-356.Bergles and Jahr, 1997

Bourdenx, M., Dovero, S., Engeln, M., Bido, S., Bastide, M. F., Dutheil, N., ... & Boraud, T. (2015). Lack of additive role of ageing in nigrostriatal neurodegeneration triggered by α-synuclein overexpression. Acta neuropathologica communications, 3(1), 46.

Braak, H., Rüb, U., Gai, W. P., & Del Tredici, K. (2003). Idiopathic Parkinson's disease: possible routes by which vulnerable neuronal types may be subject to neuroinvasion by an unknown pathogen. Journal of neural transmission, 110(5), 517-536.

Braak, H., Sastre, M., & Del Tredici, K. (2007). Development of α-synuclein immunoreactive astrocytes in the forebrain parallels stages of intraneuronal pathology in sporadic Parkinson's disease. Acta neuropathologica, 114(3), 231-241.

Brahic, M., Bousset, L., Bieri, G., Melki, R., & Gitler, A. D. (2016). Axonal transport and secretion of fibrillar forms of α-synuclein, Aβ42 peptide and HTTExon 1. Acta neuropathologica, 131(4), 539-548.

Braidy, N., Gai, W. P., Xu, Y. H., Sachdev, P., Guillemin, G. J., Jiang, X. M., ... & Chan, D. Y. (2013). Uptake and mitochondrial dysfunction of alpha-synuclein in human astrocytes, cortical neurons and fibroblasts. Translational neurodegeneration, 2(1), 20.

Brichhta, L., & Greengard, P. (2014). Molecular determinants of selective dopaminergic vulnerability in Parkinson's disease: an update. Frontiers in neuroanatomy, 8, 152.

Brown, A. M., & Ransom, B. R. (2007). Astrocyte glycogen and brain energy metabolism. Glia, 55(12), 1263-1271.

Burke, W. J., Kumar, V. B., Pandey, N., Panneton, W. M., Gan, Q., Franko, M. W., ... & Galvin, J. E. (2008). Aggregation of α-synuclein by DOPAL, the monoamine oxidase metabolite of dopamine. Acta neuropathologica, 115(2), 193-203.

Buzsáki, G., & Chrobak, J. J. (2005). Synaptic plasticity and self-organization in the hippocampus. Nature neuroscience, 8(11), 1418.

Cavaliere, F., Cerf, L., Dehay, B., Ramos-Gonzalez, P., De Giorgi, F., Bourdenx, M., ... & Bezard, E. (2017). In vitro α-synuclein neurotoxicity and spreading among neurons and astrocytes using Lewy body extracts from Parkinson disease brains. Neurobiology of disease, 103, 101-112.

Cha, S. H., Choi, Y. R., Heo, C. H., Kang, S. J., Joe, E. H., Jou, I., ... & Park, S. M. (2015). Loss of parkin promotes lipid rafts-dependent endocytosis through accumulating caveolin-1: implications for Parkinson's disease. Molecular neurodegeneration, 10(1), 63.

Chan, D., Citro, A., Cordy, J. M., Shen, G. C., & Wolozin, B. (2011). Rac1 protein rescues neurite retraction caused by G2019S leucine-rich repeat kinase 2 (LRRK2). Journal of Biological Chemistry, 286(18), 16140-16149.

Charron, G., Doudnikoff, E., Canron, M. H., Li, Q., Véga, C., Marais, S., ... & Bezard, E. (2014). Astrocytosis in parkinsonism: considering tripartite striatal synapses in physiopathology?. Frontiers in aging neuroscience, 6, 258.

Choi, B. K., Choi, M. G., Kim, J. Y., Yang, Y., Lai, Y., Kweon, D. H., ... & Shin, Y. K. (2013). Large α-synuclein oligomers inhibit neuronal SNARE-mediated vesicle docking. Proceedings of the National Academy of Sciences, 110(10), 4087-4092.

Clark, D. P., Perreau, V. M., Shultz, S. R., Brady, R. D., Lei, E., Dixit, S., ... & Boon, W. C. (2019). Inflammation in Traumatic Brain Injury: Roles for Toxic A1 Astrocytes and Microglial–Astrocytic Crosstalk. Neurochemical research, 44(6), 1410-1424.

Clarke, L. E., Liddelow, S. A., Chakraborty, C., Münch, A. E., Heiman, M., & Barres, B. A. (2018). Normal aging induces A1-like astrocyte reactivity. Proceedings of the National Academy of Sciences, 115(8), E1896-E1905.

Colosimo, C., Hughes, A. J., Kilford, L., & Lees, A. J. (2003). Lewy body cortical involvement may not always predict dementia in Parkinson's disease. Journal of Neurology, Neurosurgery & Psychiatry, 74(7), 852-856.

Cooper, O., Seo, H., Andrabi, S., Guardia-Laguarta, C., Graziotto, J., Sundberg, M., ... & Hargus, G. (2012). Pharmacological rescue of mitochondrial deficits in iPSC-derived neural cells from patients with familial Parkinson's disease. Science translational medicine, 4(141), 141ra90-141ra90.

Covarrubias-Pinto, A., Acuña, A. I., Beltrán, F. A., Torres-Díaz, L., & Castro, M. A. (2015). Old things new view: ascorbic acid protects the brain in neurodegenerative disorders. International journal of molecular sciences, 16(12), 28194-28217.

Croisier, E., & Graeber, M. B. (2006). Glial degeneration and reactive gliosis in alpha-synucleinopathies: the emerging concept of primary gliodegeneration. Acta neuropathologica, 112(5), 517-530.

Crosiers D, Theuns J, Cras P & Van Broeckhoven C (2011) Parkinson disease: insights in clinical, genetic and pathological features of monogenic disease subtypes. J Chem Neuroanat 42, 131–141

Cruz, N. F., & Dienel, G. A. (2002). High glycogen levels in brains of rats with minimal environmental stimuli: implications for metabolic contributions of working astrocytes. Journal of Cerebral Blood Flow & Metabolism, 22(12), 1476-1489.

Danbolt, N. C. (2001). Glutamate uptake. Progress in neurobiology, 65(1), 1-105.

Davalos, D., Grutzendler, J., Yang, G., Kim, J. V., Zuo, Y., Jung, S., ... & Gan, W. B. (2005). ATP mediates rapid microglial response to local brain injury in vivo. Nature neuroscience, 8(6), 752.

Dawson, T. M., Ko, H. S., & Dawson, V. L. (2010). Genetic animal models of Parkinson's disease. Neuron, 66(5), 646-661.

De Cecco, E., & Legname, G. (2018). The role of the prion protein in the internalization of α-synuclein amyloids. Prion, 12(1), 23-27.

Dehay, B., Bourdenx, M., Gorry, P., Przedborski, S., Vila, M., Hunot, S., ... & Petsko, G. A. (2015). Targeting α-synuclein for treatment of Parkinson's disease: mechanistic and therapeutic considerations. The Lancet Neurology, 14(8), 855-866.

Dehay, B., Bové, J., Rodríguez-Muela, N., Perier, C., Recasens, A., Boya, P., & Vila, M. (2010). Pathogenic lysosomal depletion in Parkinson's disease. Journal of Neuroscience, 30(37), 12535-12544.

Del Tredici, K., & Braak, H. (2016). Sporadic Parkinson's disease: development and distribution of α-synuclein pathology. Neuropathology and applied neurobiology, 42(1), 33-50.

Desplats, P., Lee, H. J., Bae, E. J., Patrick, C., Rockenstein, E., Crews, L., ... & Lee, S. J. (2009). Inclusion formation and neuronal cell death through neuron-to-neuron transmission of α-synuclein. Proceedings of the National Academy of Sciences, 106(31), 13010-13015.

Dickson, D. W., Ahmed, Z., Algom, A. A., Tsuboi, Y., & Josephs, K. A. (2010). Neuropathology of variants of progressive supranuclear palsy. Current opinion in neurology, 23(4), 394-400.

Dodson, M. W., & Guo, M. (2007). Pink1, Parkin, DJ-1 and mitochondrial dysfunction in Parkinson's disease. Current opinion in neurobiology, 17(3), 331-337.

Doengi, M., Hirnet, D., Coulon, P., Pape, H. C., Deitmer, J. W., & Lohr, C. (2009). GABA uptake-dependent Ca2+ signaling in developing olfactory bulb astrocytes. Proceedings of the National Academy of Sciences, 106(41), 17570-17575.

Dringen, R. (2000). Metabolism and functions of glutathione in brain. Progress in neurobiology, 62(6), 649-671.

Dringen, R., Gebhardt, R., & Hamprecht, B. (1993). Glycogen in astrocytes: possible function as lactate supply for neighboring cells. Brain research, 623(2), 208-214.

Dunning, C. J., Reyes, J. F., Steiner, J. A., & Brundin, P. (2012). Can Parkinson's disease pathology be propagated from one neuron to another?. Progress in neurobiology, 97(2), 205-219.

El-Agnaf, O. M., Salem, S. A., Paleologou, K. E., Curran, M. D., Gibson, M. J., Court, J. A., ... & Allsop, D. (2006). Detection of oligomeric forms of α-synuclein protein in human plasma as a potential biomarker for Parkinson’s disease. The FASEB journal, 20(3), 419-425.

Elkon, H., Don, J., Melamed, E., Ziv, I., Shirvan, A., & Offen, D. (2002). Mutant and wild-type α-synuclein interact with mitochondrial cytochrome C oxidase. Journal of Molecular Neuroscience, 18(3), 229-238.

Emdad, L., D'Souza, S. L., Kothari, H. P., Qadeer, Z. A., & Germano, I. M. (2011). Efficient differentiation of human embryonic and induced pluripotent stem cells into functional astrocytes. Stem cells and development, 21(3), 404-410.

Emmanouilidou, E., Melachroinou, K., Roumeliotis, T., Garbis, S. D., Ntzouni, M., Margaritis, L. H., ... & Vekrellis, K. (2010). Cell-produced α-synuclein is secreted in a calcium-dependent manner by exosomes and impacts neuronal survival. Journal of Neuroscience, 30(20), 6838-6851.

Eroglu, C., & Barres, B. A. (2010). Regulation of synaptic connectivity by glia. Nature, 468(7321), 223.

Fellner, L., Irschick, R., Schanda, K., Reindl, M., Klimaschewski, L., Poewe, W., ... & Stefanova, N. (2013). Toll-like receptor 4 is required for α-synuclein dependent activation of microglia and astroglia. Glia, 61(3), 349-360.

Frigerio R, Fujishiro H, Ahn TB, Josephs KA, Maraganore DM, DelleDonne A, Parisi JE, Klos KJ, Boeve BF, Dick- son DW, Ahlskog JE (2011) Incidental Lewy body disease: do some cases represent a preclinical stage of dementia with Lewy bodies? Neurobiol Aging 32:857–863.

Gallegos, S., Pacheco, C., Peters, C., Opazo, C. M., & Aguayo, L. G. (2015). Features of alpha-synuclein that could explain the progression and irreversibility of Parkinson's disease. Frontiers in neuroscience, 9, 59.

Gandhi, P. N., Wang, X., Zhu, X., Chen, S. G., & Wilson-Delfosse, A. L. (2008). The Roc domain of leucine-rich repeat kinase 2 is sufficient for interaction with microtubules. Journal of neuroscience research, 86(8), 1711-1720.

Giasson, B. I. (2004). Mitochondrial injury: a hot spot for parkinsonism and Parkinson's disease?. Science of aging knowledge environment: SAGE KE, 2004(48), pe42-pe42.

Gillardon, F. (2009). Leucine-rich repeat kinase 2 phosphorylates brain tubulin-beta isoforms and modulates microtubule stability–a point of convergence in Parkinsonian neurodegeneration?. Journal of neurochemistry, 110(5), 1514-1522.

Goedert, M., Clavaguera, F., & Tolnay, M. (2010). The propagation of prion-like protein inclusions in neurodegenerative diseases. Trends in neurosciences, 33(7), 317-325.

Goedert, M., Falcon, B., Clavaguera, F., & Tolnay, M. (2014). Prion-like mechanisms in the pathogenesis of tauopathies and synucleinopathies. Current neurology and neuroscience reports, 14(11), 495.

Goers, J., Manning-Bog, A. B., McCormack, A. L., Millett, I. S., Doniach, S., Di Monte, D. A., ... & Fink, A. L. (2003). Nuclear localization of α-synuclein and its interaction with histones. Biochemistry, 42(28), 8465-8471.

Goldwurm, S., Zini, M., Mariani, L., Tesei, S., Miceli, R., Sironi, F., ... & Pezzoli, G. (2007). Evaluation of LRRK2 G2019S penetrance: relevance for genetic counseling in Parkinson disease. Neurology, 68(14), 1141-1143.

Gordon, G. R., Choi, H. B., Rungta, R. L., Ellis-Davies, G. C., & MacVicar, B. A. (2008). Brain metabolism dictates the polarity of astrocyte control over arterioles. Nature, 456(7223), 745.

Greggio, E., Zambrano, I., Kaganovich, A., Beilina, A., Taymans, J. M., Daniëls, V., ... & Thomas, K. J. (2008). The Parkinson disease-associated leucine-rich repeat kinase 2 (LRRK2) is a dimer that undergoes intramolecular autophosphorylation. Journal of Biological Chemistry, 283(24), 16906-16914.

Grünewald, A., Arns, B., Meier, B., Brockmann, K., Tadic, V., & Klein, C. (2014). Does uncoupling protein 2 expression qualify as marker of disease status in LRRK2-associated Parkinson's disease?.

Gu, X. L., Long, C. X., Sun, L., Xie, C., Lin, X., & Cai, H. (2010). Astrocytic expression of Parkinson's disease-related A53T α-synuclein causes neurodegeneration in mice. Molecular brain, 3(1), 12.

Guillamon-Vivancos, T., Gomez-Pinedo, U., & Matias-Guiu, J. (2015). Astrocytes in neurodegenerative diseases (I): function and molecular description. Neurología (English Edition), 30(2), 119-129.

Haj-Yasein, N. N., Vindedal, G. F., Eilert-Olsen, M., Gundersen, G. A., Skare, Ø., Laake, P., ... & Nagelhus, E. A. (2011). Glial-conditional deletion of aquaporin-4 (Aqp4) reduces blood–brain water uptake and confers barrier function on perivascular astrocyte endfeet. Proceedings of the National Academy of Sciences, 108(43), 17815-17820.

Halliday, G., McCann, H., & Shepherd, C. (2012). Evaluation of the Braak hypothesis: how far can it explain the pathogenesis of Parkinson's disease?. Expert review of neurotherapeutics, 12(6), 673-686.

Halnes, G., Ostby, I., Pettersen, K. H., Omholt, S. W., and Einevoll, G. T. (2013). Electrodiffusive model for astrocytic and neuronal ion concentration dynamics. PLoS Comput. Biol. 9:e1003386.

Hansen, C., Angot, E., Bergström, A. L., Steiner, J. A., Pieri, L., Paul, G., ... & Li, J. Y. (2011). α-Synuclein propagates from mouse brain to grafted dopaminergic neurons and seeds aggregation in cultured human cells. The Journal of clinical investigation, 121(2), 715-725.

Hasegawa, M., Nonaka, T., & Masuda-Suzukake, M. (2017). Prion-like mechanisms and potential therapeutic targets in neurodegenerative disorders. Pharmacology & therapeutics, 172, 22-33.

Haston, K. M., & Finkbeiner, S. (2016). Clinical trials in a dish: the potential of pluripotent stem cells to develop therapies for neurodegenerative diseases. Annual review of pharmacology and toxicology, 56, 489-510.

Herrera-Vaquero, M., Bouquio, D., Kallab, M., Biggs, K., Nair, G., Ochoa, J., ... & Wenning, G. K. (2019). The molecular tweezer CLR01 reduces aggregated, pathologic, and seeding-competent α-synuclein in experimental multiple system atrophy. Biochimica et Biophysica Acta (BBA)-Molecular Basis of Disease, 1865(11), 165513.

Herrero-Mendez, A., Almeida, A., Fernández, E., Maestre, C., Moncada, S., & Bolaños, J. P. (2009). The bioenergetic and antioxidant status of neurons is controlled by continuous degradation of a key glycolytic enzyme by APC/C–Cdh1. Nature cell biology, 11(6), 747.

Hertz, L., Xu, J., Song, D., Yan, E., Gu, L., & Peng, L. (2013). Astrocytic and neuronal accumulation of elevated extracellular K+ with a 2/3 K+/Na+ flux ratio—consequences for energy metabolism, osmolarity and higher brain function. Frontiers in computational neuroscience, 7, 114.

Hines, D. J., Hines, R. M., Mulligan, S. J., & Macvicar, B. A. (2009). Microglia processes block the spread of damage in the brain and require functional chloride channels. Glia, 57(15), 1610-1618.

Hishikawa, N., Hashizume, Y., Yoshida, M., & Sobue, G. (2001). Widespread occurrence of argyrophilic glial inclusions in Parkinson's disease. Neuropathology and applied neurobiology, 27(5), 362-372.

Hodara, R., Norris, E. H., Giasson, B. I., Mishizen-Eberz, A. J., Lynch, D. R., Lee, V. M. Y., & Ischiropoulos, H. (2004). Functional Consequences of α-Synuclein Tyrosine Nitration Diminished Binding to Lipid Vesicles and Increased Fibril Formation. Journal of Biological Chemistry, 279(46), 47746-47753.

Holmqvist, S., Chutna, O., Bousset, L., Aldrin-Kirk, P., Li, W., Björklund, T., ... & Li, J. Y. (2014). Direct evidence of Parkinson pathology spread from the gastrointestinal tract to the brain in rats. Acta neuropathologica, 128(6), 805-820.

Hsieh, C. H., Shaltouki, A., Gonzalez, A. E., da Cruz, A. B., Burbulla, L. F., Lawrence, E. S., ... & Wang, X. (2016). Functional impairment in miro degradation and mitophagy is a shared feature in familial and sporadic Parkinson's disease. Cell Stem Cell, 19(6), 709-724.

Huang, Z., Xu, Z., Wu, Y., & Zhou, Y. (2011). Determining nuclear localization of alpha-synuclein in mouse brains. Neuroscience, 199, 318-332.

Ihse, E., Yamakado, H., van Wijk, X. M., Lawrence, R., Esko, J. D., & Masliah, E. (2017). Cellular internalization of alpha-synuclein aggregates by cell surface heparan sulfate depends on aggregate conformation and cell type. Scientific reports, 7(1), 9008.

Ilić D., Furuta, Y., Kanazawa, S., Takeda, N., Sobue, K., Nakatsuji, N., Nomura, S., ... & Aizawa, S. (1995). Reduced cell motility and enhanced focal adhesion contact formation in cells from FAK-deficient mice. Nature, 377(6549), 539.

Illes, P., & Verkhratsky, A. (2016). Purinergic neurone-glia signalling in cognitive-related pathologies. Neuropharmacology, 104, 62-75.

Imai, Y., Gehrke, S., Wang, H. Q., Takahashi, R., Hasegawa, K., Oota, E., & Lu, B. (2008). Phosphorylation of 4E-BP by LRRK2 affects the maintenance of dopaminergic neurons in Drosophila. The EMBO journal, 27(18), 2432-2443.

Ingelsson, M. (2016). Alpha-synuclein oligomers—neurotoxic molecules in parkinson's disease and other lewy body disorders. Frontiers in neuroscience, 10, 408.

Íñigo-Marco, I., Valencia, M., Larrea, L., Bugallo, R., Martínez-Goikoetxea, M., Zuriguel, I., & Arrasate, M. (2017). E46K α-synuclein pathological mutation causes cell-

autonomous toxicity without altering protein turnover or aggregation. Proceedings of the National Academy of Sciences, 114(39), E8274-E8283.

Isidoro, C., Biagioni, F., Giorgi, F. S., Fulceri, F., Paparelli, A., & Fornai, F. (2009). The role of autophagy on the survival of dopamine neurons. Current topics in medicinal chemistry, 9(10), 869-879.

Jacobson, J., & Duchen, M. R. (2002). Mitochondrial oxidative stress and cell death in astrocytes—requirement for stored Ca2+ and sustained opening of the permeability transition pore. Journal of Cell Science, 115(6), 1175-1188.

Jakel, R. J., & Stacy, M. (2014). Parkinson's disease psychosis. J Parkinsonism Restless Legs Syndrome, 4, 41-51.

Janda, E., Isidoro, C., Carresi, C., & Mollace, V. (2012). Defective autophagy in Parkinson's disease: role of oxidative stress. Molecular neurobiology, 46(3), 639-661.

Jankovic, J. (2005). Motor fluctuations and dyskinesias in Parkinson's disease: clinical manifestations. Movement disorders: official journal of the Movement Disorder Society, 20(S11), S11-S16.

Jankovic, J., & Aguilar, L. G. (2008). Current approaches to the treatment of Parkinson's disease. Neuropsychiatric disease and treatment, 4(4), 743.

Ježek, J., Cooper, K. F., & Strich, R. (2018). Reactive oxygen species and mitochondrial dynamics: the yin and yang of mitochondrial dysfunction and cancer progression. Antioxidants, 7(1), 13

Jha, M. K., Jo, M., Kim, J. H., & Suk, K. (2019). Microglia-astrocyte crosstalk: an intimate molecular conversation. The Neuroscientist, 25(3), 227-240.

Joe, E. H., Choi, D. J., An, J., Eun, J. H., Jou, I., & Park, S. (2018). Astrocytes, microglia, and Parkinson's disease. Experimental neurobiology, 27(2), 77-87.

Jones, V. C., Atkinson-Dell, R., Verkhratsky, A., & Mohamet, L. (2017). Aberrant iPSC-derived human astrocytes in Alzheimer's disease. Cell death & disease, 8(3), e2696.

Joshi, A. U., Minhas, P. S., Liddelow, S. A., Haileselassie, B., Andreasson, K. I., Dorn, G. W., & Mochly-Rosen, D. (2019). Fragmented mitochondria released from microglia trigger A1 astrocytic response and propagate inflammatory neurodegeneration. Nature neuroscience, 22(10), 1635-1648.

Julia, T. C. W., Wang, M., Pimenova, A. A., Bowles, K. R., Hartley, B. J., Lacin, E., ... & Slesinger, P. A. (2017). An efficient platform for astrocyte differentiation from human induced pluripotent stem cells. Stem Cell Reports, 9(2), 600-614

Keeney, P. M., Xie, J., Capaldi, R. A., & Bennett, J. P. (2006). Parkinson's disease brain mitochondrial complex I has oxidatively damaged subunits and is functionally impaired and misassembled. Journal of Neuroscience, 26(19), 5256-5264.

Kim, W. S., Kågedal, K., & Halliday, G. M. (2014). Alpha-synuclein biology in Lewy body diseases. Alzheimer's research & therapy, 6(5-8), 73.

Klein, C., & Westenberger, A. (2012). Genetics of Parkinson's disease. Cold Spring Harbor perspectives in medicine, 2(1), a008888.

Kleppe, R., Martinez, A., Døskeland, S. O., & Haavik, J. (2011). The 14-3-3 proteins in regulation of cellular metabolism. In Seminars in cell & developmental biology (Vol. 22, No. 7, pp. 713-719). Academic Press.

Konnova, E. A., & Swanberg, M. (2018). Animal Models of Parkinson's Disease. In Parkinson's Disease: Pathogenesis and Clinical Aspects [Internet]. Codon Publications.

Kordower, J. H., Chu, Y., Hauser, R. A., Freeman, T. B., & Olanow, C. W. (2008). Lewy body–like pathology in long-term embryonic nigral transplants in Parkinson's disease. Nature medicine, 14(5), 504.

Krencik, R., & Zhang, S. C. (2011). Directed differentiation of functional astroglial subtypes from human pluripotent stem cells. Nature protocols, 6(11), 1710.

Kuffler, S. W., & Nicholls, J. G. (1966). The physiology of neuroglial cells. In Ergebnisse der physiologie biologischen chemie und experimentellen pharmakologie (pp. 1-90).

Lawand, N. B., Saade, N. E., El-Agnaf, O. M., & Safieh-Garabedian, B. (2015). Targeting α-synuclein as a therapeutic strategy for Parkinson's disease. Expert opinion on therapeutic targets, 19(10), 1351-1360.

Leal, M. C., Casabona, J. C., Puntel, M., & PITOSSI, F. (2013). Interleukin-1β and tumor necrosis factor-α: reliable targets for protective therapies in Parkinson's Disease?. Frontiers in cellular neuroscience, 7, 53.

Lee, H. J., Khoshaghideh, F., Patel, S., & Lee, S. J. (2004). Clearance of α-synuclein oligomeric intermediates via the lysosomal degradation pathway. Journal of Neuroscience, 24(8), 1888-1896.

Lee, H. J., Suk, J. E., Patrick, C., Bae, E. J., Cho, J. H., Rho, S., ... & Lee, S. J. (2010). Direct transfer of α-synuclein from neuron to astroglia causes inflammatory responses in synucleinopathies. Journal of Biological Chemistry, 285(12), 9262-9272.

Lee, J. H., Han, J. H., Kim, H., Park, S. M., Joe, E. H., & Jou, I. (2019). Parkinson's disease-associated LRRK2-G2019S mutant acts through regulation of SERCA activity to control ER stress in astrocytes. Acta neuropathologica communications, 7(1), 68.

Lee, S. J., Jeon, H., & Kandror, K. V. (2008). Alpha-synuclein is localized in a subpopulation of rat brain synaptic vesicles. Acta Neurobiol Exp (Wars), 68(4), 509-515.

Liddelow, S. A., Guttenplan, K. A., Clarke, L. E., Bennett, F. C., Bohlen, C. J., Schirmer, L., ... & Wilton, D. K. (2017). Neurotoxic reactive astrocytes are induced by activated microglia. Nature, 541 (7638), 481.

Lindström V, Gustafsson G, Sanders LH, Howlett EH, Sigvardson J, Kasrayan A, Ingelsson M, Bergström J, Erlandsson A (2017) Extensive uptake of α-Synuclein oligomers in astrocytes results in sustained intracellular deposits and mitochondrial damage. Mol Cell Neurosci 82:143–156

Ling H, Massey L, Lees AJ, Brown P & Day BL (2012) Hypokinesia without decrement distinguishes progressive supranuclear palsy from Parkinson's disease. Brain 135, 1141–1153

Liu, G., Boot, B., Locascio, J. J., Jansen, I. E., Winder-Rhodes, S., Eberly, S., ... & Cormier-Dequaire, F. (2016). Specifically neuropathic Gaucher's mutations accelerate cognitive decline in Parkinson's. Annals of neurology, 80(5), 674-685.

Lobbestael, E., Baekelandt, V., & Taymans, J. M. (2012). Phosphorylation of LRRK2: from kinase to substrate. Biochemical Society Transactions, 40(5), 1102-1110.

Lopez-Fabuel, I., Le Douce, J., Logan, A., James, A. M., Bonvento, G., Murphy, M. P., ... & Bolaños, J. P. (2016). Complex I assembly into supercomplexes determines differential mitochondrial ROS production in neurons and astrocytes. Proceedings of the National Academy of Sciences, 113(46), 13063-13068.

Loria, F., Vargas, J. Y., Bousset, L., Syan, S., Salles, A., Melki, R., & Zurzolo, C. (2017). α-Synuclein transfer between neurons and astrocytes indicates that astrocytes play a role in degradation rather than in spreading. Acta neuropathologica, 134(5), 789-808.

Luciano, M. S., Lipton, R. B., Wang, C., Katz, M., Zimmerman, M. E., Sanders, A. E., ... & Saunders-Pullman, R. (2010). Clinical expression of LRRK2 G2019S mutations in the elderly. Movement Disorders, 25(15), 2571-2576.

Luk, K. C., Song, C., O'Brien, P., Stieber, A., Branch, J. R., Brunden, K. R., ... & Lee, V. M. Y. (2009). Exogenous α-synuclein fibrils seed the formation of Lewy body-like intracellular inclusions in cultured cells. Proceedings of the National Academy of Sciences, 106(47), 20051-20056.

Ma, B., Xu, L., Pan, X., Sun, L., Ding, J., Xie, C., ... & Cai, H. (2016). LRRK2 modulates microglial activity through regulation of chemokine (C–X3–C) receptor 1–mediated signalling pathways. Human molecular genetics, 25(16), 3515-3523.

MacLeod D, Dowman J, Hammond R, Leete T, Inoue K & Abeliovich A (2006) The familial Parkinsonism gene LRRK2 regulates neurite process morphology. Neuron 52, 587–593.

Maekawa T, Sasaoka T, Azuma S, Ichikawa T, Melrose HL, Farrer MJ, Obata F (2016) Leucine-rich repeat kinase 2 (LRRK2) regulates α-Synuclein clearance in microglia. BMC Neurosci 17(1):77.

Mahul-Mellier, A. L., Altay, F., Burtscher, J., Maharjan, N., Bouziad, N. A., Chiki, A., ... & Haikal, C. (2018). The making of a Lewy body: the role of alpha-synuclein post-fibrillization modifications in regulating the formation and the maturation of pathological inclusions. bioRxiv, 500058.

Mak, S. K., McCormack, A. L., Manning-Boğ, A. B., Cuervo, A. M., & Di Monte, D. A. (2010). Lysosomal degradation of α-synuclein in vivo. Journal of Biological Chemistry, 285(18), 13621-13629.

Makar, T. K., Nedergaard, M., Preuss, A., Gelbard, A. S., Perumal, A. S., & Cooper, A. J. (1994). Vitamin E, ascorbate, glutathione, glutathicne disulfide, and enzymes of glutathione metabolism in cultures of chick astrocytes and neurons: evidence that astrocytes play an important role in antioxidative processes in the brain. Journal of neurochemistry, 62(1), 45-53.

Mao, X., Ou, M. T., Karuppagounder, S. S., Kam, T. I., Yin, X., Xiong, Y., ... & Kang, H. C. (2016). Pathological α-synuclein transmission initiated by binding lymphocyte-activation gene 3. Science, 353(6307).

Marker DF, Puccini JM, Mockus TE, Barbieri J, Lu SM, Gel- bard HA (2012) LRRK2 kinase inhibition prevents pathological microglial phagocytosis in response to HIV-1 Tat protein. Journal of neuroinflammation, 9(1), 261.

Martinez-Vicente, M., Talloczy, Z., Kaushik, S., Massey, A. C., Mazzulli, J., Mosharov, E. V., ... & Dauer, W. (2008). Dopamine-modified α-synuclein blocks chaperone-mediated autophagy. The Journal of clinical investigation, 118(2), 777-788.

Martín-Jiménez, C. A., Salazar-Barreto, D., Barreto, G. E., & González, J. (2017). Genome-scale reconstruction of the human astrocyte metabolic network. Frontiers in aging neuroscience, 9, 23.

McCARTHY, K. D., & De Vellis, J. (1980). Preparation of separate astroglial and oligodendroglial cell cultures from rat cerebral tissue. The Journal of cell biology, 85(3), 890-902.

Meixner, A., Boldt, K., Van Troys, M., Askenazi, M., Gloeckner, C. J., Bauer, M., ... & Ueffing, M. (2011). A QUICK screen for Lrrk2 interaction partners–leucine-rich repeat kinase 2 is involved in actin cytoskeleton dynamics. Molecular & Cellular Proteomics, 10(1), M110-001172.

Mendivil-Perez, M., Velez-Pardo, C., & Jimenez-Del-Rio, M. (2016). Neuroprotective effect of the LRRK2 kinase inhibitor PF-06447475 in human nerve-like differentiated cells exposed to oxidative stress stimuli: implications for Parkinson's disease. Neurochemical research, 41(10), 2675-2692.

Mercuri, N. B., & Bernardi, G. (2005). The 'magic'of L-dopa: why is it the gold standard Parkinson's disease therapy?. Trends in pharmacological sciences, 26(7), 341-344.

Middeldorp, J., & Hol, E. M. (2011). GFAP in health and disease. Progress in neurobiology, 93(3), 421-443.

Mochizuki, H., Choong, C. J., & Masliah, E. (2018). A refined concept: α-synuclein dysregulation disease. Neurochemistry international, 119, 84-96.

Mormone, E., D'Sousa, S., Alexeeva, V., Bederson, M. M., & Germano, I. M. (2014). "Footprint-free" human induced pluripotent stem cell-derived astrocytes for in vivo cell-based therapy. Stem cells and development, 23(21), 2626-2636.

Mortiboys, H., Johansen, K. K., Aasly, J. O., & Bandmann, O. (2010). Mitochondrial impairment in patients with Parkinson disease with the G2019S mutation in LRRK2. Neurology, 75(22), 2017-2020.

Mozrzymas, J., Szczęsny, T., & Rakus, D. (2011). The effect of glycogen phosphorolysis on basal glutaminergic transmission. Biochemical and biophysical research communications, 404(2), 652-655.

Mullane, K., & Williams, M. (2013). Alzheimer's therapeutics: continued clinical failures question the validity of the amyloid hypothesis—but what lies beyond?. Biochemical pharmacology, 85(3), 289-305.

Narkiewicz, J., Giachin, G., & Legname, G. (2014). In vitro aggregation assays for the characterization of α-synuclein prion-like properties. Prion, 8(1), 19-32.

Ng, C. H., Mok, S. Z., Koh, C., Ouyang, X., Fivaz, M. L., Tan, E. K., ... & Lim, K. L. (2009). Parkin protects against LRRK2 G2019S mutant-induced dopaminergic neurodegeneration in Drosophila. Journal of Neuroscience, 29(36), 11257-11262.

Nimmerjahn, A., Kirchhoff, F., & Helmchen, F. (2005). Resting microglial cells are highly dynamic surveillants of brain parenchyma in vivo. Science, 308(5726), 1314-1318.

Niu, J., Yu, M., Wang, C., & Xu, Z. (2012). Leucine-rich repeat kinase 2 disturbs mitochondrial dynamics via Dynamin-like protein. Journal of neurochemistry, 122(3), 650-658.

Obara, M., Szeliga, M., & Albrecht, J. (2008). Regulation of pH in the mammalian central nervous system under normal and pathological conditions: facts and hypotheses. Neurochemistry international, 52(6), 905-919.

Oberheim, N. A., Takano, T., Han, X., He, W., Lin, J. H., Wang, F., ... & Ransom, B. R. (2009). Uniquely hominid features of adult human astrocytes. Journal of Neuroscience, 29(10), 3276-3287.

Obeso, J. A., Rodriguez-Oroz, M. C., Goetz, C. G., Marin, C., Kordower, J. H., Rodriguez, M., ... & Halliday, G. (2010). Missing pieces in the Parkinson's disease puzzle. Nature medicine, 16(6), 653.

Outeiro, T. F., Putcha, P., Tetzlaff, J. E., Spoelgen, R., Koker, M., Carvalho, F., ... & McLean, P. J. (2008). Formation of toxic oligomeric α-synuclein species in living cells. PloS one, 3(4), e1867.

Ozelius, L. J., Senthil, G., Saunders-Pullman, R., Ohmann, E., Deligtisch, A., Tagliati, M., ... & Lipton, R. B. (2006). LRRK2 G2019S as a cause of Parkinson's disease in Ashkenazi Jews. New England Journal of Medicine, 354(4), 424-425.

Papkovskaia, T. D., Chau, K. Y., Inesta-Vaquera, F., Papkovsky, D. B., Healy, D. G., Nishio, K., ... & Cooper, J. M. (2012). G2019S leucine-rich repeat kinase 2 causes uncoupling protein-mediated mitochondrial depolarization. Human molecular genetics, 21(19), 4201-4213.

Parisiadou, L., Xie, C., Cho, H. J., Lin, X., Gu, X. L., Long, C. X., ... & Cai, H. (2009). Phosphorylation of ezrin/radixin/moesin proteins by LRRK2 promotes the rearrangement of actin cytoskeleton in neuronal morphogenesis. Journal of Neuroscience, 29(44), 13971-13980.

Park, J. Y., Paik, S. R., Jou, I., & Park, S. M. (2008). Microglial phagocytosis is enhanced by monomeric α-synuclein, not aggregated α-synuclein: Implications for Parkinson's disease. Glia, 56(11), 1215-1223.

Parker Jr, W. D., Parks, J. K., & Swerdlow, R. H. (2008). Complex I deficiency in Parkinson's disease frontal cortex. Brain research, 1189, 215-218.

Parkkinen, L., Kauppinen, T., Pirttilä, T., Autere, J. M., & Alafuzoff, I. (2005). α-Synuclein pathology does not predict extrapyramidal symptoms or dementia. Annals of

Neurology: Official Journal of the American Neurological Association and the Child Neurology Society, 57(1), 82-91.

Parkkinen, L., Pirttilä, T., & Alafuzoff, I. (2008). Applicability of current staging/categorization of α-synuclein pathology and their clinical relevance. Acta neuropathologica, 115(4), 399-407.

Pereira, C., Martins, L. M., & Saraiva, L. (2014). LRRK2, but not pathogenic mutants, protects against H2O2 stress depending on mitochondrial function and endocytosis in a yeast model. Biochimica et Biophysica Acta (BBA)-General Subjects, 1840(6), 2025-2031.

Perrin, S. (2014). Preclinical research: Make mouse studies work. Nature News, 507(7493), 423.

Picard, M., White, K., & Turnbull, D. M. (2012). Mitochondrial morphology, topology, and membrane interactions in skeletal muscle: a quantitative three-dimensional electron microscopy study. Journal of applied physiology, 114(2), 161-171.

Piccoli, G., Condliffe, S. B., Bauer, M., Giesert, F., Boldt, K., De Astis, S., ... & Gloeckner, C. J. (2011). LRRK2 controls synaptic vesicle storage and mobilization within the recycling pool. Journal of Neuroscience, 31(6), 2225-2237.

Plotegher, N., Gratton, E., & Bubacco, L. (2014). Number and Brightness analysis of alpha-synuclein oligomerization and the associated mitochondrial morphology alterations in live cells. Biochimica et Biophysica Acta (BBA)-General Subjects, 1840(6).

Qiao, L., Hamamichi, S., Caldwell, K. A., Caldwell, G. A., Yacoubian, T. A., Wilson, S., ... & Liang, Q. (2008). Lysosomal enzyme cathepsin D protects against alpha-synuclein aggregation and toxicity. Molecular brain, 1(1), 17.

Rafikov, R., Sun, X., Rafikova, O., Meadows, M. L., Desai, A. A., Khalpey, Z., ... & Black, S. M. (2015). Complex I dysfunction underlies the glycolytic switch in pulmonary hypertensive smooth muscle cells. Redox biology, 6, 278-286.

Raha, S., & Robinson, B. H. (2000). Mitochondria, oxygen free radicals, disease and ageing. Trends in biochemical sciences, 25(10), 502-508.

Ramonet, D., Daher, J. P. L., Lin, B. M., Stafa, K., Kim, J., Banerjee, R., ... & Liu, Y. (2011). Dopaminergic neuronal loss, reduced neurite complexity and autophagic abnormalities in transgenic mice expressing G2019S mutant LRRK2. PloS one, 6(4), e18568.

Rannikko, E. H., Weber, S. S., & Kahle, P. J. (2015). Exogenous α-synuclein induces toll-like receptor 4 dependent inflammatory responses in astrocytes. BMC neuroscience, 16(1), 57.

Ransom, B. R., & Fern, R. (1997). Does astrocytic glycogen benefit axon function and survival in CNS white matter during glucose deprivation?. Glia, 21(1), 134-141.

Recasens, A., Dehay, B., Bové, J., Carballo-Carbajal, I., Dovero, S., Pérez-Villalba, A., ... & Farinas, I. (2014). Lewy body extracts from Parkinson disease brains trigger α-synuclein pathology and neurodegeneration in mice and monkeys. Annals of neurology, 75(3), 351-362.

Reeve, A. K., Krishnan, K. J., Elson, J. L., Morris, C. M., Bender, A., Lightowlers, R. N., & Turnbull, D. M. (2008). Nature of mitochondrial DNA deletions in substantia nigra neurons. The American Journal of Human Genetics, 82(1), 228-235.

Reinhardt, P., Schmid, B., Burbulla, L. F., Schöndorf, D. C., Wagner, L., Glatza, M., ... & Wu, G. (2013). Genetic correction of a LRRK2 mutation in human iPSCs links parkinsonian neurodegeneration to ERK-dependent changes in gene expression. Cell stem cell, 12(3), 354-367.

Renner, M., & Melki, R. (2014). Protein aggregation and prionopathies. Pathologie Biologie, 62(3), 162-168.

Reyes, J. F., Rey, N. L., Bousset, L., Melki, R., Brundin, P., & Angot, E. (2014). Alpha-synuclein transfers from neurons to oligodendrocytes. Glia, 62(3), 387-398.

Reyniers, L., Del Giudice, M. G., Civiero, L., Belluzzi, E., Lobbestael, E., Beilina, A., ... & Crosio, C. (2014). Differential protein–protein interactions of LRRK 1 and LRRK 2 indicate roles in distinct cellular signaling pathways. Journal of neurochemistry, 131(2), 239-250.

Rodriguez, L., Marano, M. M., & Tandon, A. (2018). Import and export of misfolded α-synuclein. Frontiers in neuroscience, 12.

Ross, C. A., & Poirier, M. A. (2004). Protein aggregation and neurodegenerative disease. Nature medicine, 10(7s), S10.

Rothstein, J. D., Dykes-Hoberg, M., Pardo, C. A., Bristol, L. A., Jin, L., Kuncl, R. W., ... & Welty, D. F. (1996). Knockout of glutamate transporters reveals a major role for astroglial transport in excitotoxicity and clearance of glutamate. Neuron, 16(3), 675-686.

Ruiz, A., Matute, C., & Alberdi, E. (2009). Endoplasmic reticulum Ca2+ release through ryanodine and IP3 receptors contributes to neuronal excitotoxicity. Cell calcium, 46(4), 273-281.

Sacino, A. N., Brooks, M., McKinney, A. B., Thomas, M. A., Shaw, G., Golde, T. E., & Giasson, B. I. (2014). Brain injection of α-synuclein induces multiple proteinopathies, gliosis, and a neuronal injury marker. Journal of Neuroscience, 34(37), 12368-12378.

Saha, S., Guillily, M. D., Ferree, A., Lanceta, J., Chan, D., Ghosh, J., ... & Hisamoto, N. (2009). LRRK2 modulates vulnerability to mitochondrial dysfunction in Caenorhabditis elegans. Journal of Neuroscience, 29(29), 9210-9218.

Schmidt, S., Linnartz, B., Mendritzki, S., Sczepan, T., Lübbert, M., Stichel, C. C., & Lübbert, H. (2011). Genetic mouse models for Parkinson's disease display severe pathology in glial cell mitochondria. Human molecular genetics, 20(6), 1197-1211.

Seifert, G., Henneberger, C., & Steinhaeuser, C. (2018). Diversity of astrocyte potassium channels: An update. Brain research bulletin, 136, 26-36.

Setsuie, R., Wang, Y. L., Mochizuki, H., Osaka, H., Hayakawa, H., Ichihara, N., ... & Kwon, J. (2007). Dopaminergic neuronal loss in transgenic mice expressing the Parkinson's disease-associated UCH-L1 I93M mutant. Neurochemistry international, 50(1), 119-129.

Sevlever, D., Jiang, P., & Yen, S. H. C. (2008). Cathepsin D is the main lysosomal enzyme involved in the degradation of α-synuclein and generation of its carboxy-terminally truncated species. Biochemistry, 47(36), 9678-9687.

Shaltouki, A., Peng, J., Liu, Q., Rao, M. S., & Zeng, X. (2013). Efficient generation of astrocytes from human pluripotent stem cells in defined conditions. Stem cells, 31(5), 941-952.

Shavali, S., Brown-Borg, H. M., Ebadi, M., & Porter, J. (2008). Mitochondrial localization of alpha-synuclein protein in alpha-synuclein overexpressing cells. Neuroscience letters, 439(2), 125-128.

Shih, A. Y., Johnson, D. A., Wong, G., Kraft, A. D., Jiang, L., Erb, H., ... & Murphy, T. H. (2003). Coordinate regulation of glutathione biosynthesis and release by Nrf2-expressing glia potently protects neurons from oxidative stress. Journal of Neuroscience, 23(8), 3394-3406.

Sinha, S., Du, Z., Maiti, P., Klärner, F. G., Schrader, T., Wang, C., & Bitan, G. (2012). Comparison of three amyloid assembly inhibitors: the sugar scyllo-inositol, the polyphenol epigallocatechin gallate, and the molecular tweezer CLR01. ACS chemical neuroscience, 3(6), 451-458.

Sian-Hulsmann, J., Monoranu, C., Strobel, S., & Riederer, P. (2015). Lewy bodies: a spectator or salient killer?. CNS & Neurological Disorders-Drug Targets (Formerly Current Drug Targets-CNS & Neurological Disorders), 14(7), 947-955.

Sickmann, H. M., Walls, A. B., Schousboe, A., Bouman, S. D., & Waagepetersen, H. S. (2009). Functional significance of brain glycogen in sustaining glutamatergic neurotransmission. Journal of Neurochemistry, 109, 80-86.

Siddiqui, A., Chinta, S. J., Mallajosyula, J. K., Rajagopolan, S., Hanson, I., Rane, A., ... & Andersen, J. K. (2012). Selective binding of nuclear alpha-synuclein to the PGC1alpha promoter under conditions of oxidative stress may contribute to losses in mitochondrial function: implications for Parkinson's disease. Free Radical Biology and Medicine, 53(4), 993-1003.

Simard, M., & Nedergaard, M. (2004). The neurobiology of glia in the context of water and ion homeostasis. Neuroscience, 129(4), 877-896.

Singh, A., Zhi, L., & Zhang, H. (2019). LRRK2 and mitochondria: recent advances and current views. Brain research, 1702, 96-104.

Singleton, A. B., Farrer, M. J., & Bonifati, V. (2013). The genetics of P arkinson's disease: Progress and therapeutic implications. Movement Disorders, 28(1), 14-23.

Sinha, S., Du, Z., Maiti, P., Klärner, F. G., Schrader, T., Wang, C., & Bitan, G. (2012). Comparison of three amyloid assembly inhibitors: the sugar scyllo-inositol, the polyphenol epigallocatechin gallate, and the molecular tweezer CLR01. ACS chemical neuroscience, 3(6), 451-458.

Smith WW, Jiang H, Pei Z, Tanaka Y, Morita H, Sawa A, Dawson VL, Dawson TM, Ross CA (2005) Endoplasmic reticulum stress and mitochondrial cell death pathways mediate A53T mutant alpha-synuclein-induced toxicity. Hum Mol Genet 14:3801–3811

Smith, G. A., Jansson, J., Rocha, E. M., Osborn, T., Hallett, P. J., & Isacson, O. (2016). Fibroblast biomarkers of sporadic Parkinson's disease and LRRK2 kinase inhibition. Molecular neurobiology, 53(8), 5161-5177.

Solano RM, Casarejos MJ, Menendez-Cuervo J, Rodriguez- Navarro JA, Garcia De Yebenes J, Mena MA (2008) Glial dysfunction in parkin null mice: effects of aging. J Neurosci 28:598-611.

Solano, R. M., Menendez, J., Casarejos, M. J., Rodriguez-Navarro, J. A., de Yebenes, J. G., & Mena, M. A. (2006). Midbrain neuronal cultures from parkin mutant mice are resistant to nitric oxide-induced toxicity. Neuropharmacology, 51(2), 327-340.

Spillantini, M. G., Schmidt, M. L., Lee, V. M. Y., Trojanowski, J. Q., Jakes, R., & Goedert, M. (1997). α-Synuclein in Lewy bodies. Nature, 388(6645), 839.

Stafa, K., Tsika, E., Moser, R., Musso, A., Glauser, L., Jones, A., ... & Dawson, T. M. (2013). Functional interaction of Parkinson's disease-associated LRRK2 with members of the dynamin GTPase superfamily. Human molecular genetics, 23(8), 2055-2077.

Su, Y. C., & Qi, X. (2013). Inhibition of excessive mitochondrial fission reduced aberrant autophagy and neuronal damage caused by LRRK2 G2019S mutation. Human molecular genetics, 22(22), 4545-4561.

Subramaniam, S. R., & Chesselet, M. F. (2013). Mitochondrial dysfunction and oxidative stress in Parkinson's disease. Progress in neurobiology, 106, 17-32.

Sugama, S., Yang, L., Cho, B. P., DeGiorgio, L. A., Lorenzl, S., Albers, D. S., ... & Joh, T. H. (2003). Age-related microglial activation in 1-methyl-4-phenyl-1, 2, 3, 6-tetrahydropyridine (MPTP)-induced dopaminergic neurodegeneration in C57BL/6 mice. Brain research, 964(2), 288-294.

Suh, S. W., Bergher, J. P., Anderson, C. M., Treadway, J. L., Fosgerau, K., & Swanson, R. A. (2007). Astrocyte glycogen sustains neuronal activity during hypoglycemia: studies with the glycogen phosphorylase inhibitor CP-316,819 ([RR*, S*]-5-chloro-N-[2-hydroxy-3-(methoxymethylamino)-3-oxo-1-(phenylmethyl) propyl]-1H-indole-2-carboxamide). Journal of Pharmacology and Experimental Therapeutics, 321(1), 45-50.

Suzuki, A., Stern, S.A., Bozdagi, O., Huntley, G.W., Walker, R.H., Magistretti, P.J., and Alberini, C.M. (2011). Astrocyte-neuron lactate transport is required for long-term memory formation. Cell 144, 810–823.

Swanson, R. A., Morton, M. M., Sagar, S. M., & Sharp, F. R. (1992). Sensory stimulation induces local cerebral glycogenolysis: demonstration by autoradiography. Neuroscience, 51(2), 451-461.

Takahashi, K., & Yamanaka, S. (2006). Induction of pluripotent stem cells from mouse embryonic and adult fibroblast cultures by defined factors. Cell, 126(4), 663-676.

Takahashi, K., Tanabe, K., Ohnuki, M., Narita, M., Ichisaka, T., Tomoda, K., & Yamanaka, S. (2007). Induction of pluripotent stem cells from adult human fibroblasts by defined factors. Cell, 131(5), 861-872.

Tamgüney, G., & Korczyn, A. D. (2018). A critical review of the prion hypothesis of human synucleinopathies. Cell and tissue research, 373(1), 213-220.

Tansey, M. G., McCoy, M. K., & Frank-Cannon, T. C. (2007). Neuroinflammatory mechanisms in Parkinson's disease: potential environmental triggers, pathways, and targets for early therapeutic intervention. Experimental neurology, 208(1), 1-25.

Terada, S., Ishizu, H., Yokota, O., Tsuchiya, K., Nakashima, H., Ishihara, T., ... & Kuroda, S. (2003). Glial involvement in diffuse Lewy body disease. Acta neuropathologica, 105(2), 163-169.

Thakur, P., Breger, L. S., Lundblad, M., Wan, O. W., Mattsson, B., Luk, K. C., ... & Björklund, A. (2017). Modeling Parkinson’s disease pathology by combination of fibril seeds and α-synuclein overexpression in the rat brain. Proceedings of the National Academy of Sciences, 114(39), E8284-E8293.

Tian, L., Ma, L., Kaarela, T., & Li, Z. (2012). Neuroimmune crosstalk in the central nervous system and its significance for neurological diseases. Journal of neuroinflammation, 9(1), 155.

Torres-Platas, S. G., Hercher, C., Davoli, M. A., Maussion, G., Labonté, B., Turecki, G., & Mechawar, N. (2011). Astrocytic hypertrophy in anterior cingulate white matter of depressed suicides. Neuropsychopharmacology, 36(13), 2650.

Tremblay, M. E., Cookson, M. R., & Civiero, L. (2019). Glial phagocytic clearance in Parkinson's disease. Molecular neurodegeneration, 14(1), 1-14.

Tsigelny, I. F., Sharikov, Y., Wrasidlo, W., Gonzalez, T., Desplats, P. A., Crews, L., ... & Masliah, E. (2012). Role of α-synuclein penetration into the membrane in the mechanisms of oligomer pore formation. The FEBS journal, 279(6), 1000-1013.

Tsika E, Kannan M, Foo CS, Dikeman D, Glauser L, Gellhaar S, Galter D, Knott GW, Dawson TM, Dawson VL et al (2014) Conditional expression of Parkinson's disease-related R1441C LRRK2 in midbrain dopaminergic neurons of mice causes nuclear abnormalities without neurodegeneration. Neurobiol Dis, 71, 345–358.

Tu, P. H., Galvin, J. E., Baba, M., Giasson, B., Tomita, T., Leight, S., ... & Lee, V. M. Y. (1998). Glial cytoplasmic inclusions in white matter oligodendrocytes of multiple system atrophy brains contain insoluble α-synuclein. Annals of neurology, 44(3), 415-422.

Uemura, N., Yagi, H., Uemura, M. T., Hatanaka, Y., Yamakado, H., & Takahashi, R. (2018). Inoculation of α-synuclein preformed fibrils into the mouse gastrointestinal tract induces Lewy body-like aggregates in the brainstem via the vagus nerve. Molecular neurodegeneration, 13(1), 21.

Vargas, J. Y., Grudina, C., & Zurzolo, C. (2019). The prion-like spreading of α-synuclein: From in vitro to in vivo models of Parkinson's disease. Ageing research reviews.

Vargas, K. J., Makani, S., Davis, T., Westphal, C. H., Castillo, P. E., & Chandra, S. S. (2014). Synucleins regulate the kinetics of synaptic vesicle endocytosis. Journal of Neuroscience, 34(28), 9364-9376.

Vargas, M. R., & Johnson, J. A. (2009). The Nrf2–ARE cytoprotective pathway in astrocytes. Expert reviews in molecular medicine, 11.

Vasile, F., Dossi, E., & Rouach, N. (2017). Human astrocytes: structure and functions in the healthy brain. Brain Structure and Function, 222(5).

Vicente-Gutierrez, C., Bonora, N., Bobo-Jimenez, V., Jimenez-Blasco, D., Lopez-Fabuel, I., Fernandez, E., ... & Bolaños, J. P. (2019). Astrocytic mitochondrial ROS modulate brain metabolism and mouse behaviour. Nature Metabolism, 1(2), 201.

Vidoni, C., Follo, C., Savino, M., Melone, M. A., & Isidoro, C. (2016). The role of cathepsin D in the pathogenesis of human neurodegenerative disorders. Medicinal research reviews, 36(5), 845-870.

Vila, M., Bové, J., Dehay, B., Rodríguez-Muela, N., & Boya, P. (2011). Lysosomal membrane permeabilization in Parkinson disease. Autophagy, 7(1), 98-100.

Volpicelli-Daley, L. A., Luk, K. C., Patel, T. P., Tanik, S. A., Riddle, D. M., Stieber, A., ... & Lee, V. M. Y. (2011). Exogenous α-synuclein fibrils induce Lewy body pathology leading to synaptic dysfunction and neuron death. Neuron, 72(1), 57-71.

Von Bartheld, C. S., Bahney, J., & Herculano-Houzel, S. (2016). The search for true numbers of neurons and glial cells in the human brain: A review of 150 years of cell counting. Journal of Comparative Neurology, 524(18), 3865-3895.

Wakabayashi, K., Hayashi, S., Yoshimoto, M., Kudo, H., & Takahashi, H. (2000). NACP/α-synuclein-positive filamentous inclusions in astrocytes and oligodendrocytes of Parkinson's disease brains. Acta neuropathologica, 99(1), 14-20.

Wallings, R., Manzoni, C., & Bandopadhyay, R. (2015). Cellular processes associated with LRRK 2 function and dysfunction. The FEBS journal, 282(15), 2806-2826.

Walls, A. B., Heimbürger, C. M., Bouman, S. D., Schousboe, A., & Waagepetersen, H. S. (2009). Robust glycogen shunt activity in astrocytes: Effects of glutamatergic and adrenergic agents. Neuroscience, 158(1), 284-292.

Walsh, D. M., & Selkoe, D. J. (2016). A critical appraisal of the pathogenic protein spread hypothesis of neurodegeneration. Nature Reviews Neuroscience, 17(4), 251.

Wang, X., Yan, M. H., Fujioka, H., Liu, J., Wilson-Delfosse, A., Chen, S. G., ... & Zhu, X. (2012). LRRK2 regulates mitochondrial dynamics and function through direct interaction with DLP1. Human molecular genetics, 21(9), 1931-1944.

West, A. B., Moore, D. J., Choi, C., Andrabi, S. A., Li, X., Dikeman, D., ... & Dawson, T. M. (2007). Parkinson's disease-associated mutations in LRRK2 link enhanced GTP-binding and kinase activities to neuronal toxicity. Human molecular genetics, 16(2), 223-232.

Wilson, J. X. (1997). Antioxidant defense of the brain: a role for astrocytes. Canadian journal of physiology and pharmacology, 75(10-11), 1149-1163.

Winkler, B. S., Orselli, S. M., & Rex, T. S. (1994). The redox couple between glutathione and ascorbic acid: a chemical and physiological perspective. Free Radical Biology and Medicine, 17(4), 333-349.

Winner, B., Jappelli, R., Maji, S. K., Desplats, P. A., Boyer, L., Aigner, S., ... & Tzitzilonis, C. (2011). In vivo demonstration that α-synuclein oligomers are toxic. Proceedings of the National Academy of Sciences, 108(10), 4194-4199.

Wu, S., Zhou, F., Zhang, Z., & Xing, D. (2011). Mitochondrial oxidative stress causes mitochondrial fragmentation via differential modulation of mitochondrial fission–fusion proteins. The FEBS journal, 278(6), 941-954.

Xing, W., Liu, J., Cheng, S., Vogel, P., Mohan, S., & Brommage, R. (2013). Targeted disruption of leucine-rich repeat kinase 1 but not leucine-rich repeat kinase 2 in mice causes severe osteopetrosis. Journal of Bone and Mineral Research, 28(9), 1962-1974.

Yamada, T., McGeer, P. L., & McGeer, E. G. (1992). Lewy bodies in Parkinson's disease are recognized by antibodies to complement proteins. Acta neuropathologica, 84(1), 100-104.

Yap, L., Tay, H. G., Nguyen, M. T., Tjin, M. S., & Tryggvason, K. (2019). Laminins in Cellular Differentiation. Trends in cell biology.

## Publications and contributions related to my PhD

### Publications

- Cavaliere, F., Cerf, L., Dehay, B., Ramos-Gonzalez, P., De Giorgi, F., Bourdenx, M., ... & Bezard, E. (2017). In vitro α-synuclein neurotoxicity and spreading among neurons and astrocytes using Lewy body extracts from Parkinson disease brains. *Neurobiology of disease*, *103*, 101-112.

- Bengoa-Vergniory, N., Faggiani, E., Ramos-González, P., Kirkiz E., Connor-Robson, N., Vingill, S., Cioroch, M., Cavaliere, F., Threlfell, S., Roberts, B., Cragg, S., Dehay, B., Bitan, G., Matute-Almau, C., Bezard E., & Wade-Martins, R. CLR01 protects dopaminergic neurons in vitro and in vivo in human neurons and mouse models of Parkinson's. *Nature communications*. Under second review.

### Conferences

- Role of Astrocytes in α-synuclein-mediated Neuronal Degeneration in Parkinson´s Disease. Poster. XI Glia Meeting. 2015, Bilbao.

- Role of Astrocytes in α-synuclein-mediated Neuronal Degeneration. Poster. Neurogune. 2016, Bilbao.

- Astrocytes contribute to the spreading of pathogenic α-synuclein. Poster. Alpha-synuclein & Parkinson's Disease Conference. 2017, Barcelona.

- Generation and characterization of human iPSc derived astrocytes from healthy and LRRK2$^{G2019S}$ Parkinson´s Pisease donors: Implications in neuronal degeneration. Poster. SENC. 2019, Santiago de Compostela.